IMPACTS OF HDAC4-MAP1S INTERACTION ON AUTOPHAGY AND DISEASES

A Dissertation

by

FEI YUE

Submitted to the Office of Graduate and Professional Studies of
Texas A&M University
in partial fulfillment of the requirements for the degree of

DOCTOR OF PHILOSOPHY

Chair of Committee,	Leyuan Liu
Committee Members,	Fen Wang
	Dekai Zhang
	Qiang Shen
Head of Department,	Van Wilson

May 2016

Major Subject: Medical Sciences

ABSTRACT

Autophagy is a cellular process to sequester cytoplasmic components for delivery to lysosomes for subsequent degradation, and plays important roles in aging and aging-associated pathogenesis. MAP1S is a ubiquitously distributed autophagy activator, which directly binds to the autophagosome marker LC3, accelerates autophagy initiation and degradation. Elucidating the mechanism of MAP1S-mediated autophagy can generate insights to control aging and aging-associated diseases. We discover that the acetylation of MAP1S maintains the stability of MAP1S protein and promotes autophagy. MAP1S interacts with HDAC4 via an HDAC4-binding domain (HBD). HDAC4 destabilizes MAP1S via deacetylation and suppresses autophagic flux.

Huntington's disease is a fatal progressive neurodegenerative disorder caused by the accumulation of aggregation-prone mutant Huntingtin protein (mHTT). Utilizing cell line stably expressing GFP-mHTT, we demonstrate that an overexpression of HDAC4 causes accumulation of mHTT aggregates by inhibiting MAP1S-mediated autophagy. Either suppression of HDAC4 or overexpression of HBD promotes the stability of MAP1S, and enhances MAP1S-regulated autophagic clearance of mHTT aggregates. This reveals a new potential strategy to treat Huntington's disease by interrupting HDAC4-MAP1S interaction.

Spermidine is a polyamine that activates autophagy and enhances longevity in some model systems. MAP1S-mediated autophagy helps mice maintain their lifespans and suppresses diethylnitrosamine-induced hepatocellular carcinomas. Thus, we

hypothesize that spermidine regulates MAP1S-mediated autophagy to prolong lifespans and suppress hepatocarcinogenesis. Our results indicate that spermidine activates autophagy by depleting cytosolic HDAC4 to reduce HDAC4-MAP1S interaction, and enhance the acetylation of MAP1S. Wild-type mice drinking spermidine-containing water have higher levels of MAP1S and autophagy activity, and extended lifespans, compared to wild-type mice drinking water; whereas $MAP1S^{-/-}$ mice drinking spermidine have no significant increase in autophagy level and medium survival time, compared to $MAP1S^{-/-}$ mice drinking water. Utilizing diethylnitrosamine-induced hepatocellular carcinoma mouse model, we find that spermidine enhances MAP1S to accelerate autophagic flux and suppress hepatocarcinogenesis in a MAP1S-dependent manner.

In sum, we uncover that HDAC4 deacetylates MAP1S, reduces the stability of MAP1S protein and impairs MAP1S-mediated autophagy. Blocking the association of MAP1S with HDAC4 leads to activation of MAP1S-mediated autophagy and suppression of aging and aging-associated diseases.

DEDICATION

This dissertation is dedicated to my family for all of their love and support.

To my mother and father who always inspired me to pursue the career of being a research scientist and set a good example for me by being passionate and conscientious about work, for their endless love, encouragement and guidance.

To my husband, my best friend and tower of strength, for love and care.

ACKNOWLEDGEMENTS

I would like to thank my committee chair, Dr. Leyuan Liu, and my committee members, Dr. Fen Wang, Dr. Dekai Zhang, Dr. Qiang Shen, for their guidance and support throughout the course of this research. Dr. Liu offered me the precious opportunity to join his lab, and trained me to think and work independently. Dr. Wang inspired me with interesting and incisive questions that broadened my perspective in research. Dr. Zhang offered me precious advice to my projects and helped me to improve my writing skills. Dr. Shen always gave me insightful suggestions to conduct advanced research and guided me on my future career.

I thank Dr. Peter Davies for always supporting me and generously offering me help whenever I need. I'm grateful to Ms. Cynthia Lewis, Ms. Janis Bender and Ms. Mary Cole for treating me as own child, comforting and encouraging me during hard times, and helping me solve all the administrative issues. I'm also thankful to all the members in Dr. Liu's lab for their friendship and kindness; especially Ms. Wenjiao Li, my good company, for sharing thoughts and techniques towards projects, and for all the assistance during my research.

I would like to express my gratitude to Drs. Sheng Zhang and Zhen Xu for providing stable cell line expressing inducible GFP-HTT72Q; and Drs. Tony Kouzarides and Paola Gallinari for providing plasmids that express HDAC4 variants. My gratitude also goes to my friends and colleagues, Dr. Wallace McKeehan for giving valuable advice on my project; Dr. Yanqing Huang, one of my best friends, for always standing by

my side and answering my numerous questions; Dr. Stefan Siwko for helping me proofreading my writings; Mr. Yifan Zhang for helping me with Real-Time PCR analyses; Mr. Ji Jing for helping me solving complicated problems while using confocal microscope; Ms. Lian He for providing me with the efficient protocol of establishing deletion construct; Mr. Yi Liang for helping me with CRISPR/Cas9 techniques; Mr. Dharmanand Ravirajan for providing me with the equipment for AGERA assay; Mr. Junchen Liu, Mr. Lei An, Mr. Peng Tan, Dr. Xiaojing Yue, Dr. Li Zeng, Dr. Yuan Dai, for generously sharing experimental materials and protocols with me; and all the staff in Institute of Biosciences and Technology-Texas A&M Health Science Center, for good memories we share with each other. In addition, I want to extend my gratitude to the funding support for my work, which includes a National Institute of Health NCI R01CA142862 to Dr. Leyuan Liu, the National Natural Science Foundation of China (No. 81472382) to Dr. Hai Huang, and the Natural Science Foundation of Guangdong Province and Science of China (2015A030310530) to Dr. Guibin Xu.

Last but not the least, I thank my mother and father for their unconditional love, dedication and encouragement, and my husband for his love, support and patience.

NOMENCLATURE

AGERA	Agarose Gel Electrophoresis for Resolving Aggregates
AFB	Aflatoxin B1
ARLD	Alcohol-related Liver Disease
ATG	Autophagy-related
BAF	Balifomycin A1
Bcl-2/xL	B-cell CLL/lymphoma 2 or xL
BSA	Bovine Serum Albumin
CCl4	Carbon Tetrachloride
ccRCC	Clear Cell Renal Cell Carcinoma
CE	Cytoplasmic Extract
CHX	Cycloheximide
CR	Calorie Restriction
CT	Comparative Threshold
DAB	3, 3'-Diaminobenzidine
DEN	Diethylnitrosamine
DHE	Dihydroethidium
DMEM	Dulbecco's Modified Eagle Medium
DMSO	Dimethyl Sulfoxide
DSB	Double-strand Breaks
EBSS	Earle's Balanced Salt Solution

EMEM	Eagle's Minimum Essential Medium
FBS	Fetal Bovine Serum
FL	Full Length
GFP	Green Fluorescent Protein
GST	Glutathione S-transferase
HAT	Histone Acetyltransferase
HBD	HDAC4-bind Domain
HBSS	Hanks' Balanced Salt Solution
HBV	Hepatitis B Virus
HC	Heavy Chain
HCC	Hepatocellular Carcinoma
HCV	Hepatitis C Virus
HD	Huntington’s Disease
HDAC	Histone Deacetylase
HDAC4	Histone Deacetylase 4
HDACi	Histone Deacetylase Inhibitor
HEK	Human Embryonic Kidney
HIF-1α	Hypoxia-inducible Factor-1α
HRP	Horseradish Peroxidase
HTT	Huntingtin
H&E	Hematoxylin and Eosin
ITS-G	Insulin-Transferrin-Selenium

IHC	Immunohistochemistry
LAMP2	Lysosome-associated Membrane Protein 2
LC	Light Chain
LC3	Microtubule-associated Protein 1A/B Light Chain 3
LRPPRC	Leucine-rich Pentatricopeptide Repeat Containing
MAP1A	Microtubule-associated Protein 1A
MAP1B	Microtubule-associated Protein 1B
MAP1S	Microtubule-associated Protein 1 Small Form
MAGD	Mitochondrial Aggregation and Genomic Destruction
MEF	Mouse Embryonic Fibroblast
MEF2	Myocyte Enhancer Factor-2
MEKK2	Mitogen-activated Protein Kinase Kinase Kinase 2
MT	Microtubule
mHTT	Mutant Huntingtin
N2α	Neuro-2α
NAD	Nicotinamide Adenine Dinucleotide
NAFLD	Non-alcoholic Fatty Liver Disease
NAM	Nicotinamide
NASH	Non-alcoholic Steatohepatitis
NE	Nuclear Extract
NMDAR	N-methyl-D-aspartate Receptor
P27	Cyclin-dependent Kinase Inhibitor 1B

PBS	Phosphate-buffered Saline
PCa	Prostate Adenocarcinoma
PE	Phosphatidylethanolamine
PI3K	Phosphoatidylinositol-3-kinase
PI3P	Phosphatidylinositol-3-phosphate
PMSF	Phenylmethanesulfonyl Fluoride
PolyQ	Polyglutamine
PP2A	Protein Phosphatase-2A
PVDF	Polyvinylidene Difluoride
RASSF1A	Ras-association Domain Family 1 Isoform A
RFP	Red Fluorescent Protein
ROS	Reactive Oxygen Species
Runx2	Runt-related Transcription Factor 2
SC	Short Chain
SDS	Sodium Dodecyl Sulfate
STAT1	Signal Transducer and Activator of Transcription 1
TBST	Tris-buffered Saline with Tween-20
TOR	Target of Rapamycin
TSA	Trichostatin A

TABLE OF CONTENTS

LIST OF FIGURES

Page

LIST OF TABLES

CHAPTER I

INTRODUCTION

Aging is the time-dependent process of functional loss that affects most organisms, and accounts for the primary risk factor for various human diseases (1). The incidence of chronic diseases, such as neurodegenerative diseases, metabolic disorders, sarcopenia, and cancers, increases dramatically in the aged population. Though global life expectancy has increased in the past fifteen years, the number of deaths increases as well over the same interval (2). Particularly, the death rate increases significantly in the group of people older than age 80. Therefore, extending healthy lifespans become a major challenge in medical sciences.

Aging is mainly resulted from the accumulation of cellular damage. Several cellular and molecular hallmarks of aging have been identified, including the primary hallmarks of genomic instability and proteostasis deficiency (3). Importantly, recent evidence shows that weak autophagy activity and high levels of oxidative stress are correlated with short lifespans (4). Thus, activation of autophagy to alleviate cellular oxidative stress is one of the most efficient approaches to prevent aging and aging-associated diseases.

Autophagy is a cellular self-degradation process that was first observed in the 1960s (5), and has been identified as the primary machinery to remove misfolded proteins, aggresomes, and dysfunctional organelles. The process of autophagy begins with the formation of cytosolic double-membrane vesicles, so-called autophagosomes,

containing sequestered substrates. Autophagosomes are sequentially transported along acetylated microtubules to fuse with lysosomes to form autolysosomes, in which autophagic substrates are degraded (6). The whole process of autophagy can be divided into several sequential steps, including autophagy induction, autophagosome formation, autophagosome-lysosome fusion, and degradation (7).

In the recent decades, significant progress has been made in understanding the molecular mechanisms of autophagy. A number of autophagy-related (ATG) gene-encoded proteins have been shown to be involved in autophagy regulation. As autophagy functions in a step-dependent manner, these ATG proteins are generally classified into three groups based on their functions at each step. The target of rapamycin (TOR) kinase and its effectors (ATG1, ATG2, ATG9, ATG13, ATG17, and ATG18) coordinately regulate autophagy induction. As the key component in autophagy regulation, TOR activity is regulated in response to nutrients availability, growth factor signaling, and cellular stress (8). TOR interacts with and inactivates ATG1 via direct phosphorylation. Under the condition of starvation or stress that induces autophagy, TOR activity is inhibited, which leads to ATG1 dissociated from TOR and dephosphorylation-induced activation of ATG1. Activated ATG1 further phosphorylates ATG13 and triggers downstream effectors for autophagy initiation. Class III phosphoatidylinositol-3-kinase (PI3K) complex (ATG6, ATG14, and VPS34) is the critical regulator of autophagosome nucleation. ATG6 interacts with class III PI3K (VPS34) to increase VPS34 kinase activity for generating phosphatidylinositol-3-phosphate (PI3P), an essential component that forms membrane and recruits proteins during autophagosome nucleation (9). Two

ubiquitin-like protein conjugation systems regulate the extension and completion of autophagosomes: the ATG12 conjugation system (ATG5, ATG12, and ATG16), and the LC3 (microtubule-associated protein 1 light chain 3, the mammalian homolog of ATG8) lipidation system (ATG3, ATG7, and LC3) (10). ATG12, an ubiquitin-like protein, can be firstly activated by ATG7 as an ubiquitin-activating enzyme E1-like protein, and then mediated by ATG10 as an ubiquitin-conjugating enzyme E2-like protein to form the ATG5-ATG12 conjugate. ATG16 interacts with ATG5-ATG12 conjugate to form a complex facilitating LC3 lipidation (11,12). In the LC3 lipidation system, LC3 precursor is firstly cleaved by ATG4 to remove its C-terminus to produce the cytosolic LC3-I. Mediated by the E1-like enzyme ATG7 and E2-like enzyme ATG3, LC3-I is conjugated to phosphatidyl-ethanolamine (PE) to generate membrane-associated LC3-II, which is recruited to both sides of the phagophore membrane. Once autophagosome formation is completed, ATG4 cleaves PE from LC3-II that localizes on the outer autophagosomal membrane, to release LC3 back to the cytosol for recycling (13).

LC3 is a commonly used marker for autophagy (14). The conversion from LC3-I to LC3-II indicates autophagosomal formation and the degradation of LC3-II indicates autolysosomal degradation. Either autophagy initiation or autophagy degradation affects levels of LC3-I and LC3-II. To perform an accurate measurement for autophagy level, lysosome inhibitors are utilized to block the degradation of autolysosomes, which leads to accumulation of LC3-II. With application of lysosome inhibitor, such as bafilomycin A1 (BAF), chloroquine, and ammonium chloride, levels of accumulated LC3-II can precisely represent autophagy activity (14).

Autophagy is the most important mechanism that regulates aging and aging-associated pathologies. Autophagy facilitates the removal of aggresomes and damaged organelles, reduces oxidative stress that further leads to cellular damage and genomic instability (15). The accumulation of aggresomes and dysfunctional organelles due to autophagy deficiency results in oxidative stress-induced toxicity in the cytoplasm which directly impacts on aging (4). In addition, autophagy serves as the primary mechanism that maintains homeostasis during nutrient fluctuation. Multiple nutrient-sensing signaling pathways, such as LKB1-AMPK-TOR signaling pathway, regulate autophagy to prolong lifespans under nutrient stress (16,17). The incidence of aging-associated pathologies increases with accumulation of cellular damage resulted from low levels of autophagy activity. Therefore, induction of autophagy is one of the most promising strategies to extend healthy lifespans and suppress aging-associated diseases, such as neurodegenerative disorders and cancers.

Neurodegenerative disorders are caused by progressive loss of neurons, due to the accumulation of toxic oligomeric and polymeric aggregates formed by altered proteins (18). As one of the most common neurodegenerative diseases, Huntington's disease (HD) occurs as a result of an autosomal dominant mutation with expansion of more than 36 trinucleotide CAG repeats which codes for polyglutamine (ployQ) in exon 1 of the *huntingtin* gene encoding Huntingtin protein (HTT) (19,20). PolyQ expansions longer than 36 residues render HTT prone to aggregate into insoluble inclusion bodies which are toxic to cells and promote neuronal death eventually (18). Striatum, primarily mediating cognition and motor function, is the most affected area in the brain by the

formation of mutant Huntingtin (mHTT) aggregates. Thus, HD patients suffer progressive cognitive impairment, uncontrolled movement ability. The incidence of HD mainly occurs in North America, Europe and Australia with an overall prevalence of 5.7 per 100,000 (21), and an increasing rate of 15-20% per decade (22). HD leads to an average age of onset around age 35-40, and ultimately death within 10-20 years after diagnosis (23).

At present, there are no treatments available to alter the course of HD. Research on curing HD mainly focuses on neuronal replacement, neuronal survival improvement, reduction of mHTT production and promotion of mHTT degradation. Autophagy is an important biological process that controls and executes the turnover of abnormally aggregated proteins, including mHTT (24). Therefore, up-regulating autophagy activity or preventing autophagy dysfunction may be a potential therapeutics for HD (23).

Cancer is a leading cause of death worldwide with increasing incidence associated with the aging of population. Among all the cancers, liver cancer is the second leading cause of cancer death (25). In the United States, both liver cancer cases and deaths have increased by more than twice during the past twenty-five years (26,27). Hepatocellular carcinoma (HCC) is the most common type of liver cancer, caused by long-term damage in the liver (28). Most HCC develops with a clinical history of liver cirrhosis, a chronic hepatic disease with excessive accumulation of extracellular matrix deposition, induced by long-term injuries, such as viral infection (Hepatitis B, HBV and Hepatitis C, HCV), alcohol-related liver disease (ARLD), non-alcoholic fatty liver disease (NAFLD) or non-alcoholic steatohepatitis (NASH) (29). Currently, most HCC

patients are diagnosed in the age of 50 or later with no effective treatment available; only small portions of HCC patients are diagnosed early enough that may be treated by surgical resection or liver transplantation (30). The prognosis of HCC is very unfavorable. In the United States, the one-year survival is less than 50%, and the five-year survival is only 10% (31). Thus, effective treatments and prevention approaches for HCC are in urgent need.

As the major pathway for removing dysfunctional organelles and misfolded proteins, autophagy is implicated in tumor suppression. Autophagy activity is elevated immediately in response to cellular stress. Activated autophagy removes aggresomes and damaged organelles that trigger DNA double-strand breaks (DSB) and genomic instability. Autophagy deficiency leads to an unstable genome and ultimately tumorigenesis. In addition to tumor initiation, tumor development induces autophagy to suppress genomic instability in tumor foci (15). Multiple animal studies confirm that autophagy deficiency promotes hepatocellular carcinogenesis (32,33). Clinical evidence also suggests that low levels of autophagy activity are associated with poor prognosis of cancer patients (34-36). Therefore, elevating autophagy activity may be helpful to prevent or treat HCC.

Microtubule-associated protein 1 small form (MAP1S) is a novel microtubule-associated autophagy activator. It was first cloned from a liver cDNA library and named as C19ORF5 based on the chromosomal location of its encoding gene (37). MAP1S is a widely distributed homologue of MAP1A and MAP1B (38,39). Similar to other members in the MAP1 family, MAP1S full length (FL) is synthesized as a precursor and

cleaved into multiple isoforms, including heavy chain (HC), short chain (SC), and light chain (LC) (40). MAP1S SC binds to microtubule and causes mitochondrial aggregation and genomic destruction (MAGD) (38); FL, HC and SC interact with mammalian autophagy marker microtubule-associated protein 1A/B light chain 3 (LC3) (41). All the MAP1S isoforms coordinately regulate autophagy initiation and autophagosome maturation. Depletion of MAP1S reduces the protein levels of B-cell CLL/lymphoma 2 or xL (Bcl-2/xL) and cyclin-dependent kinase inhibitor 1B (P27), which further results in decreased levels of autophagy initiation (41,42). As an autophagy regulator, MAP1S suppresses aging and tumorigenesis. MAP1S deficient mice have shortened lifespans (4) and develop more and larger foci of HCC after exposed to diethylnitrosamine (DEN) (33). In addition, MAP1S has been identified as a novel prognostic marker of patients suffering from prostate adenocarcinomas (PCa) (35) and clear cell renal carcinomas (ccRCC) (36). Cancer patients with low levels of MAP1S have shortened survival span. Thus, MAP1S is a potential target to induce autophagy to suppress aging and aging-associated diseases. A better understanding of the molecular detail of MAP1S can generate more insights on MAP1S-mediated autophagy and contribute to drug discovery of autophagy inducer in future.

Histone deacetylases (HDACs) are classes of enzymes that can remove acetyl groups from lysine on either histones or non-histone proteins (43). Mammalian HDACs are classified into four groups based on the homology to yeast proteins. All HDACs have one or two zinc-containing catalytic domains except Class III HDACs. Class I HDACs that are mainly localized in nucleus include HDAC1, HDAC2, HDAC3, and HDAC8.

Class II HDACs can be further divided into two subgroups. Class IIa HDACs, consisted of HDAC4, HDAC5, HDAC7 and HDAC9, have a binding domain for myocyte enhancer factor-2 (MEF2) and conserved phosphorylation sites that are important for the interaction with 14-3-3 protein for nucleus/cytoplasm trafficking. Class IIb HDACs include HDAC6 and HDAC10, and mainly function in cytoplasm. Class III HDACs are the sirtuins family of deacetylases that require nicotinamide adenine dinucleotide (NAD) for deacetylase activity. HDAC11 is classified individually into Class IV, due to the conserved residues shared by both Class I and Class II HDACs in the catalytic domain (44).

Histone deacetylation leads to condensed nucleosomes that block the binding of transcription factors to the targeted genes. Thus, deacetylation of histones represses gene expression through epigenetic regulation (45). Acetylation and deacetylation process in non-histone proteins is one of the major post-translational modifications that regulates protein stability, activity, cellular localization, and binding affinity (46). Recently, protein acetylation and deacetylation process has been identified as an important mechanism involved in autophagy regulation (17). Reduction in levels of acetyltransferases or acetyl-CoA can stimulate autophagy and prolong lifespans (47). In addition, activation of sirtuins promotes autophagy-dependent lifespan extension (48). Interestingly, histone deacetylase inhibitors (HDACi), the novel treatments for cancers, are reported as autophagy inducers (49,50), though the mechanism is still unclear. Therefore, further study is necessary to understand acetylation and deacetylation regulation in individual proteins involved in autophagy, such as MAP1S.

As autophagy is critical in extending lifespans and suppressing aging-associated diseases, pharmacologic intervention that induces autophagy is a novel direction for drug development. Spermidine has been identified as an autophagy inducer and longevity enhancer recently (51). It is a polyamine synthesized from putrescine and serves as a precursor of spermine. The name of spermidine is given for its high concentration in sperm, in addition to its abundance in citrus fruits, soybeans, and wheat germ (52). Studies have shown that spermidine extends the lifespans of yeast, nematodes, and flies in an autophagy-dependent fashion (51). The mechanism by which spermidine induces autophagy is suggested to be a combination of transcription-dependent and independent regulatory events but still not well understood (53). Unlike canonical autophagy inducers that have severe immunosuppressive effects, such as rapamycin, spermidine is a natural compound in food and should have fewer side effects. Besides, spermidine is a small molecule that can easily enter cells to execute its biological function. Thus, spermidine is a potential treatment to induce autophagy. At present, the impact of spermidine-induced lifespan extension has not been studied on mammals. The role of spermidine in cancer prevention and suppression is worth studying as well. Meanwhile, determining the mechanism of how spermidine modulates autophagy can contribute to the development of novel autophagy inducers for improving healthy lifespans.

CHAPTER II

MAP1S IS NEGATIVELY REGULATED BY HDAC4 VIA DEACETYLATION*

Introduction

Microtubule-associated protein 1 small form (MAP1S, previously called C19ORF5) associates with microtubules (38,54). Like its neuronal specific sequence homologues microtubule-associated protein 1A and 1B (MAP1A and MAP1B), widely distributed MAP1S interacts with the autophagosome-associated light chain 3 of MAP1A/B (LC3), and bridges autophagic components with microtubules to affect autophagosomal biogenesis and degradation (41).

B-cell CLL/lymphoma 2 (Bcl-2) is originally characterized as an anti-apoptotic protein, and also exhibits opposite roles in autophagy. By directly interacting with Beclin 1, the mammalian homolog of ATG6, Bcl-2 prevents the association of Beclin1 with class III PI3K and inhibits Beclin 1-dependent autophagy. On the other hand, Bcl-2 elevates levels of cyclin-dependent kinase inhibitor 1B (P27) that enhances ATG5 level to activate autophagy through a Beclin 1-independent pathway (42,55,56). Ablation of the *Map1s* gene in mice results in reduction in levels of Bcl-2 and P27, suggesting MAP1S enhances autophagy initiation by sustaining levels of Bcl-2 and P27 (41).

---

*Part of this chapter is reprinted with permission from "Blocking the Association of HDAC4 with MAP1S Accelerates Autophagy Clearance of Mutant Huntingtin" by Yue, F., Li, W., Zou, J., Chen, Q., Xu, G., Huang, H., Xu, Z., Zhang, S., Gallinari, P., Wang, F., McKeehan, W. L., and Liu, L, 2015, *Aging* **7**, 839-853, Copyright [2015] by Fei Yue.

In addition, MAP1S may regulate autophagy through one of its interactive proteins. Leucine-rich pentatricopeptide repeat containing (LRPPRC) is a mitochondrial inner membrane protein that associates with MAP1S (38,57) and has been suggested to play a suppressive role in autophagy initiation. LRPPRC interacts with Beclin 1 and Bcl-2 simultaneously to form a ternary complex to maintain the stability of Bcl-2, and further inhibits autophagy initiation (58). Therefore, MAP1S may bind with LRPPRC and participate in regulating the association between Beclin 1 and Bcl-2 complex to affect autophagy activity.

Both the direct function of MAP1S association with microtubules and autophagosome-associated LC3, and indirect positive impact of MAP1S on autophagy initiation through Bcl-2 and P27 enhance the overall rate of autophagic flux (20,41). However, the upstream regulators of MAP1S have not been identified. Elucidating the mechanism by which MAP1S is regulated can generate new knowledge in autophagy regulation.

Histone deacetylases 4 (HDAC4) belongs to the Class II subgroup a of the HDACs family (44), which can shuttle between the nucleus and cytoplasm. In the nucleus, HDAC4 binds with the myocyte enhancer factor-2 (MEF2) through a conserved MEF2 binding domain in the N-terminal of HDAC4 and represses MEF2 transcriptional activation (59). In addition, emerging evidence indicates that HDAC4 interacts with and regulates a variety of non-histone proteins, such as runt-related transcription factor 2 (Runx2), hypoxia-inducible factor-1α (HIF-1α), signal transducer and activator of transcription 1(STAT1), and mitogen-activated protein kinase kinase kinase 2 (MEKK2),

via direct deacetylation (60-63). Though HDAC4 plays global roles in the regulation of gene transcription and further controls cell growth, survival and proliferation (64), its impact on autophagy is poorly understood.

To characterize the molecular detail of MAP1S protein and identify the upstream regulator of MAP1S, we first focus on the post-translational modification of MAP1S protein. In addition to the fact that acetylation and deacetylation process is an important mechanism to regulate protein function and stability, a yeast two-hybrid screen result suggests a potential interaction between HDAC4 and MAP1S (65), which encourages us to investigate whether HDAC4 regulates MAP1S via deacetylation and further affects autophagy activity through MAP1S.

Herein we show that depletion of MAP1S leads to suppression of autophagic flux and confirm MAP1S as an autophagy activator in multiple cell lines. Importantly, we discover that MAP1S can interact with HDAC4, but have no impact on the protein level of HDAC4. However, HDAC4 decreases the stability of MAP1S protein by catalyzing deacetylation of acetylated MAP1S and inhibits autophagic flux through MAP1S (20).

Materials and Methods

Animals

Animal protocols were approved by the Institutional Animal Care and Use Committee (IACUC), Institute of Biosciences and Technology, Texas A&M Health Science Center. All animals received human care according to the criteria outlined in the 'Guide for the Care and Use of Laboratory Animals' prepared by the National Academy of Sciences and published by the National Institutes of Health (NIH publication 86-23 revised 1985). C57BL/6 wild-type and MAP1S$^{-/-}$ mice were bred and genotyped as previously described (41). Primers used for verification of mouse genotypes are listed in the Table 1.

Table 1. Primers Used for Verification of Mouse Genotypes.

Primer	Sequence
P31	5'-CACCTGCCTAAGCCATCTGTGTC-3'
P32	5'-CTCAGTCTGTCTGAGACAAGGTC-3'
Pneo	5'-GGTAGAATTGGTCGAGGTCGAC-3'

Cell Culture

Most cell lines, including HeLa, HepG2, human embryonic kidney (HEK)-293T, COS-7 cells, HeLa cells stably expressing ERFP-LC3 (HeLa-RFP-LC3), and mouse embryonic fibroblast (MEF) cells that were established as described (41), were cultured in the Dulbecco's Modified Eagle Medium (DMEM) (GenDEPOT, #CM001) containing

10% Fetal Bovine Serum (FBS) (Invitrogen, #26140) and antibiotics (Thermo Scientific, #SV30010). Primary mouse hepatocytes were grown in William's E culture media (Sigma, #W4125) with 10% FBS, Insulin-Transferrin-Selenium (ITS-G) (Invitrogen, #51300-044), antibiotics and 100 nM dexamethasone (Sigma, D4902). Phosphate-buffered saline (PBS), pH 7.4 and 0.25% trypsin (Thermo Scientific, #SV30031.01) were used for subculture.

Cell Transfection

Cell lines used for transfection included HeLa, HepG2, HEK-293T, COS-7 cells, HeLa-RFP-LC3 cells, or MEF cells. For transient knockdown experiments, cells were cultured at 30% confluence on the cell culture plates or coverslips and transfected with negative control siRNA or specific siRNA by Oligofectamine (Invitrogen, #12252-011) according to the manufacturer's recommended instruction. For transient overexpression experiments in HeLa, HepG2, COS-7 cells, HeLa-RFP-LC3 cells, or MEF cells, cells were cultured at 70% confluence on the cell culture plates or coverslips and transfected with control vector or plasmids encoding specific genes by Lipofectamine 2000 (Invitrogen, #11668019) according to the manufacturer's recommended instruction. For transient overexpression in HEK-293T, cells were cultured at 60% confluence on the cell culture plates and transfected with control vector or plasmids encoding specific genes by using calcium phosphate transfection kit (Clontech, #631312) according to the manufacturer's recommended instruction.

Plasmids and siRNAs

Plasmids encoding HA-MAP1S, GFP–HDAC4, Flag-HDAC4, Flag-HDAC4 H976Y, Flag-HDAC4 H976F, Myc-HDAC4 H803A, or Myc-HDAC4 D840N were previously described (38,59,66,67). The control siRNA (Invitrogen, #AM4635) and siRNA specific to human MAP1S (Invitrogen, #AM16708, ID45347) were from Invitrogen. The siRNAs specific to human HDAC4 (Santa Cruz, #35540) or mouse HDAC4 (Santa Cruz, #35541) were from Santa Cruz Biotechnology.

Establishment of Stable MAP1S Knockout HeLa Cell Line by CRISPR/Cas9

Guide RNAs targeting human MAP1S gene listed in the Table 2 were designed using Optimized CRISPR Design (http://crispr.mit.edu/). DNA oligos were synthesized by Integrated DNA Technologies and annealed by using T4 Polynucleotide Kinase (New England Biolabs, #M0201S) according to the manufacturer's recommended instruction. Annealed DNA oligos were inserted into CRISPR/CAS9 vector pSpCas9(BB)-2A-Puro (PX459) (Addgene, #48139) via digestion-ligation reaction to construct plasmids encoding Cas9 nuclease and guide RNAs targeting for human *Map1s*. Sequence verification was then performed by GENEWIZ. HeLa cells were transiently transfected with a pool of five MAP1S CRISPR/Cas9 knockout plasmids or the vector for wild-type control. Cells were selected with 1.5 μg/ml puromycin (Sigma, #P9620) starting at 48 hours after transfection. Multiple monoclonal single cell clones were picked and cultured individually in separate wells. Immunoblot analyses of MAP1S protein level were used to determine the knockout efficiency.

Table 2. DNA Oligos for gRNAs Targeting Human MAP1S.

DNA Oligo for gRNAs	Sequence
MAP1S gRNA-1 Forward	5'-CACCGATGGCGGCGGTGGCTGGATC-3'
MAP1S gRNA-1 Reverse	5'-AAACGATCCAGCCACCGCCGCCATC-3'
MAP1S gRNA-2 Forward	5'-CACCGTCGTGGTGGGCAGCGAGTTC-3'
MAP1S gRNA-2 Reverse	5'-AAACGAACTCGCTGCCCACCACGAC-3'
MAP1S gRNA-3 Forward	5'-CACCGGGGCTCCTCACCTACGTCC-3'
MAP1S gRNA-3 Reverse	5'-AAACGGACGTAGGTGAGGAGCCCC-3'
MAP1S gRNA-4 Forward	5'-CACCGCGGTCTTGGGATGTCGATCC-3'
MAP1S gRNA-4 Reverse	5'-AAACGGATCGACATCCCAAGACCGC-3'
MAP1S gRNA-5 Forward	5'-CACCGTCCACCTCGGTCGAGTGCG-3'
MAP1S gRNA-5 Reverse	5'-AAACCGCACTCGACCGAGGTGGAC-3'

Isolation of Primary Mouse Hepatocytes

Primary mouse hepatocytes were isolated from 12-week-old male mice. Mice were anesthetized and laparotomized with U shape incision. The portal vein was cannulated and the inferior vena cava was sectioned. The liver was simultaneously perfused with Earle's Balanced Salt Solution (EBSS) (Invitrogen, #14115-063) containing 0.5 mM EGTA (Sigma, #E4378), followed by Hanks' Balanced Salt Solution (HBSS) (Invitrogen, #14170-112) supplied with 0.3mg/ml type IV collagenase (Roche, #11088874103). After perfusion, the liver was cut out and gently squeezed until most of the hepatocytes got out. The cells were filtered through sterile 70-μm-mesh nylon (Greiner Bio-one, #542070), washed by centrifugation and resuspended in the culture

media. Cell viability was assessed by trypan blue (Invitrogen, #15250-061) staining and cells were seeded at 1×10^6 in the 60 mm dish.

Immunoblot Analyses

Cells were lysed in the cell lysis buffer (50 mM HEPES, pH 7.5, 150 mM NaCl, 1 mM EDTA, 2.5 mM EGTA, 0.1% Triton X-100, 10% Glycerol, 1 mM NaF) with 1 mM phenylmethanesulfonyl fluoride (PMSF) (Sigma, #P7626) on ice for 30 minutes. The total protein concentration of the cell lysates was determined by using BCA protein assay kit (Thermo Scientific, #23225). The cell lysates were then mixed with sodium dodecyl sulfate (SDS) loading buffer and boiled for 10 minutes. Cell lysates were loaded on SDS-polyacrylamide gels containing 8, 10, 12 or 15% (w/v) acrylamide. Proteins were separated by electrophoresis, transferred on to polyvinylidene difluoride (PVDF) membranes (GE Health, #10600023). The membranes were then blocked with 5% (w/v) non-fat milk in Tris-buffered Saline with Tween-20 (TBST) for 1 hour at room temperature, bound with primary antibodies overnight at 4 °C and incubated with horseradish peroxidase (HRP)-conjugated secondary antibodies (Bio-Rad, #172-1011, #170-6515, dilution 1:10000) for 2 hours at room temperature. Proteins were detected by ECL Prime Western Blotting Detection Reagents (GE Health, #RPN2232). The exposed X-ray films (Pheonix, #F-BX57) were processed using developer (Carestream, #1900984) and fixer (Carestream, #1902485), and scanned into image files. The relative intensity of a band to internal control was measured using ImageJ software (NIH). The catalog numbers and dilutions of primary antibodies are listed in the Table 3.

Table 3. Catalog Numbers and Dilutions of Primary Antibodies-I.

Antibody	Catalog Number	Dilution
MAP1S	Precision, #AG10006	1:2000
LC3	Novus, #NB100-2331	1:3000
β-Actin	Santa Cruz, #47778	1:5000
GAPDH	Santa Cruz, #25778	1:2000
HDAC4	Cell Signaling, #7628	1:1000
Acetyl-lysine	EMD Millipore, #05515	1:1000
HA	Covance, #MMS-101P	1:1000

Immunoprecipitation

To analyze levels of acetylated MAP1S by immunoprecipitation, cell lysates were prepared by using RIPA buffer (50 mM Tris-Hcl, pH 7.4, 150 mM NaCl, 1% Triton X-100, 0.5% sodium dexycholate, 1 mM EDTA, pH 7.4, 0.5 mM EDTA, 0.1% SDS) with 1 mM PMSF, protease inhibitor cocktails (Sigma, #P8340), 5 mM nicotinamide (NAM) (Sigma, #72340) and 10 μM Trichostatin A (TSA) (Sigma, #T8552); and centrifuged at 14,000 rpm for 15 minutes at 4 °C to isolate the supernatants. Lysates of same amount of total proteins were mixed with 30 μl anti-acetyl-lysine agarose conjugate (EMD Millipore, #16-272) overnight at 4 °C for precipitation of total acetylated lysine proteins.

To study the interaction between MAP1S and HDAC4, cell lysates were prepared by using NP-40 buffer (50 mM Tris-Hcl, pH 7.4, 150 mM NaCl, 5 mM EDTA, pH 7.4, 1% NP-40) with 1 mM PMSF and protease inhibitor cocktails. The supernatants were collected after centrifugation at 14,000 rpm for 15 minutes at 4 °C. Same amount of

lysates with 1.5 mg of total protein were subjected to immunoprecipitation with 2 μg antibodies against MAP1S, HDAC4, HA, or the respective IgG control, and incubated with 30 μl Protein G-Sepharose beads (GE Health, #17-0618-01). Beads binding with antibodies and the bound proteins were precipitated and washed extensively with the relative lysis buffer four times. The final precipitates were resuspended in 100 μl lysis buffer containing SDS loading buffer and processed for immunoblot analyses.

GST Pull-down Assay

HEK-293T cells overexpressing Flag-HDAC4 or a control were lysed with binding buffer containing 1% NP-40 in PBS, 2 mM dithiothreitol (Sigma, #D0632) and protease inhibitor cocktails. The supernatants were collected after centrifugation at 14,000 rpm for 15 minutes at 4 °C. Lysates of 200 μg protein were mixed with 25 μl equilibrated Glutathione-Sepharose 4B beads (GE Health, #17-0756-01) in a final volume of 400 μl and rotated for 30 minutes at 4 °C for per-cleaning. A total of 7.5 μg purified Glutathione S-transferase (GST) or GST-tagged proteins bound to 25 μl glutathione beads were mixed with 200 μg pre-cleaned cell lysates, and rotated for 1 hour at 4 °C and then washed three times with binding buffer. The pellets were resuspended in 50μl binding buffer containing SDS loading buffer and processed for immunoblot analyses. Purified GST and GST-tagged proteins were stained by coomassie blue.

RNA Expression

Total RNA was extracted from HeLa cells transfected with control siRNA, HDAC4-specific siRNA, control vector plasmid, or HDAC4 expression plasmid with Trizol reagent (Invitrogene, #15596-026) according to the manufacturer's recommended instructions. The Invitrogene SuperScript III First-Strand System was used for reverse transcription with random primers for cDNA synthesis. Real-time PCRs were performed with SYBR Premix ExTaq (TaKaRa, #RR820A) according to the manufacturer's recommended instructions. Primers for human MAP1S included a forward primer 5'-CGCTGGAAGAACTCCTCATC-3' and a reverse primer 5'-GAGTGAGCCCAGTGA GAAGG-3' and those for human β-Actin included a forward primer 5'-ACTCTTCCA GCCTTCCTTCC-3' and a reverse primer 5'-CAGTGATCTCCTTCTGCATCC-3'. The comparative threshold (CT) cycle method was used to calculate the mRNA level. The relative mRNA level of *Map1s* was quantified by normalizing the amount of *Map1s* mRNA to the amount of *β-actin* mRNA.

Protein Half-life Measurement

HeLa cells were seeded in 10cm culture dishes and transfected with control siRNA or HDAC4-specific siRNA. After transfection for 48 hours, cells were processed for subculture. Cell pellet harvested after centrifugation at 600 rpm for 5 minutes were resuspended and split evenly into 35 mm culture dishes. Then, the protein synthesis inhibitor 10 μg/ml cycloheximide (CHX) (Sigma, #C1988) was added into the culture media. Cell lysates were harvested at the indicated time points for immunoblot analyses.

In vitro *Deacetylation*

As described previously (61), 293T cells were transfected with the plasmid expressing HA-MAP1S and treated with 1 μM apicidin (Sigma, #A8851) to induce acetylated HA-MAP1S 24 hours prior to the harvest. Cell lysates were prepared by using RIPA buffer with 1 mM PMSF, protease inhibitor cocktails, 5 mM NAM and 10 μM TSA; and purified with anti-MAP1S antibody by immunoprecipitation. Flag-HDAC4, Flag-HDAC4 H976Y, Flag-HDAC4 H976F, Myc-HDAC4 H803A, or Myc-HDAC4 D840N was overexpressed in 293T cells and purified with conjugated anti-Flag M2-agarose (Sigma, #M8823) or anti-Myc antibody (Cell Signaling, #2276) and Protein G-agarose beads by immunoprecipitation. The agarose beads containing immunopurified HDAC4 were mixed with agarose beads containing HA-MAP1S in deacetylation buffer (10 mM Tris-HCl, pH 8.0, 150 mM NaCl and 10% glycerol). Mixture was incubated at 37°C for the indicated amount of time; each reaction was terminated with SDS loading buffer.

Fluorescence Microscopy

HeLa-RFP-LC3 cells transfected with the plasmid expressing GFP or GFP-HDAC4 were treated with 10 nM balifomycin A1 (BAF) (Sigma, #11707) for 6 hours before fixation. Cells were fixed with 4% (w/v) paraformaldehyde (Sigma, #P6148) in PBS at room temperature for 30 minutes and processed for fluorescence microscopy analyses. Images were captured with a Zeiss LSM 510 Meta Confocal Microscope. The

acquired images were converted into 8-bit binary files, and the number of RFP-LC3 punctate foci on each image was calculated using ImageJ software.

Transmission Electron Microscopy

HeLa cells, transfected with control siRNA, HDAC4-specific siRNA, control vector plasmid or Flag-HDAC4 plasmid, were treated with 10 nM BAF for 12 hours before fixation. As described previously (58), cells were fixed for 1 hour with a solution containing 3% (w/v) glutaraldehyde, 2% (w/v) paraformaldehyde and 0.1M cacodylate buffer, pH 7.3. After fixation, cells were washed and treated with 0.1% Millipore-filtered cacodylate-buffered tannic acid, post-fixed with 1% (w/v) buffered osmium tetroxide for 30 minutes, and stained *en bloc* with 1% (w/v) Millipore-filtered uranyl acetate. The samples were dehydrated in increasing concentrations of ethanol, infiltrated and embedded in LX-112 medium followed by polymerization in a 70 °C oven for 2 days. Ultrathin sections were cut in a Leica Ultracut microtome (Leica), stained with uranyl acetate and lead citrate in a Leica EM Stainer, and examined in a JEM 1010 transmission electron microscope (JEOL) at an accelerating voltage of 80 kV. Digital images were obtained using the Advanced Microscopy Techniques imaging systems. The percentages of areas occupied by autophagic vacuoles were measured using ImageJ software.

Statistical Analyses

Statistical significance was determined by Student's t-test, with significance set to *, $p \leq 0.05$; **, $P \leq 0.01$; and ***, $P \leq 0.001$. Error bars indicate standard deviation.

Results

MAP1S Deficiency Results in Autophagy Suppression

To study the impact of MAP1S on regulating autophagic flux, lysosome inhibitor bafilomycin 1A (BAF) was applied to inhibit autolysosomal degradation and levels of accumulated LC3-II was measured to represent autophagic flux by immunoblot analyses. Effective transient siRNA knockdown of MAP1S in HeLa (Figure 1A) and HepG2 (Figure 1B) cells leads to increased levels of LC3-II but decreased levels of accumulated LC3-II when cells were treated with 10 nM BAF for 4 hours, which suggested that MAP1S knockdown inhibited both autophagy initiation and degradation.

The suppressive role of MAP1S deficiency in autophagy was further confirmed in HeLa cell lines with stable knockout of MAP1S. CRISPR/Cas9 technique was applied to establish $MAP1S^{-/-}$ HeLa cells and three single cell colonies were isolated. As shown in the results of immunoblot analyses, $MAP1S^{-/-}$ HeLa cells accumulated less LC3-II compared to $MAP1S^{+/+}$ HeLa cells after BAF treatment (Figure 1C), which suggested depletion of MAP1S suppressed autophagic flux. Meanwhile, mouse embryonic fibroblasts (MEF) and primary mouse hepatocytes isolated from wild-type or $MAP1S^{-/-}$ mice were treated with BAF to study the role of MAP1S on autophagy. Significant decrease in levels of LC3-II was observed in $MAP1S^{-/-}$ MEF cells (Figure 1D) or $MAP1S^{-/-}$ hepatocytes (Figure 1E) in contrast to wild-type MEF cells or wild-type hepatocytes after BAF treatment, which also demonstrated MAP1S deficiency resulted in autophagy suppression. All the results confirm that MAP1S is a positive regulator of autophagic flux.

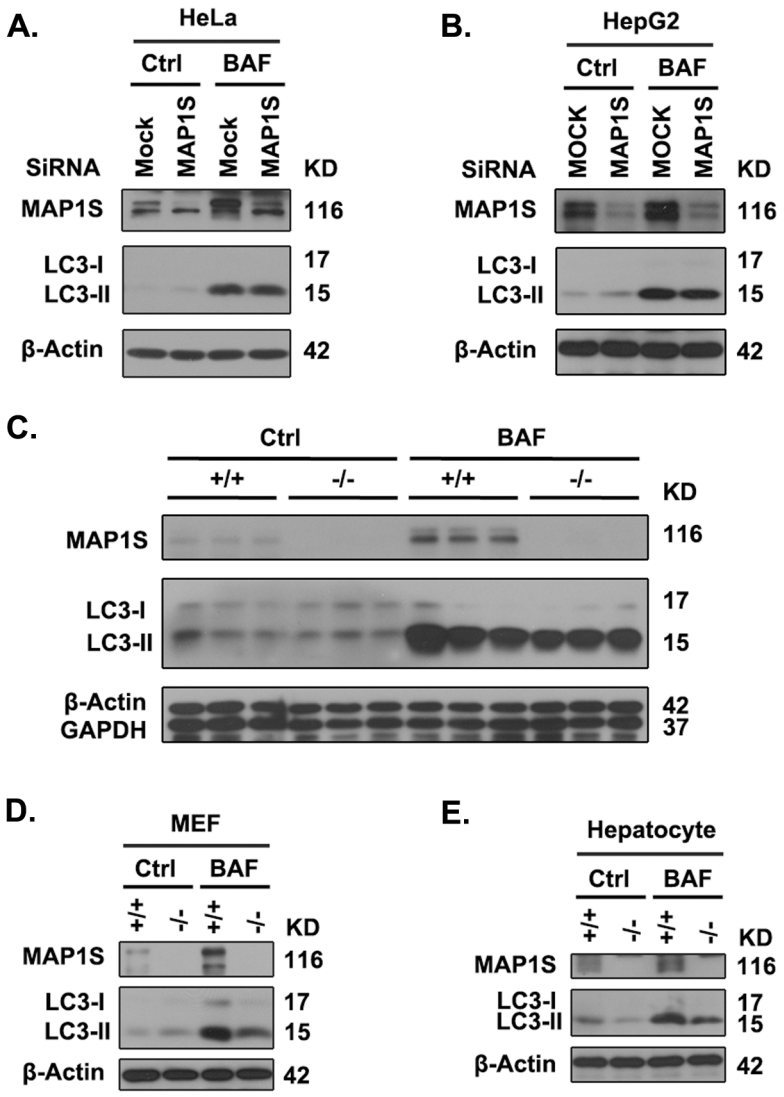

Figure 1. Depletion of MAP1S Suppresses Autophagic Flux. (**A**, **B**) Transient siRNA knockdown of MAP1S inhibits autophagic flux. Representative immunoblot results show the impact of MAP1S suppression with siRNA on levels of LC3-II in HeLa (**A**) or HepG2 cells (**B**) in the absence (Ctrl) or presence of BAF. (**C-E**) Knockout of MAP1S suppresses autophagic flux. Representative immunoblot results of levels of LC3-II in wild-type and MAP1S$^{-/-}$ HeLa cells (**C**), wild-type and MAP1S$^{-/-}$ MEF cells (**D**), wild-type and MAP1S$^{-/-}$ primary mouse hepatocytes (**E**), in the absence (Ctrl) or presence of BAF, are shown.

HDAC Inhibitor Apicidin Enhances Levels of Acetylated MAP1S and Promotes Autophagic Flux

Similarly to the previous results (68), the histone deacetylase inhibitor, apicidin was able to induce autophagy. HeLa cells treated with 1μM apicidin for 24 hours had increased levels of LC3-II compared to HeLa cells treated with dimethyl sulfoxide (DMSO) control in the absence or presence of BAF for 4 hours (Figure 2A, B), which suggested apicidin promoted autophagic flux. As shown in the immunoblot results, apicidin also led to increased levels of MAP1S protein in both HeLa and COS-7 cells (Figure 2C), suggesting MAP1S may participate in the regulation of apicidin-induced autophagy. In addition, the total acetyl-lysine proteins were first precipitated by anti-acetyl-lysine agarose conjugate, and then levels of acetylated MAP1S were analyzed by immunoblot analyses. Apicidin enhanced levels of acetylated MAP1S as well (Figure 2D, E), suggesting the acetylation of MAP1S may be involved in regulating MAP1S and apicidin-induced autophagy.

HDAC4 Interacts with MAP1S

A yeast two-hybrid screen result reported previously suggested MAP1S might bind to HDAC4 (65). Here, the interaction between endogenous MAP1S and HDAC4 was confirmed in HeLa cells by immunoprecipitation using MAP1S-specific monoclonal antibodies (Figure 3A). Further examination of the interaction was characterized with either HA- or MAP1S-specific antibodies in 293T cells transiently overexpressing both HDAC4 and HA-fused MAP1S (HA-MAP1S) (Figure 3B, C).

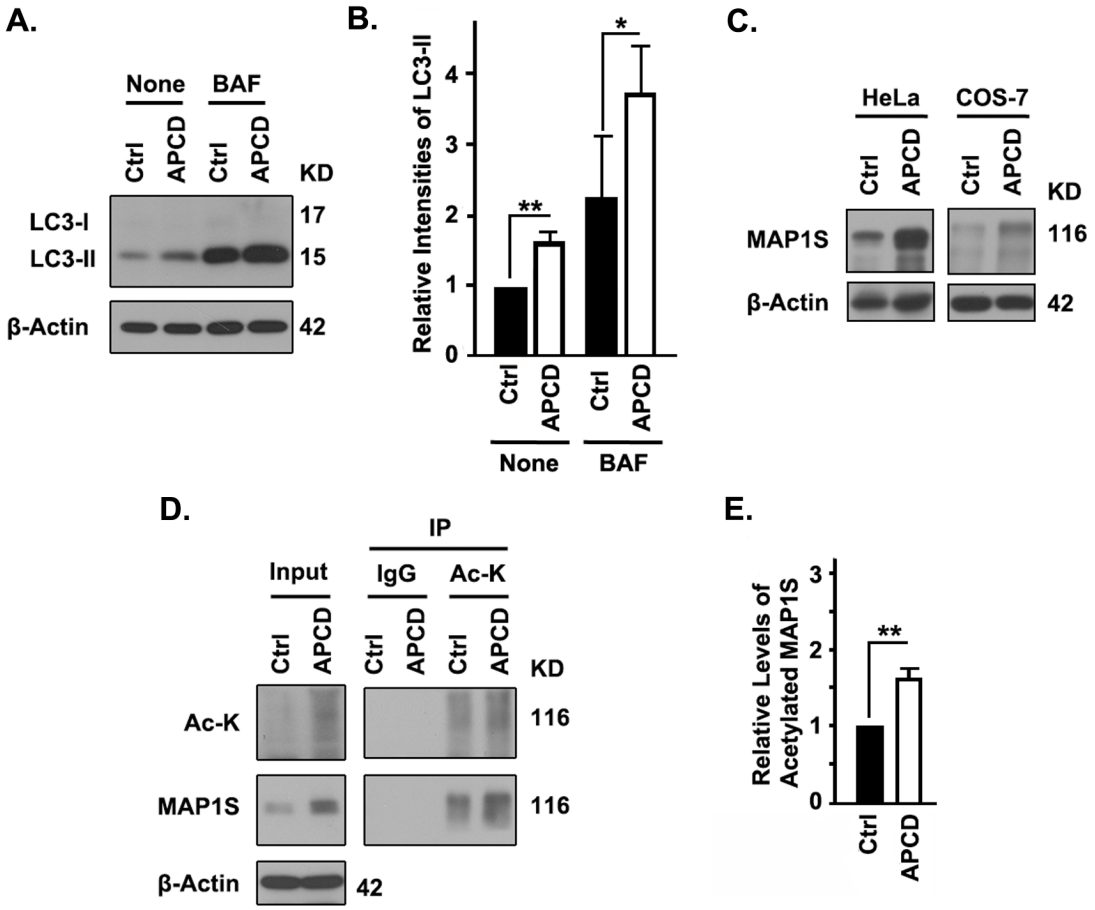

Figure 2. HDAC Inhibitor Apicidin Enhances the Acetylation of MAP1S and Promotes Autophagic Flux. (**A**, **B**) Apicidin induces autophagic flux. Representative immunoblot results (**A**) and quantification (**B**) show the impact of apicidin on levels of LC3-II in HeLa cells, in the absence (None) or presence of BAF. (**C**) Apicidin enhances levels of MAP1S protein. Representative immunoblot results show the impact of apicidin on levels of MAP1S protein in HeLa or COS-7 cells. (**D**, **E**) Apicidin enhances levels of acetylated MAP1S. Representative immunoblot results (**D**) and quantification (**E**) show the impact of apicidin on levels of acetylated MAP1S in HeLa cells.

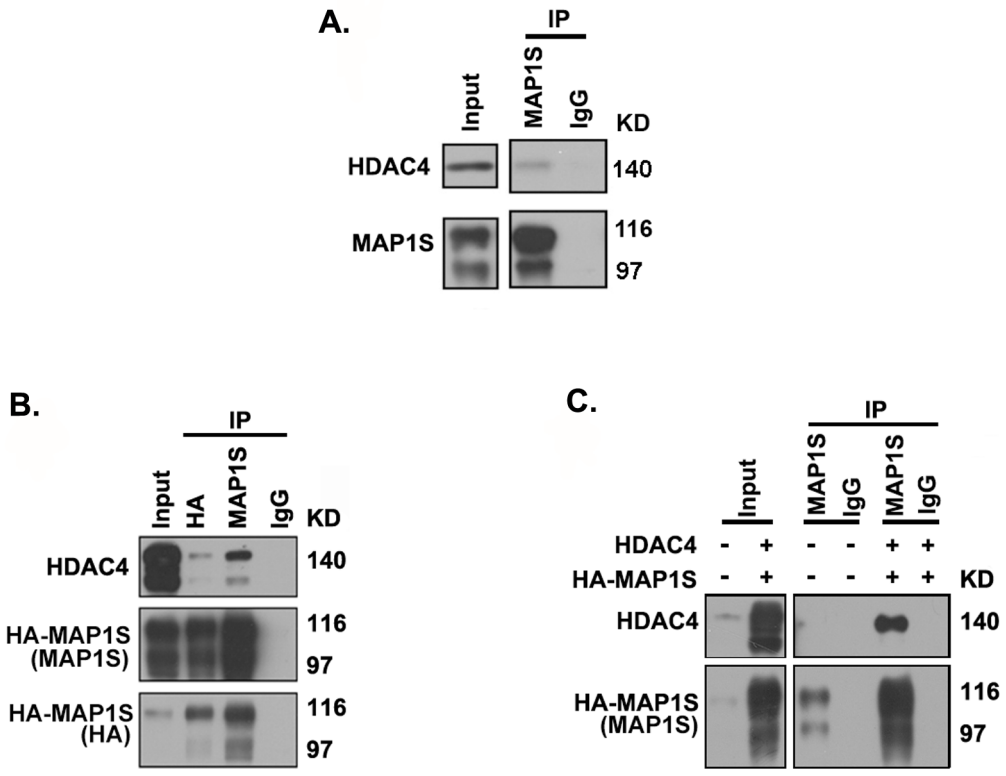

Figure 3. HDAC4 Interacts with MAP1S. (**A**) Endogenous HDAC4 interacts with MAP1S. HeLa cell lysates were precipitated with MAP1S-specific antibodies or IgG control. (**B**, **C**) Exogenous HDAC4 interacts with MAP1S in 293T cells overexpressing both HDAC4 and MAP1S. Lysates of 293T cells overexpressing both HDAC4 and HA-MAP1S were precipitated with specific antibodies against HA, MAP1S, or IgG control (**B**). Lysates of normal 293T cells and 293T cells overexpressing both HDAC4 and HA-MAP1S were precipitated with MAP1S-specific antibodies or IgG control (**C**).

HDAC4 Negatively Regulates MAP1S

To assess potential function of the interaction between HDAC4 and MAP1S, the impact of cellular levels of one on the other was analyzed by immunoblot analyses. The siRNA-mediated transient knockdown of MAP1S in HeLa cells (Figure 4A), transgenic deletion of MAP1S in MEF cells (Figure 4B) or multiple mouse tissues (Figure 4C), or overexpression of MAP1S isoforms (Figure 4D) in HeLa cells had no obvious impact on levels of HDAC4 protein. Meanwhile, levels of HDAC4 protein were altered to test if levels of MAP1S protein would be changed concomitantly. Transient transfection of 293T cells with increasing amounts of HDAC4 plasmid caused gradient decrease in levels of MAP1S protein (Figure 4E). In contrast, suppression of HDAC4 expression with siRNA caused elevation in levels of MAP1S protein in both HeLa and COS-7 cells (Figure 4F.) All the results suggest that HDAC4 negatively regulates MAP1S.

HDAC4 Destabilizes MAP1S via Deacetylation

To explore the mechanism by which HDAC4 regulates MAP1S, levels of *Map1s* mRNA were first analyzed by quantitative real-time PCR. Neither suppression of HDAC4 by transient siRNA knockdown nor enhancement of HDAC4 protein by transient overexpression in HeLa cells had any impact on levels of *Map1s* mRNA (Figure 5A), which suggested that HDAC4 might regulate MAP1S through post-translational modification rather than transcriptional regulation. Meanwhile, the half-life of MAP1S protein was measured in the presence of protein synthesis inhibitor cycloheximide (CHX) in HeLa cells transfected with control or HDAC4-specific siRNA.

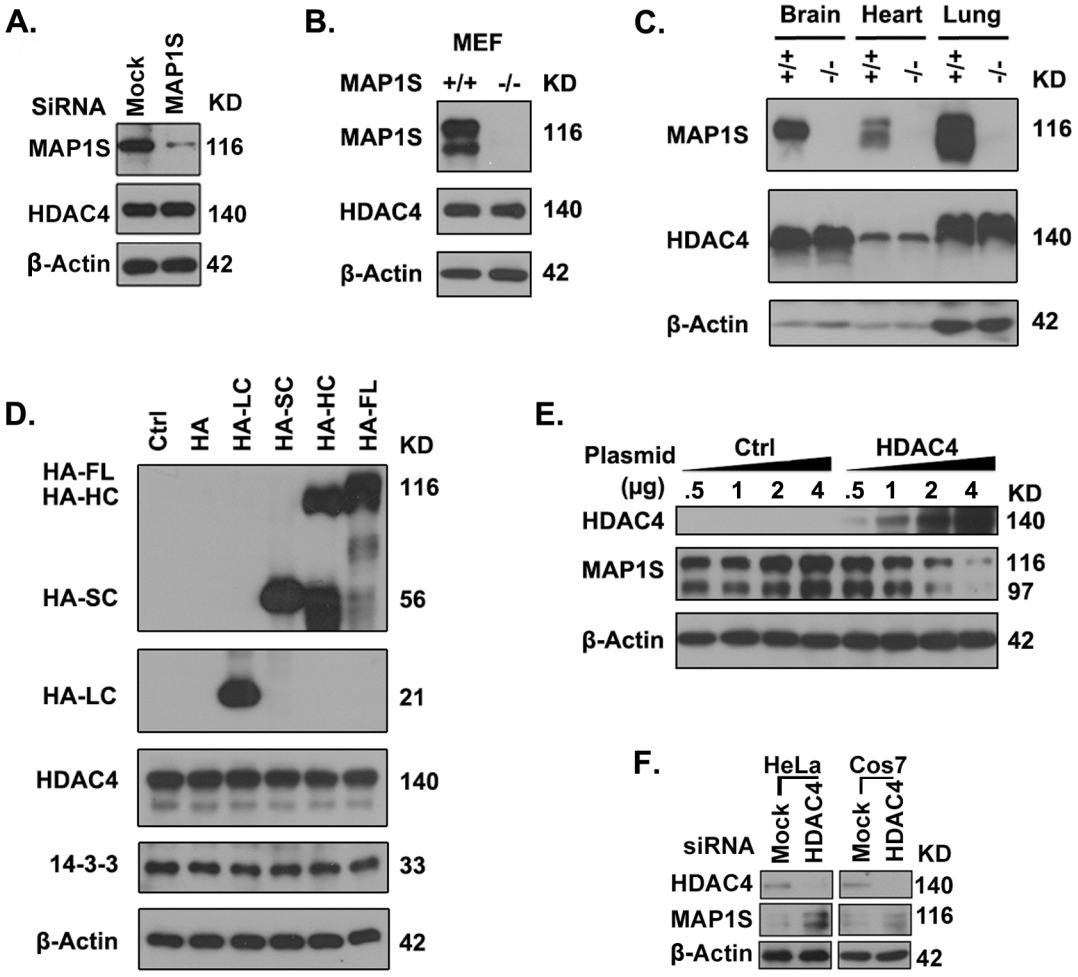

Figure 4. HDAC4 Negatively Regulates MAP1S. (**A**-**C**) MAP1S depletion has no impact on levels of HDAC4 protein in HeLa cells treated with MAP1S-specific siRNA (**A**), MEF cells (**B**) or mouse tissues (**C**) derived from wild-type or MAP1S$^{-/-}$ mice. Representative immunoblot results are shown. (**D**) Overexpression of MAP1S isoforms has no impact on levels of HDAC4 protein in HeLa cells. Representative immunoblot results are shown. (**E**) Overexpression of HDAC4 results in decreased levels of MAP1S. Representative immunoblot results show increasing expression of HDAC4 causes dose-dependent reduction in levels of MAP1S protein in 293T cells. (**F**) Suppression of HDAC4 results in increased levels of MAP1S protein. Representative immunoblot results show HDAC4 depletion with siRNA increases levels of MAP1S in HeLa or COS-7 cells.

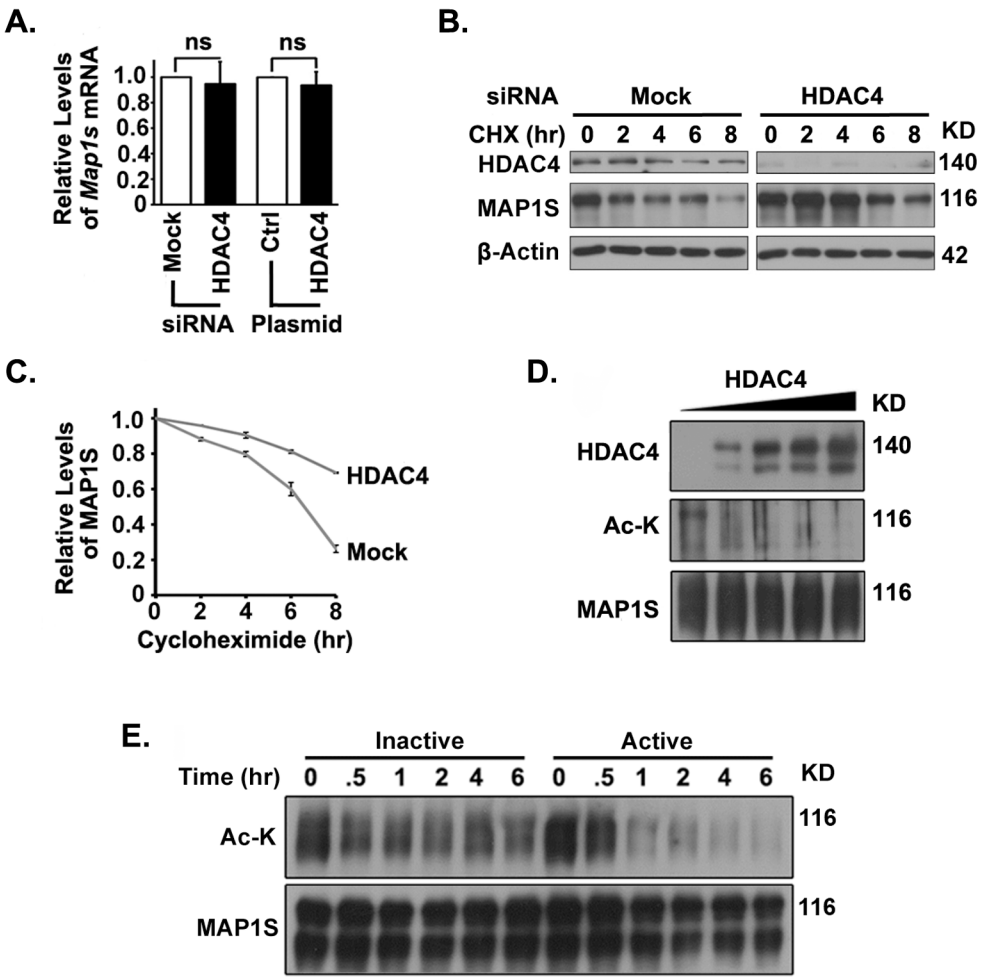

Figure 5. HDAC4 Destabilizes MAP1S via Deacetylation. (**A**) HDAC4 suppression or overexpression does not alter levels of *Map1s* mRNA. The plot shows relative levels of *Map1s* mRNA in HeLa cells transfected with siRNA to suppress the expression of HDAC4 or with plasmid to overexpress HDAC4. (**B, C**) HDAC4 depletion increases the stability of MAP1S protein. HeLa cells were treated with random (Mock) or HDAC4-specific siRNA (HDAC4), and cellular protein synthesis was then terminated with 10 μg/ml cycloheximide (CHX). Samples were collected at different times after CHX treatment. Representative immunoblot results (**B**) and quantification (**C**) are shown. (**D**, **E**) HDAC4 reduces levels of acetylated MAP1S. HDAC4 was purified from 293T cells overexpressing HDAC4 by immunoprecipitation with specific antibodies against HDAC4; purified HDAC4 (Active) was inactivated by boiling (Inactive). MAP1S purified from 293T cells overexpressing MAP1S with specific antibodies against MAP1S was incubated with increasing amounts of active HDAC4 for 2 hours (**D**) or same amount of HDAC4 for increasing amounts of incubation time (**E**). Representative immunoblot results are shown.

Results indicated that suppression of HDAC4 increased the stability of MAP1S protein (Figure 5B, C).

To demonstrate that HDAC4 activity directly could directly affect the acetylation of MAP1S, immunoprecipitates of HA-MAP1S were incubated with immuno-purified active HDAC4. Levels of acetylated MAP1S were inversely proportional to increasing levels of HDAC4 (Figure 5D) as well as the time of incubation with HDAC4 (Figure 5E). In contrast, no significant decrease in levels of acetylated MAP1S was observed when immunoprecipitates of HA-MAP1S were incubated with heat-inactivated HDAC4 (Figure 5E).

The degree of MAP1S acetylation when incubated with gain or loss of function mutants of HDAC4 (59,66) was further investigated. As expected, mutant H976Y that has a reported gain in activity relative to wild-type HDAC4 exhibited significantly higher MAP1S-deacetylation activity and lower levels of acetylated MAP1S than wild-type HDAC4. HDAC4 mutant H803A and D840N that have compromised catalytic activity each exhibited significantly lower MAP1S-deacetylation activity and higher levels of acetylated MAP1S than wild-type HDAC4. Unexpectedly, incubation of MAP1S with the H976F mutant resulted in decreased deacetylation and increased levels of acetylated MAP1S relative to wild-type HDAC4 (Figure 6A, B). The H976F mutant has been reported to be similar to wild-type HDAC4 using other substrates. These results show clearly that HDAC4 regulates MAP1S deacetylation.

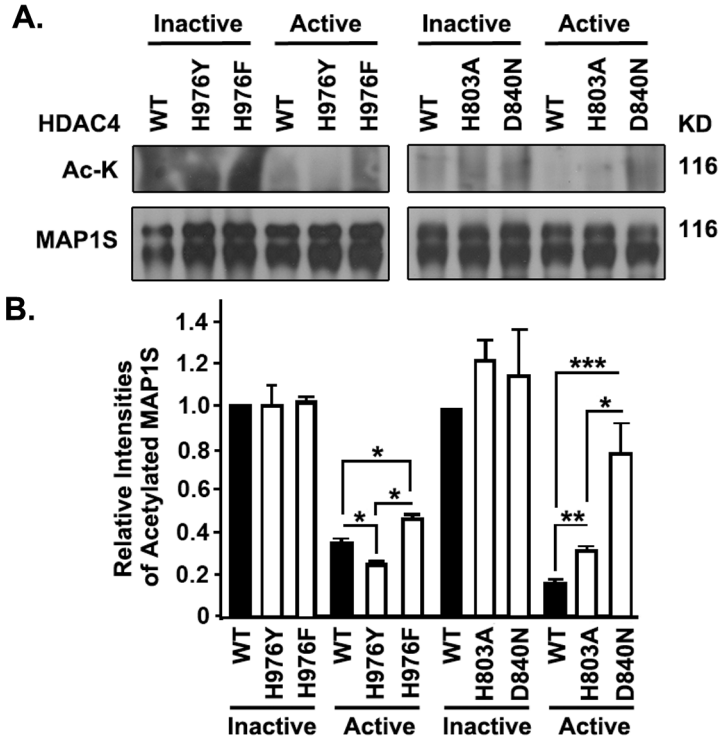

Figure 6. HDAC4-induced Deacetylation of MAP1S Depends on HDAC4 Catalytic Activity. (**A**, **B**) HDAC4 mutants with increased or reduced activity exhibit reduced or enhanced catalytic activity on deacetylating MAP1S. HDAC4 mutant proteins purified in the same method as wild-type HDAC4 were incubated with purified MAP1S for 1 hour. Representative immunoblot results (**A**) and quantification (**B**) are shown.

HDAC4 Inhibits Autophagic Flux through MAP1S

MAP1S functions as an autophagy activator, but is negatively regulated by HDAC4. To study the impact of HDAC4 on autophagy, levels of LC3 were examined when cells transfected with HDAC4 plasmid or HDAC4-specific siRNA in the presence of BAF. Impairment of autophagic flux due to HDAC4 overexpression was confirmed by reduced levels of LC3-II in HeLa cells in the presence of BAF (Figure 7A, B). Suppression of HDAC4 with siRNA (Figure 7C, D) resulted in increased levels of MAP1S, which was accompanied by increased levels of LC3-II in the presence of BAF.

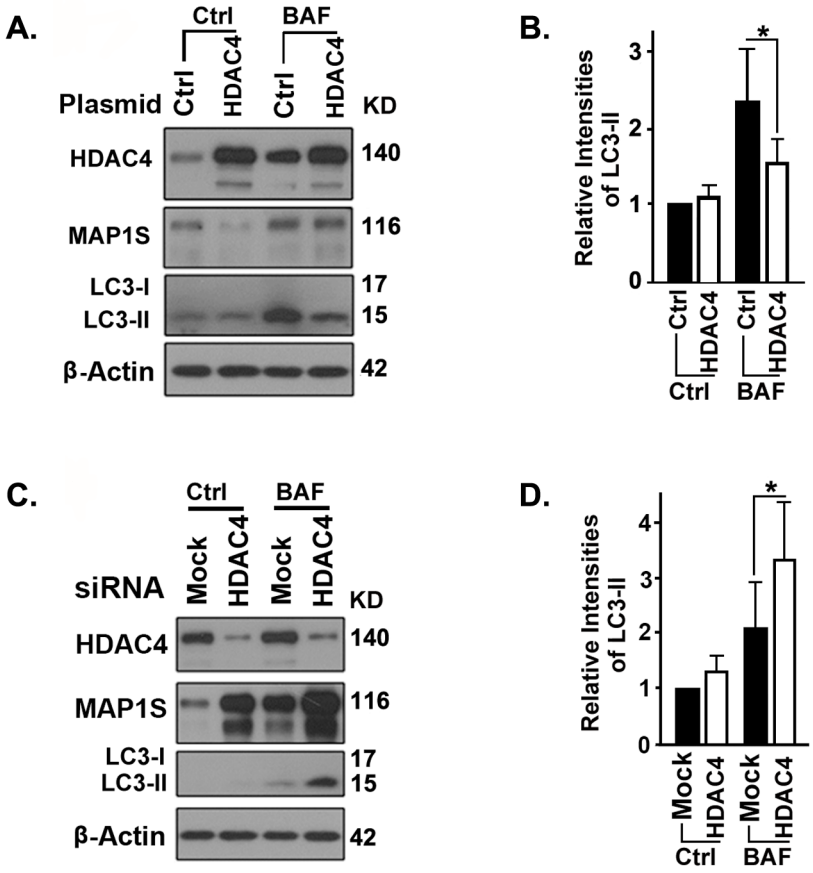

Figure 7. HDAC4 Inhibits Autophagic Flux Indicated by Immunoblot Analyses. (**A-D**) HDAC4 affects levels of MAP1S and LC3-II. Representative immunoblot results (**A**, **C**) and respective quantification (**B**, **D**) show the impact of HDAC4 overexpression (**A**, **B**) or HDAC4 suppression with siRNA (**C**, **D**) on levels of MAP1S and LC3 in HeLa cells, in the absence (Ctrl) or presence of BAF.

Autophagic flux measured at the cellular level by punctate foci of RFP-LC3 observed by fluorescence microscopy was impaired by HDAC4 overexpression (Figure 8A, B). Autophagic flux measured by autophagy vacuoles observed under the electron microscope was impaired by overexpression of HDAC4 (Figure 8C, D), or enhanced by suppression of HDAC4 (Figure 8C, E).

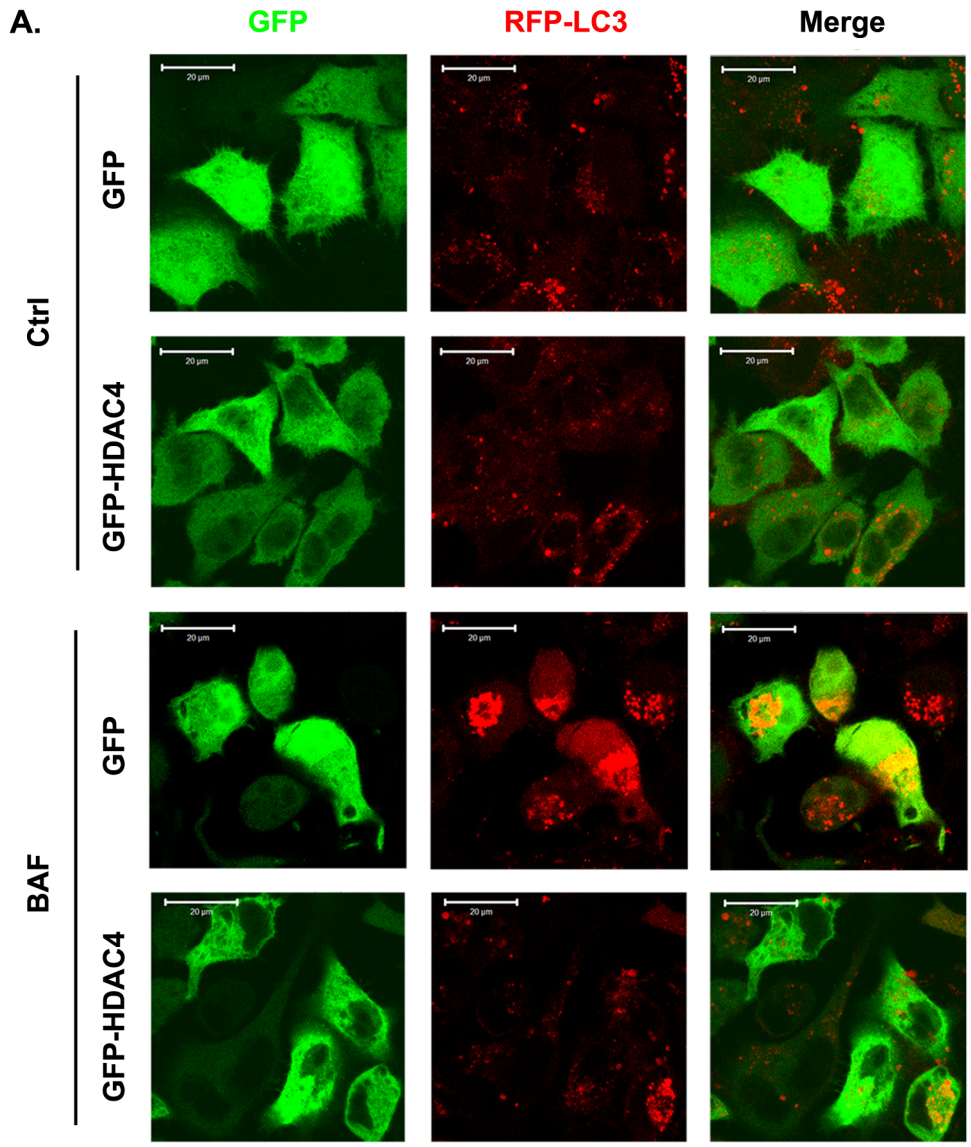

Figure 8. HDAC4 Inhibits Autophagic Flux Indicated by Fluorescence and Electron Microscopy. (**A**, **B**) HDAC4 overexpression reduces the number of punctate foci of RFP-LC3 in HeLa cells stably expressing RFP-LC3. Fluorescence microscopy images (**A**) and quantification (**B**) of punctate foci of RFP-LC3 in the absence (Ctrl) or presence of BAF are shown. (**C-E**) HDAC4 overexpression (**C**, **D**) or siRNA suppression (**C**, **E**) alters the vacuolar areas in HeLa cells. Transmission electron microscopic images (**C**) and quantification (**D**, **E**) are shown. Symbol "*****" indicates vacuoles in (**C**).

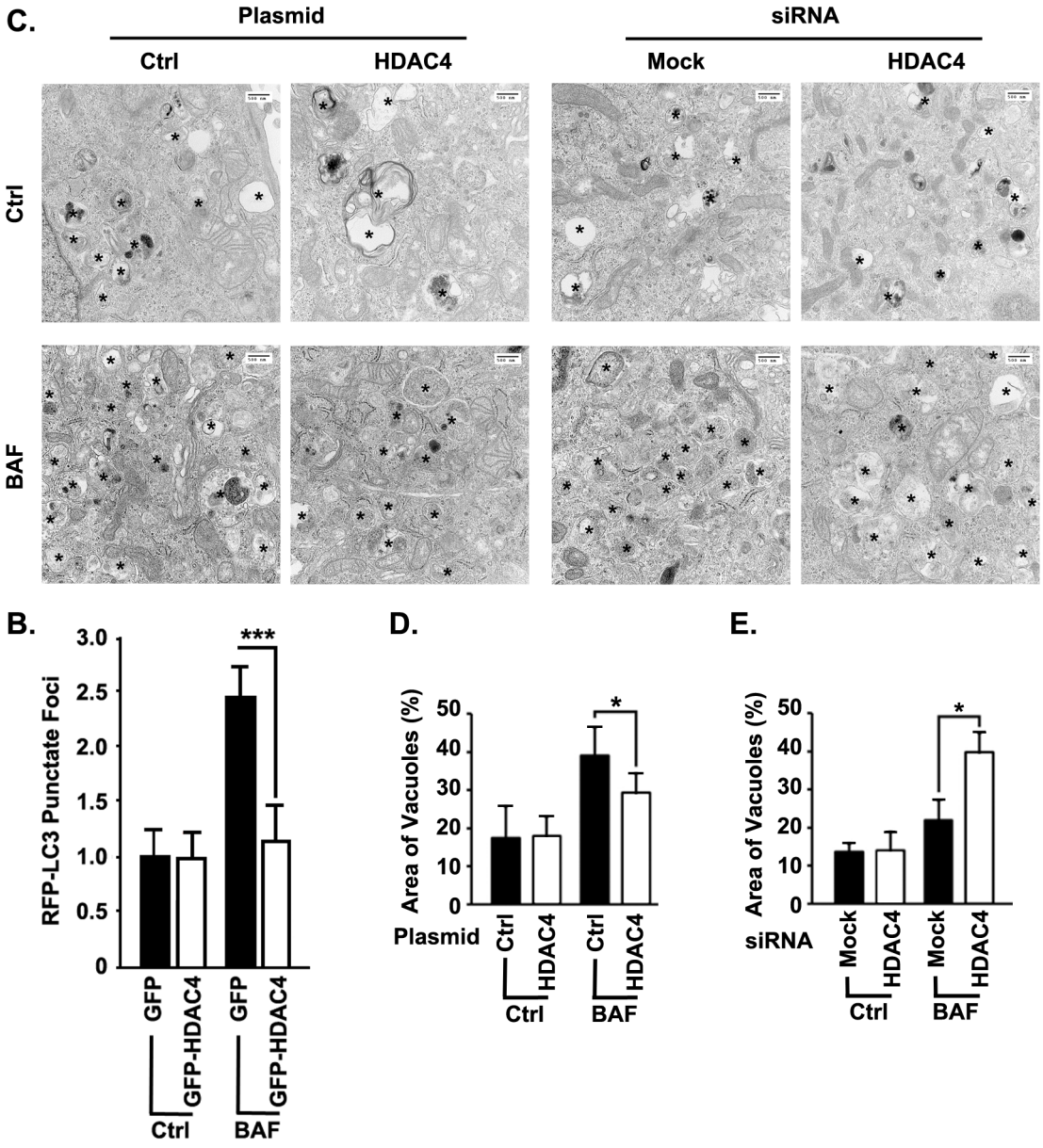

Figure 8. Continued.

To determine whether the regulation of autophagic flux by HDAC4 depends on MAP1S, MAP1S$^{-/-}$ MEF cells or MAP1S$^{-/-}$ HeLa cells were utilized. Impairment of autophagic flux by overexpression of HDAC4 (Figure 9A, B) or the activation of

autophagic flux by suppression of HDAC4 (Figure 9C, D) was only evident in wild-type cells where MAP1S was present; and the effect of alteration in levels of HDAC4 protein was abrogated in MAP1S$^{-/-}$ cells (Figure 9A-D). All the results suggest that HDAC4 inhibits autophagic flux through MAP1S.

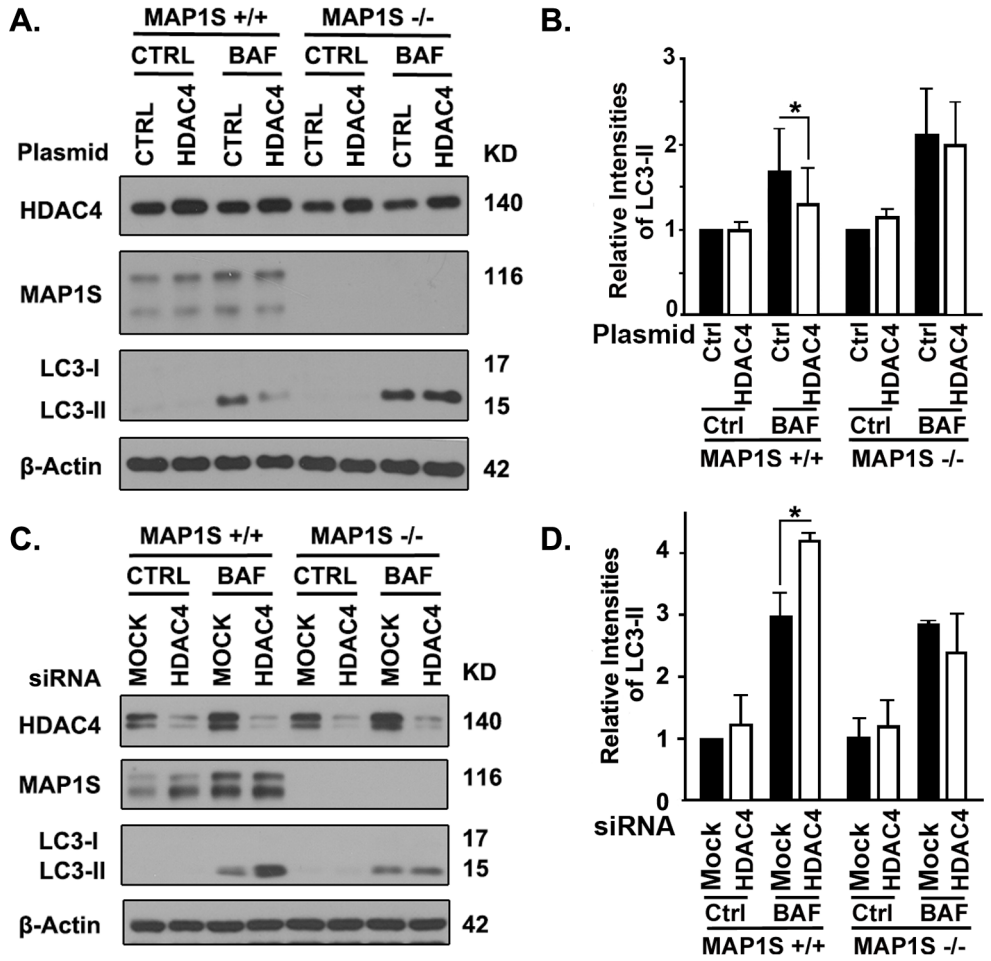

Figure 9. HDAC4 Inhibits Autophagic Flux through MAP1S. (**A-D**) MAP1S is required for HDAC4 to affect levels of LC3-II. Representative immunoblot results (**A**, **C**) and quantification (**B**, **D**) show the impact of MAP1S deletion on the effect of HDAC4 overexpression in wild-type and MAP1S$^{-/-}$ MEF cells (**A**, **B**) or HDAC4 suppression with siRNA in wild-type and MAP1S$^{-/-}$ HeLa cells (**C**, **D**) on levels of LC3-II in the absence (Ctrl) or presence of BAF.

Discussion

HDACs-mediated histone deacetylation is a key epigenetic modification that has attracted enormous attention (20,69). Deacetylation of non-histone proteins uncovers the roles of HDACs in controlling cellular function as well (70). P53 is the first reported transcription factor regulated via acetylation (71), among other acetylation-regulated transcription factors including STAT3, c-Myc, NF-κB, etc (70). Acetylation of P53 increases its protein stability and the binding affinity with DNA, resulting in increased transcriptional activity (71,72). HDAC1 interacts with and deacetylates P53, promoting the proteasomal degradation of P53 (73). In addition to transcription factors, deacetylation of α-tubulin is catalyzed by HDAC6 to increase microtubule depolymerization and cell motility (74,75). By regulating microtubule dynamics, HDAC6 is involved in the regulation of autophagy and mitophagy (76-79). Herein, we, for the first time, report that another member in ClassII HDACs, HDAC4, regulates autophagy by inducing deacetylation of autophagy activator MAP1S. Meanwhile, our study implies that HDAC5 may participate in autophagy, in addition to HDAC4 and HDAC6. LRPPRC is a binding protein of MAP1S and suppressor of autophagy initiation by enhancing levels of Bcl-2 (58). The interaction between HDAC5 and LRPPRC potentiates the ability of HDAC5 in autophagy regulation (80).

HDAC4 was originally characterized as a transcriptional regulator that associates and regulates transcription factor MEF2-mediated gene expression together with HDAC5 (59,81,82). It seems that HDAC4 regulates transcription of a specific set of genes by affecting the stability of the related transcriptional factors instead of the general

epigenetic modification of genome-associated histones (20). Though HDAC4 was suggested to directly deacetylate HIF-1α *in vitro* (61), it was reported that HDAC4 alone does not show deacetylase activity on histone substrates but regulates histone deacetylation through the formation of a functional complex by interacting with HDAC3 (83). In this study, we demonstrate that HDAC4 catalyzes the deacetylation of MAP1S; no matter HDAC4 exerts its deacetylase activity on MAP1S directly or indirectly through HDAC3 (20).

MAP1S is a microtubule-associated protein that binds with autophagy marker LC3 to facilitate autophagosomal formation and degradation. It may also regulate autophagy initiation through Bcl-2 and P27 in a Beclin 1-independent pathway (41). By accelerating autophagic flux, MAP1S reduces cellular oxidative stress and prolongs lifespans in mice (4). Besides, activation of MAP1S-mediated autophagy suppresses tumorigenesis (33) and extends survival of cancer patients (35,36). Unraveling the mechanism for enhancing levels of MAP1S protein provides insights on activation of MAP1S-mediatied autophagy. In this study, we, for the first time, report that MAP1S is regulated via acetylation and deacetylation, and identify HDAC4 as a negative regulator of MAP1S. The acetylation of MAP1S increases the stability of MAP1S protein and further promotes autophagic flux. HDAC4 interacts with MAP1S and catalyzes the deacetylation of MAP1S, leading to destabilization of MAP1S and further inhibits autophagic flux. The suppressive role of HDAC4 in autophagy is mediated by decreased levels of MAP1S protein. This study reveals a new strategy to activate MAP1S-mediated autophagy by inhibiting HDAC4. At present, the specific lysine acetylation sites of

MAP1S regulated by HDAC4 have not been determined. A mass spectrometry analysis may be conducted to identify the specific lysine acetylation sites in the future, which will contribute to understanding the molecular detail of MAP1S protein.

A variety of ATG proteins are regulated by acetylation and deacetylation process, including ATG5, ATG7, ATG8, and ATG12 (84). As reported, these autophagy components are acetylated by p300 acetyltransferase (85) or deacetylated by SIRT1 deacetylase (86). Interestingly, the acetylation of these ATG proteins plays a negative role in autophagy, which is opposite to the positive role of acetylation in MAP1S and MAP1S-mediated autophagy. Thus, our study opens a new field of discovery on the roles of acetylation and deacetylation in other autophagy-relevant proteins.

CHAPTER III

ACETYLATED MAP1S ACCELERATES AUTOPHAGIC CLEARANCE OF MUTANT HUNTINGTIN AGGREGATES*

Introduction

Huntington's disease (HD) is a fatal progressive neurodegenerative disorder caused by the accumulation of mutant Huntingtin proteins (mHTT) in neurons. Wild-type Huntingtin (HTT) has 6-35 ploy glutamine (polyQ) expansion in the N-terminus of HTT protein, while mHTT has more than 36 polyQ expansion, which leads to mHTT prone to form insoluble aggregates by both hydrogen and covalent bonds. These aggregates are toxic to neurons and further lead to neuronal degeneration. As there is no effective treatment for HD at present, HD patients suffer from progressive loss of cognition and motor function, and ultimately death within 10-20 years after first appearance of the symptom for diagnosis (23).

Autophagy is a cellular self-digestion process that begins with the formation of isolation membranes that recognize and engulf substrates, including aggregated proteins, to form autophagosomes. These autophagosomes migrate along acetylated microtubules and fuse with lysosomes to generate autolysosomes in which autophagosomal cargos are

---

*Part of this chapter is reprinted with permission from "Blocking the Association of HDAC4 with MAP1S Accelerates Autophagy Clearance of Mutant Huntingtin" by Yue, F., Li, W., Zou, J., Chen, Q., Xu, G., Huang, H., Xu, Z., Zhang, S., Gallinari, P., Wang, F., McKeehan, W. L., and Liu, L, 2015, *Aging* **7**, 839-853, Copyright [2015] by Fei Yue.

degraded (6,20,87). Autophagy deficiency causes accumulation of toxic mHTT aggregates in neurons and further results in neuronal death (88). Therefore, enhancement of autophagy activity to accelerate the turnover of mHTT aggregates is one of the directions to develop therapeutics for HD.

As a novel microtubule-associated autophagy activator, microtubule-associated protein 1 small form (MAP1S) can enhance autophagy initiation and accelerate autophagy degradation. Based on previous reports, MAP1S is suggested to be involved in neurodegenerative disorders, such as Alzheimer's disease, Parkinson's disease, and Huntington's disease. N-methyl-D-aspartate receptor (NMDAR) facilitates endocytic removal and replacement of surface receptor at synapses, which is essential in mediating learning and memory (89,90). MAP1S can interact with NR3A, one of the subunits of NMDAR, and have a potential role in the degradation of NMDAR and development of dementia which is a major symptom of Alzheimer's disease (91). In addition, MAP1S can bind with leucine-rich pentatricopeptide repeat containing (LRPPRC) (37) that also interacts with mitophagy initiator Parkin and protects mitochondria from autophagy degradation (58,92), suggesting MAP1S may participate in the regulation of molecular pathogenesis of Parkinson's disease. Histone deacetylases 4 (HDAC4) has been identified as a potential target to ameliorate Huntington's disease. Studies showed that HDAC4 interacts with mHTT and co-localizes in the cytoplasmic inclusion bodies (93). As discussed in chapter II, HDAC4 interacts with MAP1S and decreases the stability of MAP1S protein via deacetylation (20), which suggests MAP1S may regulate mHTT degradation through autophagy.

In the mouse models of Huntington's disease, HDAC4 reduction alleviates cytoplasmic formation of mHTT aggregates and rescues neuronal and cortico-striatal synaptic function, but does not repair the global transcriptional dysfunction (93). However, the mechanism by which HDAC4 reduction delays cytoplasmic formation of mHTT aggregates is unknown (20). HDAC4 suppresses autophagy by negatively regulating autophagy activator MAP1S, which prompts us to study whether HDAC4 regulates autophagy to affect mHTT aggregation through MAP1S. Elevating levels of MAP1S protein by either inhibition of HDAC4 or interruption of the interaction between HDAC4 and MAP1S may promote autophagic clearance of mHTT and ameliorate Huntington's disease.

Herein, we first confirm that HDAC4 associates with mHTT aggregates in the cytoplasm. HDAC4 leads to accumulation of mHTT aggregates by down-regulating MAP1S and inhibiting MAP1S-mediated autophagic turnover of mHTT aggregates. In addition, we identify an HDAC4-binding domain (HBD) within the overlapping region between the heavy chain (HC) and short chain (SC) of MAP1S, which is responsible for the interaction between HDAC4 and MAP1S. Overexpression of HBD interrupts the association of MAP1S with HDAC4 and leads to increased levels of MAP1S protein. Inhibition of HDAC4 or overexpression of HBD promotes stabilization of MAP1S and restores MAP1S-regulated autophagic flux and degradation of mHTT aggregates, suggesting a novel approach to treat Huntington's disease (20).

Materials and Methods

Cell Culture

Most cell lines, including HeLa, HEK-293T, HeLa cells stably expressing inducible GFP-HTT72Q (HeLa-GFP-HTT72Q), and MEF cells were cultured in the DMEM culture media containing 10% FBS and antibiotics. Neuro-2α (N2α) cells were grown in Eagle's Minimum Essential Medium (EMEM) (ATCC, #30-2003) with 10% FBS and antibiotics. PBS and 0.25% trypsin were used for subculture.

Cell Transfection

Cell lines used for transfection included HeLa, HEK-293T, HeLa-GFP-HTT72Q cells, MEF cells, or N2α cells. For transient knockdown experiments, cells were cultured at 30% confluence on the cell culture plates or coverslips and transfected with negative control siRNA or specific siRNA by Oligofectamine according to the manufacturer's recommended instruction. For transient overexpression experiments in HeLa, HeLa-GFP-HTT72Q cells, MEF cells, or N2α cells, cells were cultured at 70% confluence on the cell culture plates or coverslips and transfected with control vector or plasmids encoding specific genes by Lipofectamine 2000 according to the manufacturer's recommended instruction. For transient overexpression in HEK-293T cells, cells were cultured at 60% confluence on the cell culture plates and transfected with control vector or plasmids encoding specific genes by using calcium phosphate transfection kit according to the manufacturer's recommended instruction.

Establishment of Stable Cell Line Expressing Inducible GFP-HTT72Q

Lenti-XTM Tet-Off Advanced Inducible Expression System (Clontech, #632163) was used according to the manufacturer's recommended instruction to generate the inducible GFP-HTT72Q stable cell lines. Briefly, an EGFP-tagged Huntingtin fragment encoded by human *huntingtin* exon 1 plus 72Q repeats was amplified from the pUAST-Httex1-Q72-eGFP construct as previously described (94) and subcloned into the pLVX-Tight-Puro vector. Lenti-viruses containing Httex1-Q72 plasmid (pLVX-tight-Q72) and the regulator plasmids (pLVX-Tet-OFF advanced) were produced using the Lenti-X HTX packaging system (Clontech, #PT5135-2) and used to infect HeLa cells as instructed. A combination of 2 μg/ml puromycin and 200 μg/ml neomycin was applied to screen for positive clones that were maintained in the "off" state in the presence of 100 ng/ml doxycycline during the whole selection process to turn off the expression of potentially toxic HTT72Q proteins.

Fluorescence Microscopy

HeLa-GFP-HTT72Q cells transfected with the control vector or plasmid expressing Flag-HDAC4 were treated with 10 nM BAF for 12 hours before fixation. Cells were fixed with 4% (w/v) paraformaldehyde in PBS at room temperature for 30 minutes and then permeabilized with 0.1% Triton X-100 (Sigma, #T9284) in PBS for 20 minutes. Cells were blocked with 1% Bovine Serum Albumin (BSA) (EMD Millipore, #2960) in PBS for 20 minutes, and then incubated with primary antibodies against HDAC4 (Santa Cruz, #11418, dilution 1:50) or LAMP2 (Santa Cruz, #18822, dilution

1:50) for 1 hour at room temperature, and the corresponding rhodamine-conjugated secondary antibodies (Invitrogen, #R-6394, #R-6393, dilution 1:400) for 1 hour at room temperature for fluorescence microscopy analyses. Primary and secondary antibodies were diluted in PBS with 1% BSA. Images were captured with a Zeiss LSM 510 Meta Confocal Microscope. The ImageJ software was used to calculate the intensities of GFP-HTT72Q and analyze the lysosome-associated GFP-HTT72Q aggregates on each image.

Plasmids and Site-directed Mutagenesis

HA-MAP1S isoforms (HA-LC, HA-SC, HA-HC and HA-FL) have been described earlier (38). Plasmid encoding GFP-HTT74Q (Addgene, #40262) was purchased from Addgene. HA-MAP1S R653-Q855 fragment, representing the HDAC4-binding domain (HBD) of MAP1S, was PCR-amplified with forward primer 5'-ACGCG TCGACACGGCTGTCGCTGAGCCCACT-3' and reverse primer 5'-GAAGATCTCT ATTGCCGTGCTGTCTTGGG-3'. The fragment was inserted into HA-PCMV plasmid (Clontech, #631604) via digestion-ligation reaction to construct plasmid encoding HA-HBD. Sequence verification was then performed by GENEWIZ. To delete the HBD fragment from the full length MAP1S to generate a deletion construct HA-HBDΔ, a pair of primers (5'-CTCGCTGCCCTCTGCGGGGCT-3' and 5'-ACGGAGAACGTCAGC CGCACC-3') were phosphorylated with T4 polynucleotide kinase and mixed with HA-MAP1S plasmid template to amplify the HA-HBDΔ by PCR using the KOD hot start DNA polymerase from TOYOBO. The restriction enzyme DpnI was added to the PCR reaction mixture to digest the template. T4 DNA Ligase (New England Biolabs, #M0202)

was used to ligate the PCR product to become a circular plasmid which was then verified by DNA sequencing.

Immunoblot Analyses

Cells were lysed in the cell lysis buffer with 1mM PMSF on ice for 30 minutes. The total protein concentration of the cell lysates was determined by using BCA protein assay kit. The cell lysates were then mixed with SDS loading buffer and boiled for 10 minutes. To analyze levels of aggregated GFP-HTT72Q/74Q, cells were lysed in isolation buffer (50 mM Tris-HCl, pH 8.0, 100 mM NaCl, 5 mM MgCl2, 0.5% NP-40, and protease inhibitor cocktails). Insoluble pellets were isolated after 10 minutes centrifugation at 14,000 rpm at 4 °C and resuspended in buffer containing 20 mM Tris-HCl, pH 8.0, 15 mM MgCl2 and 0.5 mg/ml DNase, and then incubated at 37 °C for 1 hour. Insoluble fractions were diluted in SDS loading buffer and boiled for 5 minutes. Cell lysates were loaded on SDS-polyacrylamide gels containing 8, 10, 12 or 15% (w/v) acrylamide. Proteins were separated by electrophoresis, transferred on to PVDF membranes. The membranes were then blocked with 5% (w/v) non-fat milk in TBST for 1 hour at room temperature, bound with primary antibodies overnight at 4 °C and incubated with HRP-conjugated secondary antibodies for 2 hours at room temperature. Proteins were detected by ECL Prime Western Blotting Detection Reagents. The exposed X-ray films were processed using developer and fixer, and scanned into image files. The relative intensity of a band to internal control was measured using ImageJ

software. Antibody against GFP (Santa Cruz, #8334, dilution 1:2000) was applied to detect GFP-HTT72Q/74Q.

Agarose Gel Electrophoresis for Resolving Aggregates

Agarose gel electrophoresis for resolving aggregates (AGERA) was performed following a described protocol (95). Cell lysates containing 100 μg of total protein were loaded to a 1.5% agarose gel containing 0.1% SDS for AGERA. The agarose gel was run at 100 V and semi-dry transfer was conducted at 200 mA for 1 hour. After transfer, the PVDF membrane was further processed for immunoblot analyses.

Co-immunoprecipitation

Cell lysates were prepared by using NP-40 buffer with 1 mM PMSF and protease inhibitor cocktails. The supernatants were collected after centrifugation at 14,000 rpm for 15 minutes at 4 °C. Same amount of lysates with 1.5 mg of total protein were subjected to immunoprecipitation with 2 μg antibodies against MAP1S, HDAC4, HA, or the respective IgG control, and incubated with 30 μl Protein G-Sepharose beads. After overnight rotation at 4 °C, beads that bind with antibodies and the bound proteins were precipitated and washed extensively with the NP-40 buffer four times. The final precipitates were resuspended in 100 μl lysis buffer containing SDS loading buffer and boiled for 10 minutes for further immunoblot analyses.

Protein Half-life Measurement

HEK-293T cells were seeded in 10cm culture dishes and transfected with plasmids encoding HA, HA-HBD, or HA-HBDΔ by using calcium phosphate transfection kit according to the manufacturer's recommended instruction. After transfection for 24 hours, cells overexpressing HA, HA-HBD, or HA-HBDΔ were processed for subculture respectively. Cell pellets harvested after centrifugation at 600 rpm for 5 minutes were resuspended and split evenly into 35 mm culture dishes. Then, the protein synthesis inhibitor 10 μg/ml CHX was added into the culture media once cells were attached on the dishes. Cell lysates were harvested at the indicated time points for further immunoblot analyses.

Statistical Analyses

Statistical significance was determined by Student's t-test, with significance set to *, $p \leq 0.05$; **, $P \leq 0.01$; and ***, $P \leq 0.001$. Error bars indicate standard deviation.

Results

Overexpression of HDAC4 Induces Mutant Huntingtin Aggregation

GFP-HTT72Q, a GFP-tagged mHTT variant, includes a polypeptide encoded by exon 1 of the *huntingtin* gene plus 72 expanded polyQ repeats in the N-terminus (96,97). The acetylation of Huntingtin at K444 residue promotes autophagic degradation of Huntingtin itself (98). The K444 residue is out of the sequence covered by HTT72Q so that HTT72Q degradation is not affected by the acetylation of K444. To study the impact of HDAC4 on mHTT aggregation, HeLa cells stably expressing inducible GFP-HTT72Q were established first (20). Overexpression of HDAC4 in cells expressing GFP-HTT72Q

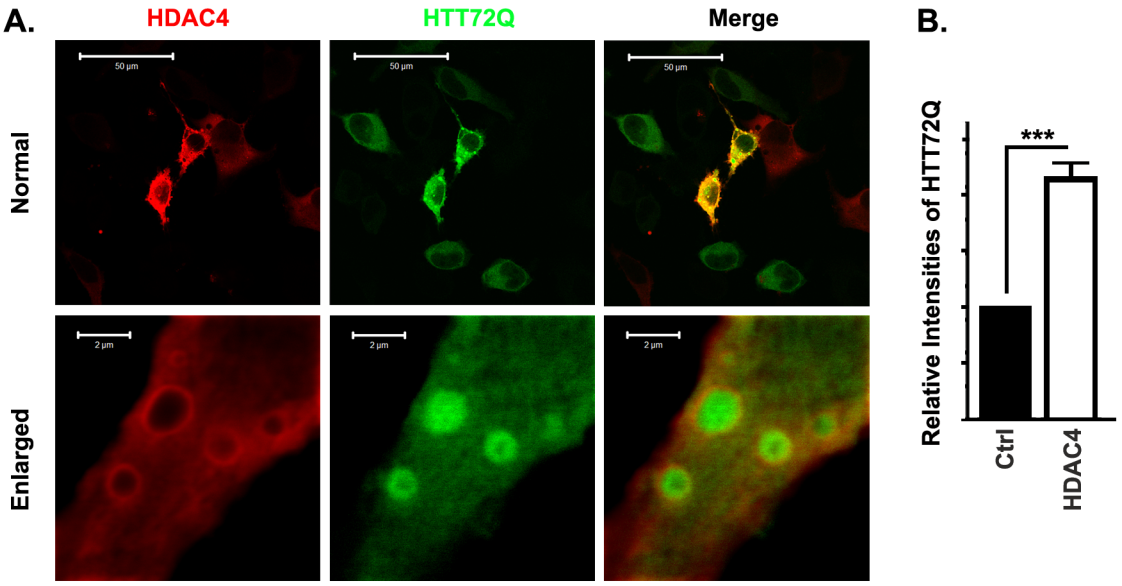

Figure 10. HDAC4 Induces Mutant Huntingtin Aggregation Indicated by Fluorescence Microscopy. (**A**, **B**) Overexpression of HDAC4 increases levels of GFP-HTT72Q (HTT72Q) in HeLa cells stably expressing HTT72Q. Representative fluorescent images (**A**) and the respective quantification (**B**) are shown. Bars in (**A**) were 50 μm in the normal view on the top or 2 μm in the enlarged view on the bottom.

led to enhancement of GFP-HTT72Q fluorescence (Figure 10A, B) and increased levels of GFP-HTT72Q aggregates detected by immunoblot analyses using anti-GFP antibodies (Figure 11A, B). As shown in the fluorescent images, increased levels of HDAC4 were distributed surrounding the HTT72Q aggregates (Figure 10A). In contrast, suppression of HDAC4 with HDAC4-specific siRNA led to reduction in levels of mHTT aggregates (Figure 11C, D). Furthermore, analyses with agarose gel electrophoresis for resolving aggregates (AGERA) (Figure 11F) were utilized to measure levels of mHTT aggregates, and revealed the same results as in the normal immunoblot analyses of aggregates in the stacking gel (Figure 11E). Accumulation of another mHTT variant, GFP-HTT74Q, with a similar role as GFP-HTT72Q in HD, was observed when GFP-HTT74Q and HDAC4 were transiently co-overexpressed in neuroblastoma Neuro-2α (N2α) cells (Figure 11E-G). Thus, overexpression of HDAC4 significantly increases the severity of mHTT aggregation.

Consistent with a previous report (24), GFP-HTT72Q was degraded in lysosomes. Inhibition of lysosomal activity with BAF led to accumulation of mHTT aggregates together with the autophagy marker LC3-II (Figure 12A). The percentage of GFP-HTT72Q aggregates that overlapped with lysosome-associated membrane protein 2 (LAMP2)-labeled lysosomes was significantly increased in the presence of BAF (Figure 12B, C). This suggests that small aggregates are efficiently degraded through lysosomes in the absence of BAF, but large aggregates accumulate due to compromised lysosomal degradation.

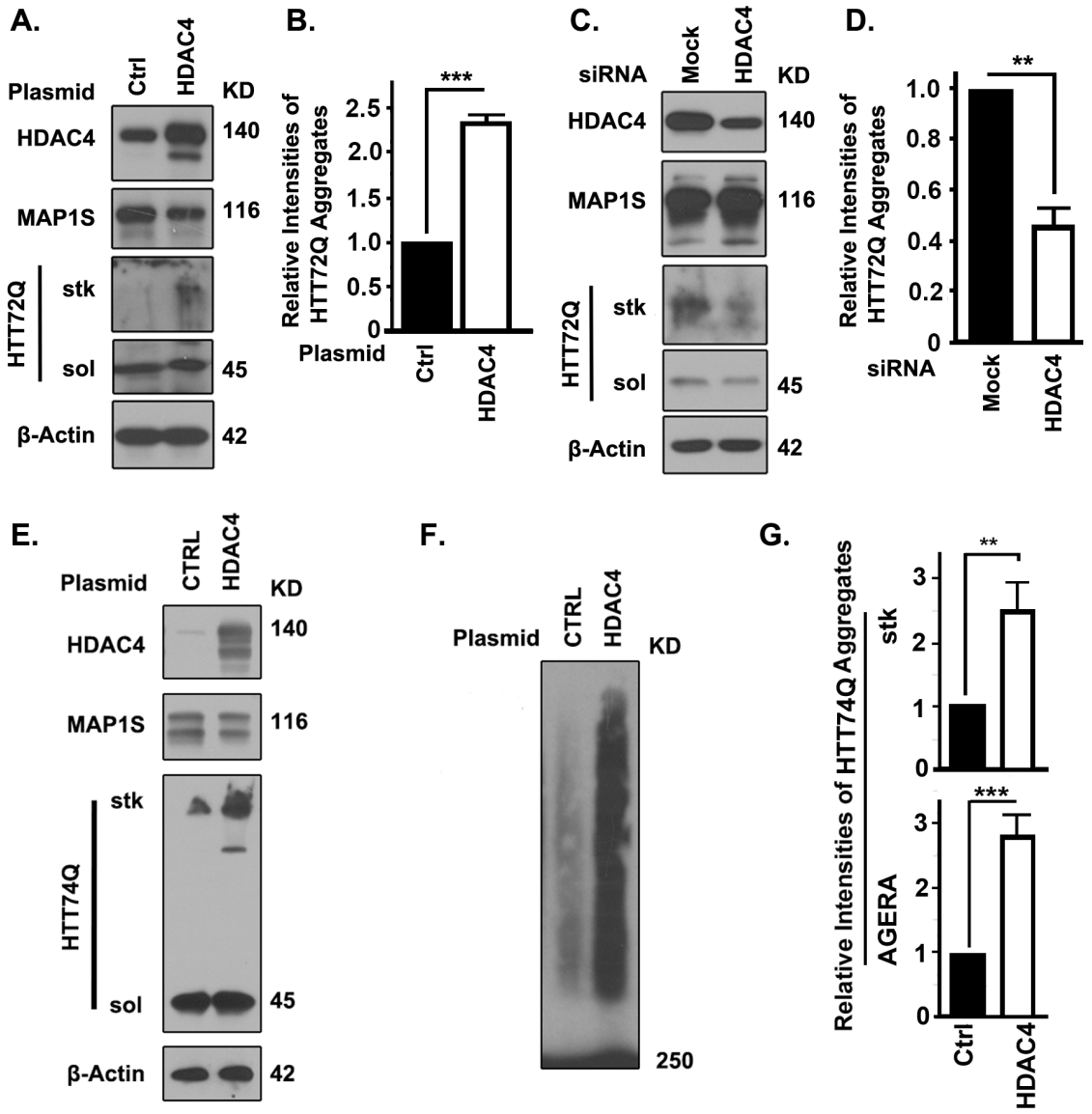

Figure 11. HDAC4 Induces Mutant Huntingtin Aggregation Indicated by Immunoblot Analyses. (**A**, **B**) Overexpression of HDAC4 increases levels of GFP-HTT72Q (HTT72Q) in HeLa cells stably expressing HTT72Q. Representative immunoblot results (**A**), and the respective quantification (**B**) are shown. HTT72Q aggregates retained in stacking gel (stk) and soluble HTT72Q (sol) were labeled. The 45 KD HTT72Q formed aggregates that failed to penetrate into stacking gel. (**C**, **D**) Suppression of HDAC4 decreases levels of HTT72Q aggregates in HeLa cells stably expressing HTT72Q. Representative immunoblot results (**C**) and quantification (**D**) show the impact of HDAC4 suppression with siRNA on levels of HTT72Q aggregates. (**E**-**G**) Overexpression of HDAC4 increases levels of GFP-HTT74Q (HTT74Q) in N2α cells transiently expressing HTT74Q. Representative results from immunoblot analyses of aggregates in stacking gel (**E**) or AGERA (**F**), and the respective quantification (**G**) are shown.

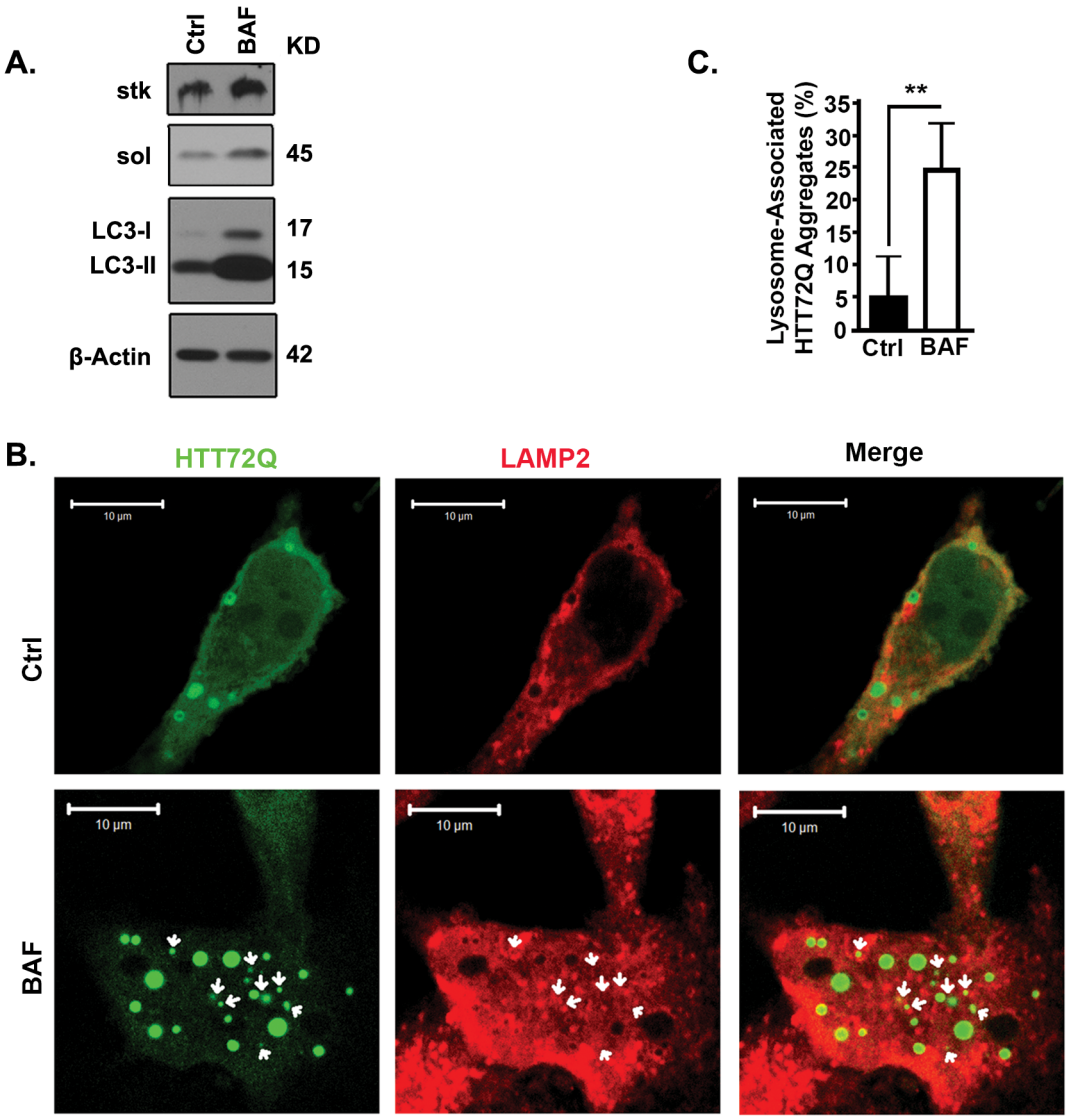

Figure 12. Mutant Huntingtin Is Degraded in Lysosomes. (**A**) Lysosome inhibitor BAF causes accumulation of both HTT72Q and LC3-II in the cells expressing HTT72Q. (**B**, **C**) HTT72Q aggregates co-localize with LAMP2-labelled lysosomes (red) in cells stably expressing HTT72Q and transiently expressing Flag-HDAC4 in the absence (Ctrl) or presence of BAF. Representative fluorescent images (**B**) are shown and white arrows indicate HTT72Q aggregates that co-localize with LAMP2. The plot (**C**) shows the percentage of HTT72Q aggregates associated with LAMP2-labelled lysosomes to total aggregates in Ctrl or BAF-treated cells.

HDAC4 Inhibits MAP1S-mediated Autophagic Clearance of Mutant Huntingtin Aggregates

As discussed in chapter II, HDAC4 suppresses autophagy through MAP1S. HDAC4 binds to and deacetylates MAP1S, which leads to MAP1S destabilization and further inhibits MAP1S-mediated autophagy. To study the role of HDAC4 in regulating autophagic turnover of mHTT aggregates, the interaction between HDAC4 and MAP1S was further examined in N2α cells (Figure 13A) and brain tissue lysates from wild-type or MAP1S$^{-/-}$ mice (Figure 13B). In addition, suppression of MAP1S with specific siRNA in the HeLa cells stably expressing GFP-HTT72Q led to inhibition of autophagic flux (Figure 13C, D). Consequently, autophagy defects induced by silencing MAP1S caused accumulation of GFP-HTT72Q aggregates (Figure 13E, F). Accumulation of GFP-HTT74Q was also observed in MAP1S$^{-/-}$ MEF cells transiently overexpressing GFP-HTT74Q. The MAP1S-deficiency-triggered accumulation of HTT74Q aggregates was confirmed when the same cell lysates were analyzed by AGERA (Figure 13G-I). Enhancement of mHTT aggregation by overexpression of HDAC4 was only observed in wild-type but not MAP1S$^{-/-}$ MEF cells (Figure 13J, K). These results indicate that HDAC4-mediated suppression of autophagic degradation of mHTT aggregates is MAP1S-dependent.

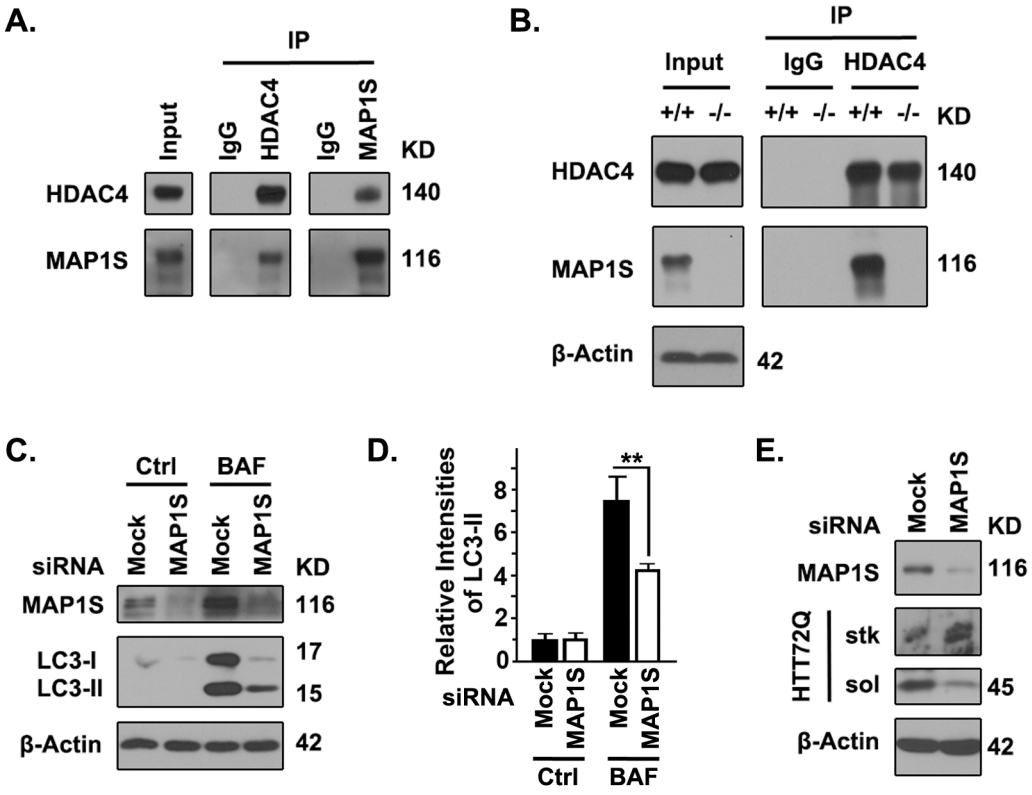

Figure 13. HDAC4 Inhibits MAP1S-mediated Autophagic Clearance of Mutant Huntingtin Aggregates. (**A**, **B**) Endogenous HDAC4 interacts with MAP1S. Lysates of N2α cells (**A**) or brain tissues of wild-type ($^{+/+}$) and MAP1S$^{-/-}$ mice (**B**) were precipitated with specific antibodies against HDAC4 or MAP1S, or IgG control. (**C**, **D**) MAP1S suppression with siRNA reduces levels of LC3-II in cells stably expressing HTT72Q in the absence (Ctrl) or presence of BAF. Representative immunoblot analyses (**C**) and quantification (**D**) are shown. (**E**, **F**) Suppression of MAP1S with siRNA increases levels of HTT72Q aggregates in cells stably expressing HTT72Q. Representative immunoblot results (**E**) and quantification (**F**) are shown. (**G-I**) Depletion of MAP1S increases levels of HTT74Q aggregates in wild-type and MAP1S$^{-/-}$ MEF cells transiently expressing HTT74Q. Representative immunoblot results (**G**, **H**) and quantification (**I**) of levels of HTT74Q aggregates in wild-type and MAP1S$^{-/-}$ MEF cells analyzed by stacking gel electrophoresis (**G**) or AGERE (**H**) are shown. (**J**, **K**) MAP1S is required for the HDAC4-dependent increase in levels of HTT74Q aggregates. Representative immunoblot results (**J**) and quantification (**K**) of the differences between wild-type and MAP1S$^{-/-}$ MEF cells are shown.

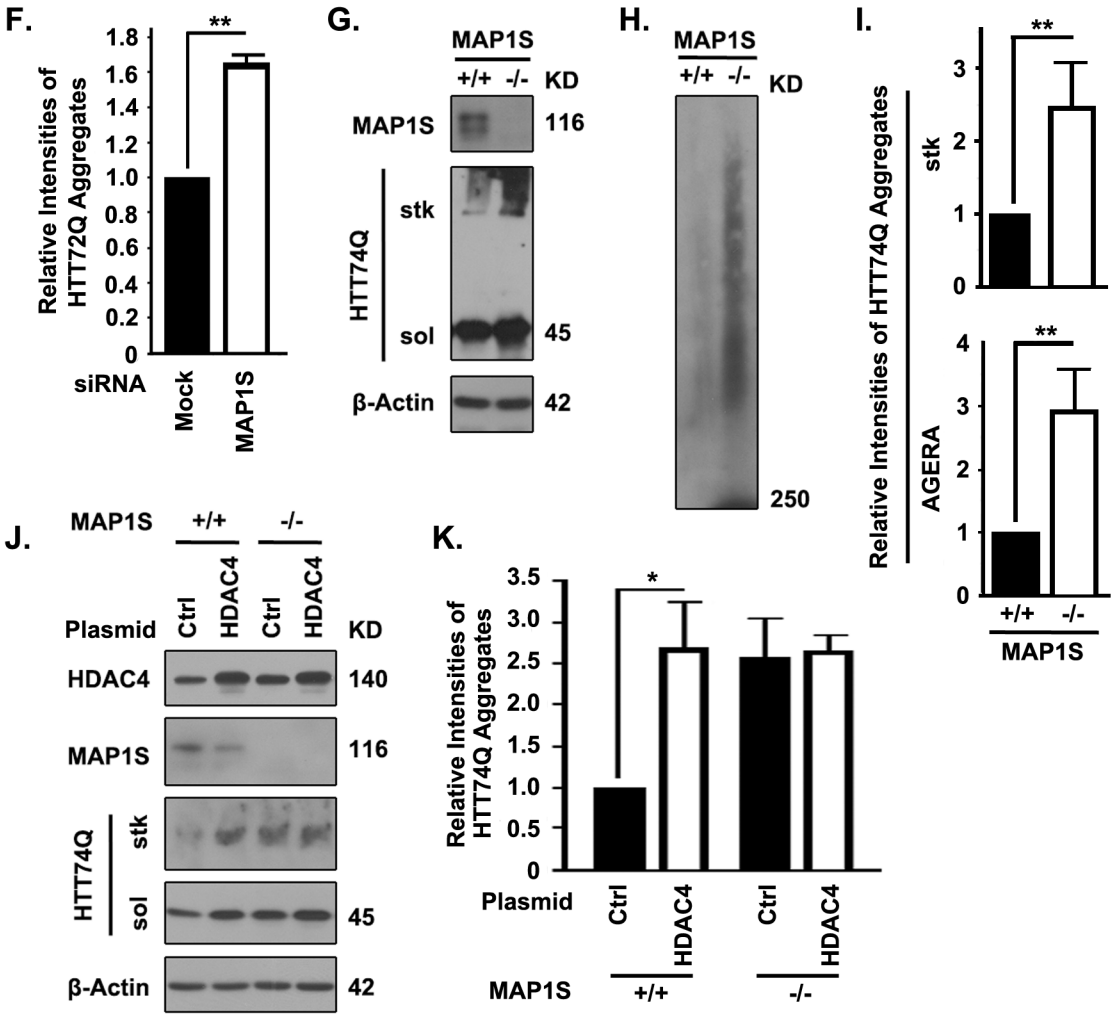

Figure 13. Continued.

HDAC4 Interacts with MAP1S via an HDAC4-binding Domain (HBD)

Full length MAP1S (FL) is processed by post-translational modification to multiple isoforms that include heavy chain (HC), short chain (SC) and light chain (LC) (Figure 14A) (38,41,54). Association of HDAC4 with MAP1S HC and SC products in addition to FL was apparent (Figure 14B), which suggested that a domain localized between R653 and Q855 (Figure 14A), the overlapping region between the HC and SC,

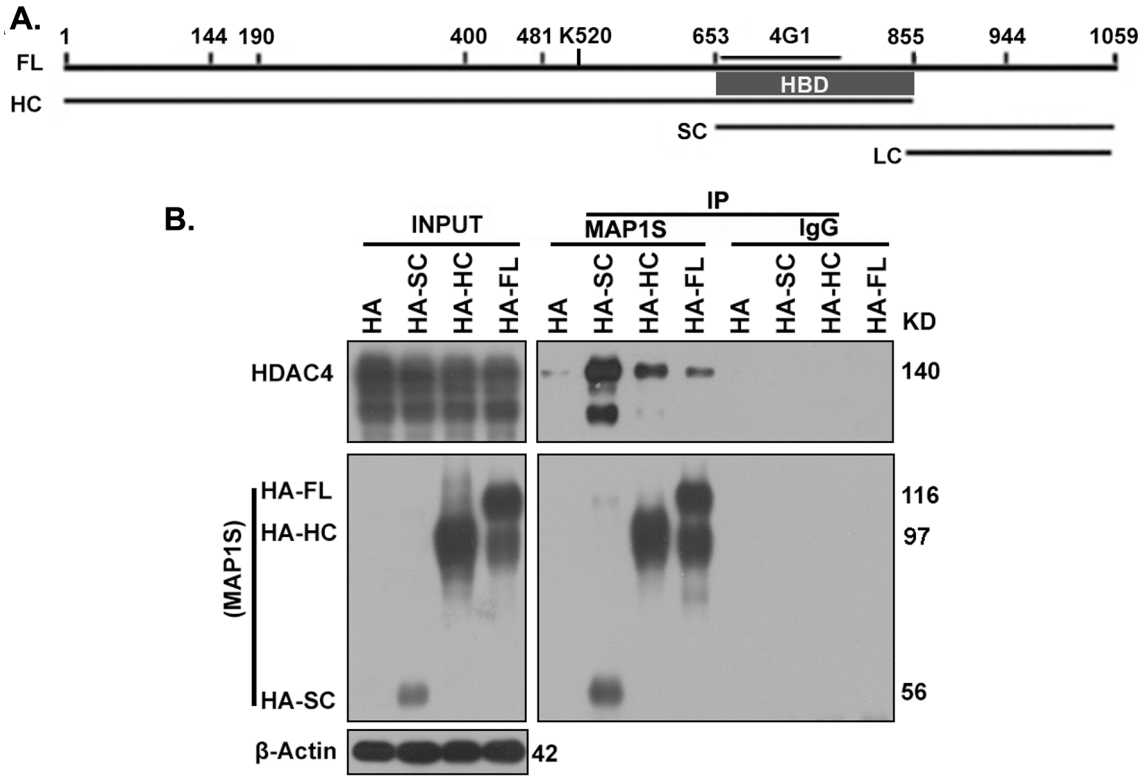

Figure 14. MAP1S Interacts with HDAC4 via an HDAC4-binding Domain (HBD) in the Overlapping Region between the Heavy Chain (HC) and Short Chain (SC) of MAP1S. (**A**) A diagram shows the sequence domains of MAP1S protein. FL, full length; HC, heavy chain; SC, short chain; LC, light chain; 4G1, region recognized by MAP1S monoclonal antibody; HBD, HDAC4-binding domain with the R653-Q855 fragment. All sequence numbers were deduced based only on experiment results. (**B**) HDAC4 interacts with MAP1S isoforms SC, HC, and FL. Lysates of 293T cells overexpressing HDAC4 and HA-fused MAP1S isoforms were precipitated with MAP1S-specific antibodies or IgG control. (**C**) HDAC4 interacts with MAP1S SC but not LC. Lysates of 293T cells overexpressing HDAC4 and HA-fused MAP1S SC or LC were precipitated with HA-specific antibodies or IgG control. (**D**, **E**) HDAC4 binds with GST-SC but not GST-LC. GSH beads bound with purified GST-fused MAP1S SC, but not LC (**E**) pulled down HDAC4 in cell lysates (**D**). HDAC4 was revealed on immunoblots with specific antibodies and GST fusion proteins were visualized with coomassie blue staining. (**F**) HDAC4 interacts with an overlapping domain between MAP1S HC and SC. Lysates of 293T cells overexpressing HDAC4 and HA-fused MAP1S sequence R653-Q855 (HA-HBD) were immunoprecipitated with HA-specific antibodies or IgG control and immunoblotted with HA or MAP1S-specific antibodies. (**G**) The interaction between MAP1S and HDAC4 is abolished when the HBD is deleted. Lysates of 293T cells overexpressing HDAC4 and HA-fused full length MAP1S (HA-FL) or mutant MAP1S with sequence R653-Q855 deleted (HA-HBDΔ) were precipitated with HA- or HDAC4-specific antibodies or IgG control and blotted with antibodies against HA and HDAC4.

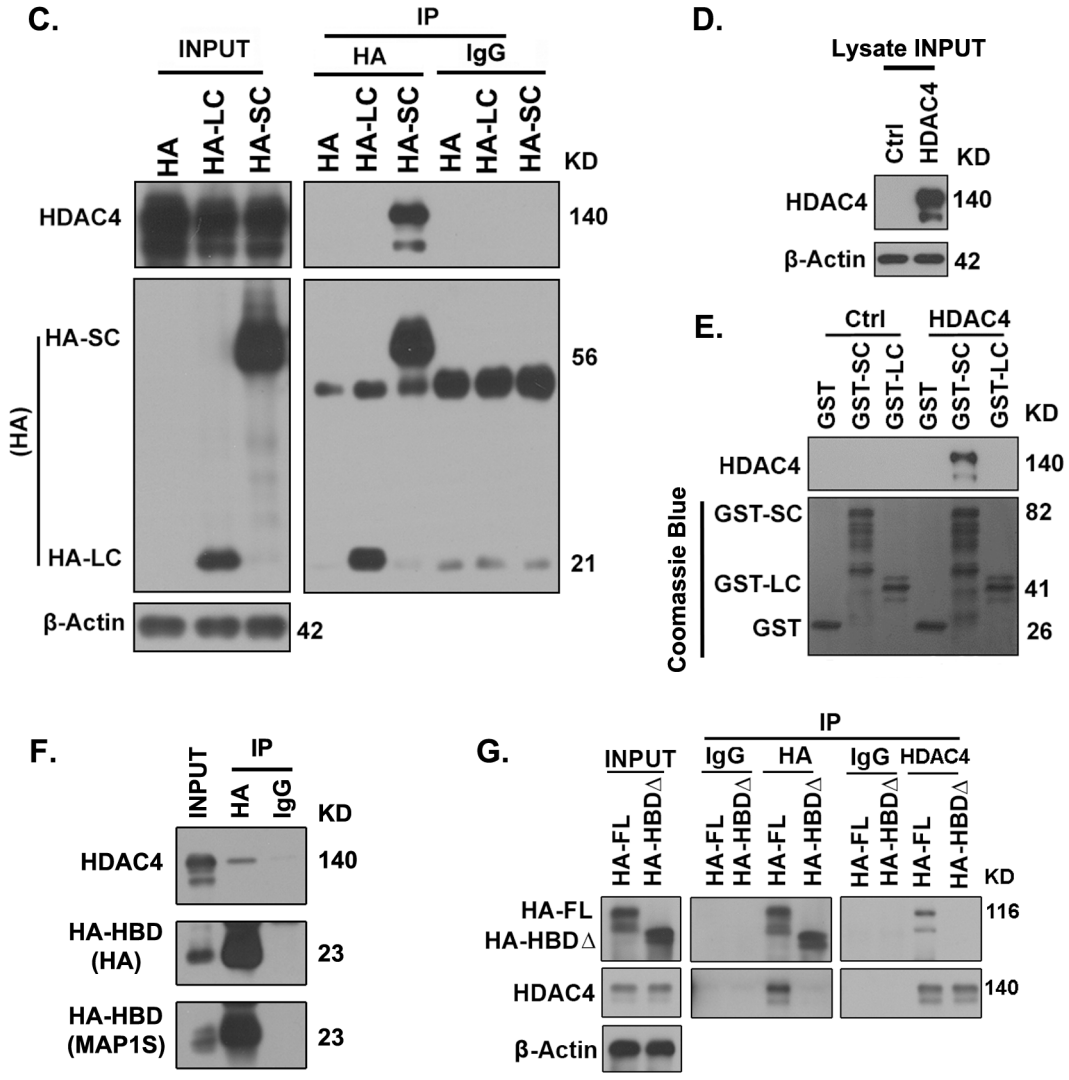

Figure 14. Continued.

was necessary and sufficient for the interaction between HDAC4 and MAP1S. MAP1S LC, lacking the sequence R652-Q855, exhibited no interaction with HDAC4 (Figure 14C). The isoform-specific interaction was further confirmed using purified MAP1S SC or LC variants tagged with glutathione S-transferase (GST) (GST-SC or GST-LC) to pull down HDAC4 from lysates of 293T cells overexpressing HDAC4. Notably, GST-

SC pulled down HDAC4, but GST-LC did not (Figure 14D, E). Immunoprecipitation by using HA-tagged R653-Q855 fragment (HA-HBD) alone further indicated HBD localized within the fragment (Figure 14F). Deletion of HBD in MAP1S led to the abolishment of its interaction with HDAC4 (Figure 14G). All the results indicate that MAP1S interacts with HDAC4 within cells and the interaction occurs through HBD.

Overexpression of HBD Promotes Autophagy by Sustaining MAP1S Level

To further confirm that the impact of HDAC4 on autophagy is specifically through its association with MAP1S, the impact of HBD and HBDΔ on MAP1S-mediated autophagy was first examined. When either HBD or HBDΔ was overexpressed in HeLa cells, HBD but not HBDΔ reduced the amount of MAP1S co-precipitated with HDAC4 (Figure 15A, B), suggesting that HBD competed with full length MAP1S for binding with HDAC4. In addition, the stability of endogenous MAP1S was examined when cells were overexpressed with either HBD or HBDΔ. The results showed that overexpression of HBD but not HBDΔ enhanced the stability of endogenous MAP1S (Figure 15C, D), and only overexpression of HBD increased levels of endogenous MAP1S protein (Figure 15E, F). Consequently, autophagic flux represented by levels of LC3-II in the presence of BAF was enhanced by overexpression of HBD but not HBDΔ; and such enhancive effect was only observed in the presence of endogenous MAP1S (Figure 15E, G). HDAC4 overexpression-induced decrease in levels of MAP1S was abolished when cells were overexpressed with HBD but not HBDΔ (Figure 15H, I).

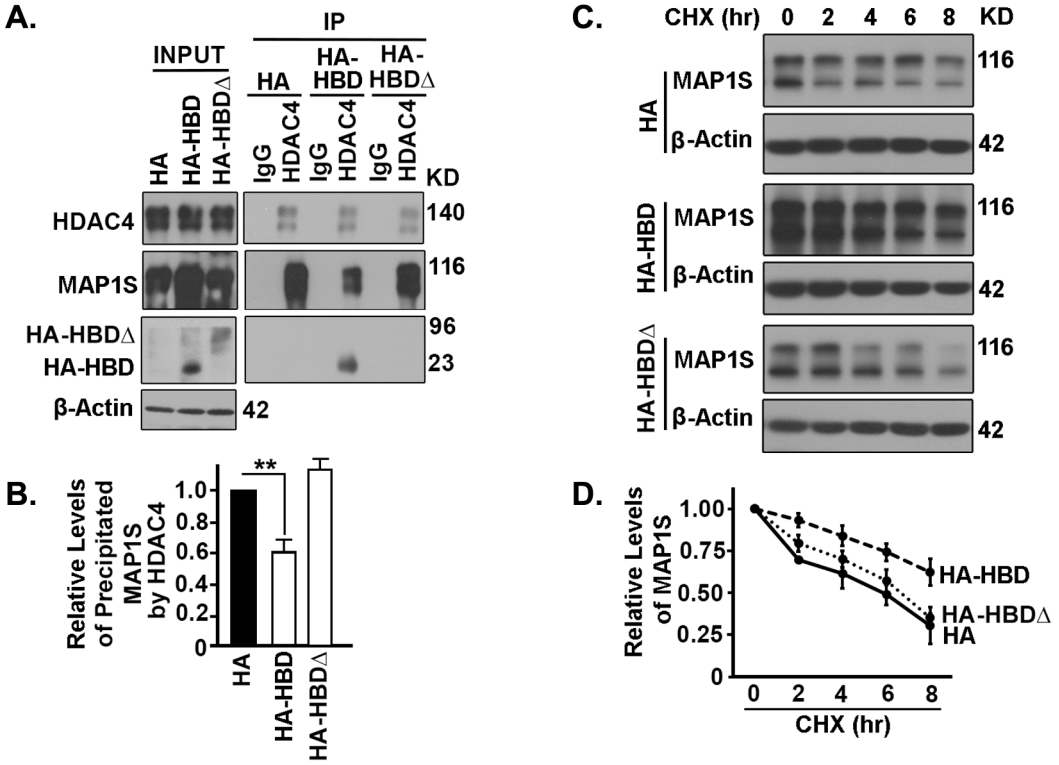

Figure 15. Overexpression of HBD Interrupts HDAC4-MAP1S Interaction, Activates MAP1S-mediated Autophagy. (**A**, **B**) Overexpression of HBD but not HA-HBDΔ reduces HDAC4-bound MAP1S. Equal amounts of lysates collected from HeLa cells expressing control HA vector, HA-HBD or HA-HBDΔ were subjected to immunoprecipitation with HDAC4-specific antibodies. Representative immunoblot results (**A**) and quantification of the precipitated MAP1S (**B**) are shown. (**C**, **D**) Overexpression of HBD but not HBDΔ enhances the stability of endogenous MAP1S in HeLa cells. Lysates of HeLa cells transiently transfected with HA vector, HA-HBD or HA-HBDΔ were collected at different time after 10 μg/ml cycloheximide treatment. Representative immunoblot results (**C**) and quantification (**D**) are shown. (**E**-**G**) Overexpression of HBD but not HBDΔ enhances autophagic flux in the presence of MAP1S. Lysates were collected from wild-type or MAP1S$^{-/-}$ HeLa cells transiently transfected with HA vector, HA-HBD or HA-HBDΔ in the absence (Ctrl) or presence of BAF. Representative immunoblot results (**E**) and quantification of relative levels of MAP1S in wild-type cells in the absence of BAF (**F**) or relative levels of LC3-II in the presence of BAF (**G**) are shown. (**H**-**J**) Overexpression of HBD but not HBDΔ prevents HDAC4-induced destabilization of MAP1S and suppression of autophagic flux. Lysates were collected from HeLa cells transiently co-transfected with HDAC4 and HA vector, HA-HBD or HA-HBDΔ in the absence (Ctrl) or presence of BAF. Representative immunoblot results (**H**) and quantification of relative levels of MAP1S in the absence of BAF (**I**) or LC3-II in the presence of BAF (**J**) are shown.

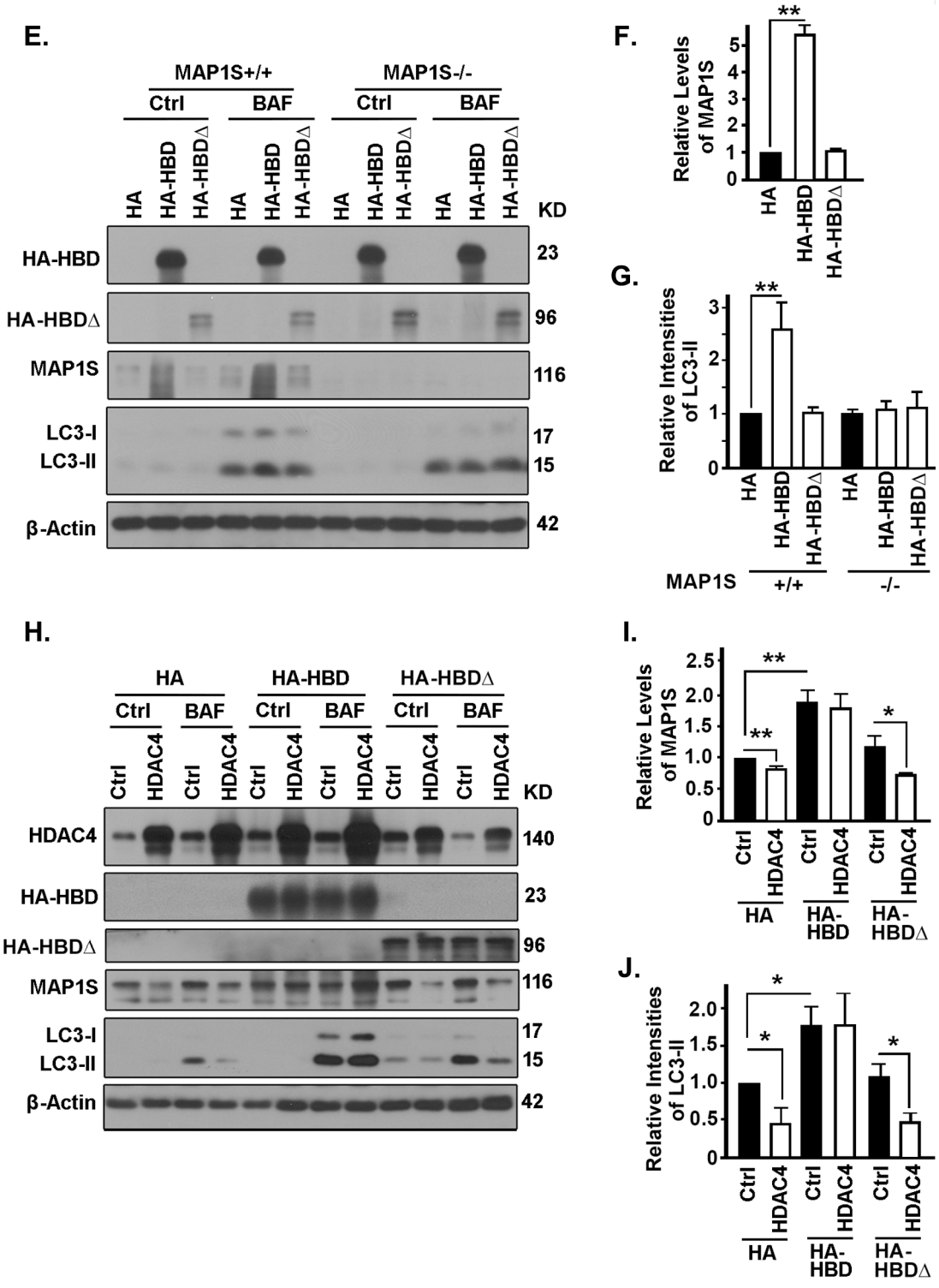

Figure 15. Continued.

HDAC4 overexpression-induced impairment of autophagic flux was inhibited when cells were overexpressed with HBD but not HBDΔ (Figure 15H, J).

Overexpression of HBD Enhances Levels of MAP1S and Alleviates HDAC4-induced Mutant Huntingtin Aggregation

To study the impact of HBD on HDAC4-induced mHTT aggregation, HBD or HBDΔ were overexpressed in the N2α cells co-overexpressed with GFP-HTT74Q. Overexpression of HBD but not HBDΔ sustained levels of endogenous MAP1S and led to significant decrease in levels of mHTT aggregates (Figure 16A-C). In addition, overexpression of HBD but not HBDΔ protected the stability of endogenous MAP1S when the cells were simultaneously overexpressed with HDAC4, and inhibited HDAC4-induced accumulation of mHTT aggregates (Figure 16A-C). These results suggest that the interaction between HDAC4 and MAP1S is required for HDAC4 to exert suppressive effect on MAP1S-mediated autophagic turnover of mHTT aggregates. Therefore, the HBD interrupts MAP1S-HDAC4 interaction and promotes MAP1S-mediated autophagic clearance of mHTT aggregates.

A diagram shows the potential mechanism by which HDAC4 regulates MAP1S-mediated autophagic turnover of mHTT aggregates (Figure 17). Under normal condition, isolation membrane-associated acetylated-MAP1S is deacetylated and destabilized by microtubule or aggregate-associated HDAC4. In the presence of excessive HBD, HBD competes with acetylated MAP1S for interaction with HDAC4, which leads to the exposure of mHTT aggregates to be packaged by the MAP1S-associated isolation

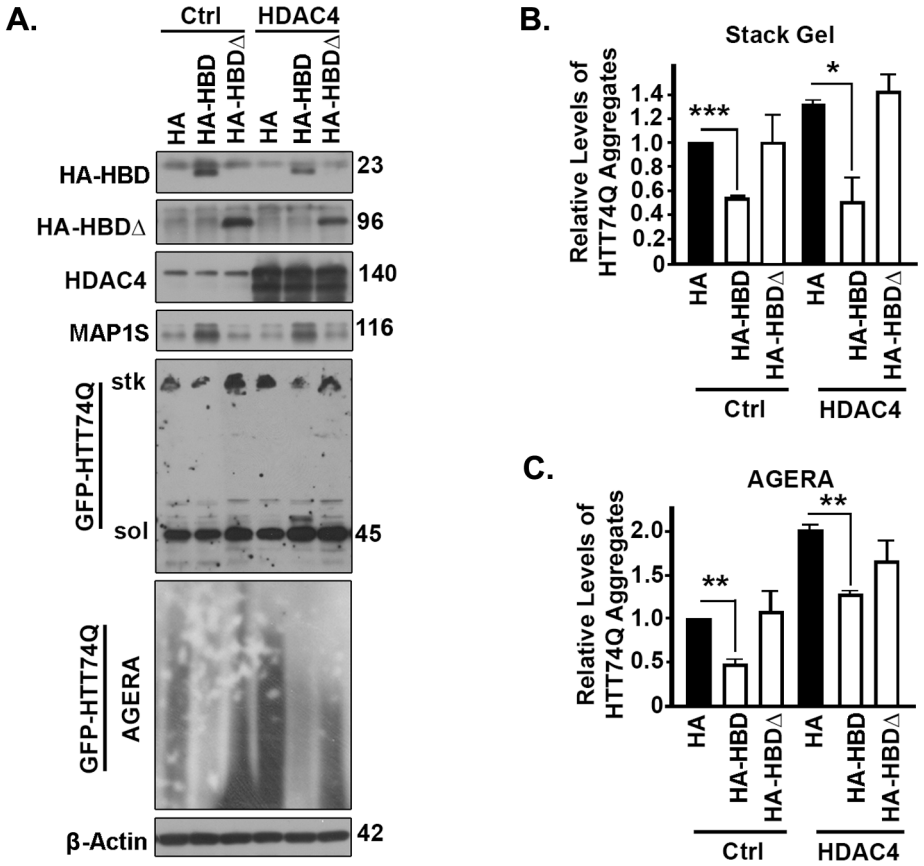

Figure 16. Overexpression of HBD Alleviates HDAC4-induced Mutant Huntingtin Aggregation. (**A-C**) Overexpression of HBD but not HBDΔ reduces levels of HTT74Q aggregates. N2α cells transiently expressing GFP-HTT74Q were simultaneously transfected with two additional plasmids with one to express HA control, HA-HBD or HA-HBDΔ, and another to express control or HDAC4, respectively. Representative immunoblot results of HTT74Q resolved by stacking gel or AGERA (**A**) and the respective quantification in stack gel (**B**) or AGERA (**C**) are shown.

membrane. Autophagosomes that contain mHTT aggregates associate with microtubules through acetylated MAP1S and fuse with lysosome to become autolysosomes in which mHTT aggregates are degraded by lysosomal enzymes (20).

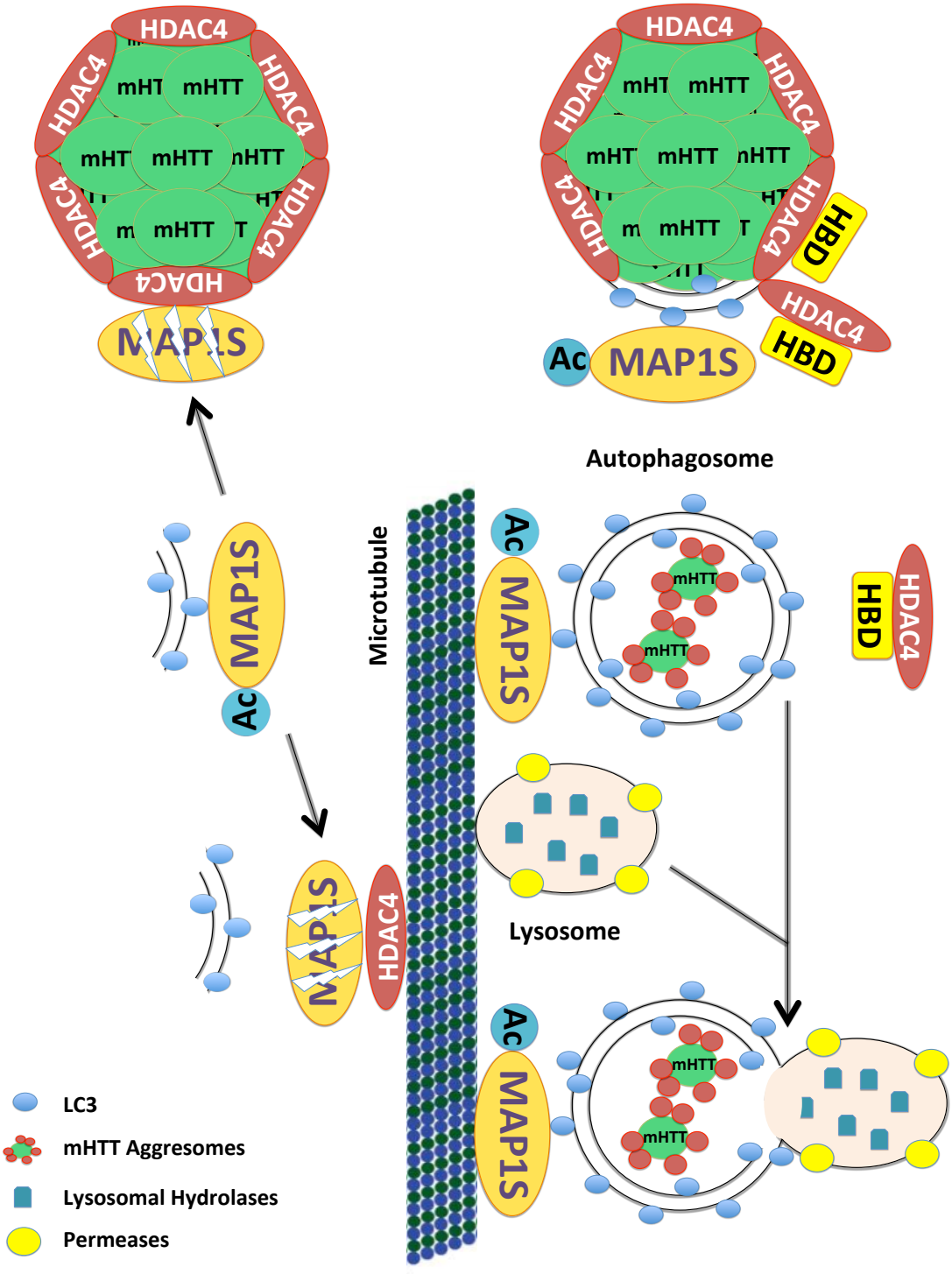

Figure 17. Potential Mechanism of HDAC4 in MAP1S-mediated Autophagic Clearance of Mutant Huntingtin Aggregates.

Discussion

Wild-type Huntingtin (HTT) is a large protein consisted of about 3,144 amino acids, widely distributed but most concentrated in the neurons (99) (100). Wild-type HTT contains a 6-35 glutamine-repeats region that is also called polyglutamine (ployQ) region in the N-terminus of the protein. Mutant HTT is the protein that has a ployQ expansion longer than 36 residues and forms insoluble aggregates that are toxic to the neurons and cause Huntington's disease (HD) (101). Although there is no efficient treatment that has been developed specifically for this devastating disease, enhancing clearance of mHTT aggregates is considered as one of the feasible approaches to slow down the neurodegeneration in HD and has revealed some beneficial effects in animal models (20,102).

Recently, HDAC4 reduction is identified as a potential treatment to target mHTT aggregates in the HD mouse model (93). The mechanistic study suggests HDAC4 regulates mHTT in ways different from transcriptional regulation, as deletion of HDAC4 in mouse brain has no effect on histone acetylation profiles and global transcription (103). In our study, we decipher the mechanism that HDAC4 induces mHTT aggregation by suppressing MAP1S-mediated autophagy. HDAC4 associates with and forms shells surrounding mHTT aggregates in the cytoplasm (20,93). HDAC4 directly interacts with the autophagy activator MAP1S, reduces the stability of MAP1S protein, consequently suppresses the autophagic flux mediated by MAP1S, and impairs the degradation of mHTT aggregates.

Wild-type HTT plays important roles during embryogenesis and brain development (104). It can not only interact with microtubules and regulate vesicle trafficking (105-107), but also bind to transcription factors to modulate gene expression in neurons (108). In addition, both *in vitro* and *in vivo* studies indicate wild-type HTT can disrupt the activation of caspases to execute apoptosis (109). The homology between regions of HTT and the yeast autophagy regulatory proteins predicts a normal regulatory function in autophagy (110). Recent studies also suggest an essential role of wild-type HTT in autophagy as a scaffold protein (23,111). Importantly, HDAC4 only interacts with aggregate-prone mHTT that has long ployQ stretches but not with wild-type HTT (93). Thus, HDAC4 and MAP1S-mediated autophagic clearance does not affect wild-type HTT and its cellular functions.

In this study, we define the role of MAP1S in the HD development through its function in multiple steps of autophagy. Our results show that it is the inhibition of HDAC4 and its associated deacetylase activity that enhances the stability of MAP1S, increases autophagic flux and improves clearance of mHTT aggregates. The mHTT disrupts the wild-type HTT-mediated regulation of autophagosomal dynamics and causes defects in cargo degradation (112). We reason that soluble mHTT protein may function similar as wild-type HTT in association with motor protein complexes on microtubules. However, mHTT sequesters HDAC4 on microtubules, which further impairs the stability and microtubule-associated functions of MAP1S through HDAC4-induced deacetylation and consequently interrupts autophagic flux. This defect leads to accumulation of mHTT and consequent formation of mHTT aggregates. The mHTT

aggregates further sequester HDAC4 that protects the aggregates from degradation by MAP1S-mediated autophagy (20).

HDACs facilitate the removal of acetyl groups during epigenetic regulation, which results in transcriptional repression. Because high expression levels or hyperactiviton of multiple HDACs are the mechanisms that promote epigenetic dysregulation in cancer (113), HDACs emerge as a druggable class of enzymes in cancer treatment. Disruption of HDAC activity with HDAC inhibitors (HDACi) shows pleiotropic effects in cancer cells in pharmacodynamics studies in that HDACi may also exhibit effects on neurodegeneration (113,114). However, several studies show that pan-HDACi is unsuitable for treating HD, as genetic knockdown of HDAC3 or HDAC7, or knockout of HDAC6 has no effects on ameliorating HD in mouse model (115-118). Consistent with the result that genetic knockout of HDAC4 in mouse delays cytosolic mHTT aggregation and improves motor coordination, neurological phenotypes and longevity (93), our study shows that inhibition of HDAC4 with specific siRNA results in stabilization of MAP1S protein, activation of MAP1S-mediated autophagic flux and fast degradation of mHTT (20). This provides a mechanism by which therapeutic reduction of HDAC4-associated activity can reduce accumulation of cytoplasmic mHTT aggregates and alleviate neurodegeneration (20).

Since a series of cellular processes are regulated by HDAC4, any small molecule inhibitor of HDAC4 will inhibit the general activity of HDAC4 and is surely expected to cause unnecessary side effects besides the clearance of mHTT aggregates. Here we have identified an HDAC4-binding domain (HBD) from MAP1S, which is the overlapping

region between the heavy chain (HC) and short chain (SC) of MAP1S. HBD specifically interrupts HDAC4-MAP1S interaction and protects MAP1S from being deacetylated by HDAC4-associated deacetylase activity. Since the approach of HIV TAT-mediated protein transduction is widely utilized, TAT-tagged HBD can be first synthesized to directly validate its biological effects on autophagy *in vitro* and *in vivo*. Further development of short peptides to disrupt the interaction between HDAC4 and MAP1S may specifically enhance the MAP1S-mediated autophagic clearance of mHTT aggregates (20).

CHAPTER IV

SPERMIDINE ACTIVATES MAP1S-MEDIATED AUTOPHAGY TO PROLONG LIFESPANS AND SUPPRESS DIETHYLNITROSAMINE-INDUCED HEPATOCARCINOGENESIS

Introduction

Hepatocellular carcinoma (HCC) is the primary malignancy of the liver caused by long-term hepatic injuries. Due to late-diagnosis and few effective drugs available, HCC is a leading cause of cancer mortality worldwide (25). The incidence and mortality rate of HCC also rise dramatically in recent decades in the United States (26,27). Only small portions of HCC patients with early diagnosis may be treated with surgery or liver transplantation, but have poor prognosis (30). Though it is an FDA approved drug for advanced HCC, Sorafenib has severe toxicity and only extends survival for 3 months (119). Prescribed medications such as statins, metformin and aspirin have shown chemopreventive effects for HCC, but each simultaneously exhibits other unintended effects (30). Thus, development of therapeutics and effective prevention approach for HCC is in urgent need.

Several experimental animal models have been developed to investigate the pathogenesis of HCC and the potential treatment for HCC (120). There are three types of mouse models to study HCC currently based on the mechanism of how HCC is triggered, including chemical-induced HCC mouse models, genetically modified HCC mouse models and xenograft models. Diethylnitrosamine (DEN)-induced HCC mouse model is

one of the most commonly used models to define HCC pathogenesis. A single injection of DEN in 15-day-old male mice leads to tumor development in a dose-dependent manner (120,121). DEN induces genomic instability via DNA alkylation mediated by cytochrome P450 which is most activated in the centrilobular hepatocytes. In addition, DEN induces cellular oxidative stress which further contributes to hepatocellular carcinogenesis (122). High incidence of HCC in developing countries is in partially due to the consumption of food contaminated with *Aspergillus* fungi which produce aflatoxin B1 (AFB) (25). Thus, AFB is another frequently used carcinogen to induce HCC in mice. Carbon tetrachloride (CCl4) exposure induces hepatic injuries associated with a series of inflammatory responses which result in liver fibrosis and ultimately HCC (120). Therefore, CCl4-treated mice develop HCC in a context of liver fibrosis. Since viral infection is a main cause of HCC, transgenic mouse models expressing viral genes are generated to study the pathogenesis of HCC involved with Hepatitis B (HBV) and Hepatitis C (HCV). Besides, several HCC mouse models are established by overexpression of specific oncogenes, such as *c-myc* and *β-catenin* (123,124). Xenograft mouse models are generated by injecting HCC cell lines in immune deficient mice to develop HCC and are usually used for drug screening (120).

Autophagy is the primary mechanism for removal of misfolded proteins, aggresomes and dysfunctional organelles through lysosomal degradation, and further reduces cellular oxidative stress to suppress accumulation of cellular damages, which is the common underlying process for aging and cancers (3,125). Autophagy has essential roles in lifespan extension. Calorie restriction (CR) and pharmacologic intervention that

regulates growth-related signaling or anti-aging pathways can prolong lifespans by enhancing autophagy activity (17). In addition to aging, autophagy suppresses tumorigenesis by alleviating levels of cellular oxidative stress which further induces genomic instability and tumorigenesis (15). Impaired autophagy results in tumor initiation and development (32,33), and leads to shortened lifespans in cancer patients as well (34-36). Therefore, elevating autophagy activity may be utilized to prevent and treat HCC. Induction of autophagy by pharmacologic agents has attracted enormous attention for cancer prevention.

Microtubule-associated protein 1 small form (MAP1S) associates with microtubules stabilized by either chemotherapeutic drug and microtubule stabilizer taxanes or tumor suppressive protein Ras-association domain family 1 isoform A (RASSF1A) (38,54). Specific accumulation of MAP1S short chain (SC) responding to mitotic arrest leads to mitochondrial collapse on mitotic spindle and mitotic cell death (40). Importantly, MAP1S has been identified as a novel autophagy activator. The association of MAP1S with microtubule and LC3 promotes autophagosome formation and transportation. Meanwhile, MAP1S regulates autophagy initiation through Bcl-2 and P27 (41). Autophagy defects caused by MAP1S depletion lead to enhancement of cellular oxidative stress, liver sinusoidal dilation and fibronectin-induced liver fibrosis, and reduction in mouse lifespans (4). In DEN-induced HCC mouse model, MAP1S suppresses tumor initiation and development through autophagy regulation (33). In the early stage of tumorigenesis, DEN treatment leads to immediate elevation in levels of MAP1S protein to activate autophagic turnover of P62-associated aggresomes and

inhibit DNA double-strand breaks (DSB) induced by accumulated oxidative stress. MAP1S is also maintained in high levels in tumor foci to accelerate autophagy and prevent genomic instability during tumor development (15,33). In addition, clinical evidence suggests that higher levels of MAP1S in tumor tissues predict longer survival for cancer patients (35,36). Thus, elevating levels of MAP1S can activate autophagic flux to extend lifespans and suppress tumorigenesis.

Spermidine is a polyamine originally isolated from semen and also enriched in wheat germ, citrus fruits, and soybeans (52). It has been recently characterized as a longevity enhancer through induction of autophagy in multiple model systems (51). However, the mechanism by which spermidine induces autophagy remains mysteries of molecular biology, though previous studies suggest that a combination of transcription-dependent and independent regulatory events may be involved (53,126). Acetylproteomic analyses indicate spermidine alters the acetylation status of multiple autophagy-relevant proteins including MAP1S (127). Notably, spermidine enhances levels of acetylated MAP1S by 24-fold in cytoplasm, which encourages us to further characterize the molecular mechanism of how spermidine elevates the acetylation of MAP1S. As discussed in chapter II, HDAC4 negatively regulates MAP1S through deacetylation, which also prompts us to study the roles of HDAC4 and MAP1S in spermidine-induced autophagy. In addition, the impact of spermidine-induced lifespan extension needs further study on mammals, and the role of spermidine in tumor suppression is still unknown. Elucidating the molecular mechanism of spermidine-induced autophagy and defining the effects of spermidine on aging and tumorigenesis

can provide insights on the drug development for lifespan extension and cancer treatment.

Herein, we discover that spermidine-induced autophagy depends on MAP1S and is mediated by MAP1S-HDAC4 complex. Spermidine increases the acetylation and stability of MAP1S protein by suppressing cytosolic HDAC4. Spermidine dephosphorylates HDAC4 on serine 246 and serine 632 residues, leading to the release of HDAC4 from its cytoplasmic partner 14-3-3 and nuclear import of HDAC4. Spermidine-induced HDAC4 nuclear translocation further results in the dissociation of MAP1S from HDAC4 to maintain its acetylation and protein stability. Lysine 520 residue of MAP1S, the spermidine-induced acetylation site, facilitates autophagosome-lysosome fusion and is critical in spermidine-induced autophagy. *In vivo* results also indicate that spermidine activates MAP1S-mediated autophagic flux to prolong lifespans and suppress DEN-induced HCC in wild-type mice. The suppressive roles of spermidine in aging and HCC is abolished in $MAP1S^{-/-}$ mice, suggesting the presence of MAP1S is essential in spermidine-induced lifespan extension and tumor suppression.

Materials and Methods

Animals

Animal protocols were approved by the Institutional Animal Care and Use Committee (IACUC), Institute of Biosciences and Technology, Texas A&M Health Science Center. All animals received human care according to the criteria outlined in the 'Guide for the Care and Use of Laboratory Animals' prepared by the National Academy of Sciences and published by the National Institutes of Health (NIH publication 86-23 revised 1985). C57BL/6 wild-type and MAP1S$^{-/-}$ mice were bred and genotyped as previously described (41). Mice were fed with drinking water or water containing 3 mM spermidine (Sigma, #S4139) and were observed to record survival times when found to be moribund. Diethylnitrosamine (DEN) (Sigma, #0756) was used to induce hepatocellular carcinogenesis in mice as previously described (33). A single intraperitoneal administration of 10 μg/g body weight of DEN dissolved in saline was applied to 15-day-old wild-type and MAP1S-depleted male littermates. Mice were sacrificed with euthanasia techniques at 7 months after birth. The body weight, liver weight, and the ratio of liver weight to body weight were recorded. Liver tissues were frozen or fixed for further analyses.

Cell Culture

Most cell lines, including HeLa, HepG2, HEK-293T, HeLa-RFP-LC3 cells, and MEF cells, were cultured in the DMEM culture media containing 10% FBS and antibiotics. Primary mouse hepatocytes were grown in William's E culture media with

10% FBS, ITS-G and 100 nM dexamethasone. PBS and 0.25% trypsin were used for subculture.

Cell Transfection

Cell lines used for transfection included HeLa, HEK-293T, HeLa-RFP-LC3 cells, and MEF cells. For transient knockdown experiments, cells were cultured at 30% confluence on the cell culture plates or coverslips and transfected with negative control siRNA or specific siRNA by Oligofectamine according to the manufacturer's recommended instruction. For transient overexpression experiments in HeLa, HeLa-RFP-LC3 cells, and MEF cells, cells were cultured at 70% confluence on the cell culture plates or coverslips and transfected with control vector or plasmids encoding specific genes by Lipofectamine 2000 according to the manufacturer's recommended instruction. For transient overexpression in HEK-293T cells, cells were cultured at 60% confluence on the cell culture plates and transfected with control vector or plasmids encoding specific genes by using calcium phosphate transfection kit according to the manufacturer's recommended instruction.

Fluorescence Microscopy

HeLa-RFP-LC3 cells were treated with 100 μM spermidine, or 10 nM BAF for 4 hours before fixation. Cells were fixed with 4% (w/v) paraformaldehyde in PBS at room temperature for 30 minutes and processed for fluorescence microscopy analyses. HeLa cells or MEF cells transfected with plasmids encoding GFP or GFP-HDAC4 were

treated with 100 μM spermidine for 4 hours before fixation. Cells were fixed with 4% (w/v) paraformaldehyde in PBS at room temperature for 30 minutes, stained DNA with TO-PRO-3 (Invitrogen, #T3605) for 5 minutes and processed for fluorescence microscopy analyses. HeLa or HeLa-RFP-LC3 cells were transfected with the plasmids expressing HA-MAP1S, or HA-MAP1S K520R. HeLa cells transfected with the plasmids expressing GFP-HDAC4 and HA-MAP1S were treated with 100 μM spermidine for 4 hours. Cells were fixed with 4% (w/v) paraformaldehyde in PBS at room temperature for 30 minutes and then permeabilized with 0.1% Triton X-100 in PBS for 20 minutes. Cells were blocked with 1% BSA in PBS for 20 minutes, and then incubated with primary antibodies against HDAC4, LAMP2, HA-tag (Covance, #MMS-101P, dilution 1:1000) for 1 hour at room temperature, and the corresponding rhodamine or alexa fluor 488 (Invitrogen, #A21206, #A21202, dilution 1:400)-conjugated secondary antibodies for 1 hour at room temperature for fluorescence microscopy analyses. Images were captured with a Zeiss LSM 510 Meta Confocal Microscope. The number of RFP-LC3 punctate foci on each image was calculated and lysosome-associated RFP-LC3 punctate foci were analyzed using ImageJ software.

Cell Fractionation

Cells were seeded in 10 cm culture dishes and treated with 100 μM spermidine for 4 hours. Cell pellets were collected after centrifugation at 6,000 rpm for 5 minutes and resuspended in five times of volume of cytoplasmic extract (CE) buffer (10 mM HEPES, pH 7.9, 10 mM KCl, 0.1 M EDTA) containing 0.3% NP-40 and protease

inhibitor cocktails for 5 minutes 4 °C. Cells were lysed with vortex all the time. The cytoplasmic extracts were the supernatants that collected after centrifugation at 3,000 rpm for 5 minutes at 4 °C. The pellets were washed by centrifugation in CE buffer without NP-40 twice, and resuspended in equal volume of nuclear extract (NE) buffer (20 mM HEPES, pH 7.9, 0.4 M NaCl, 1 mM EDTA, 25% Glycerol) containing protease inhibitor cocktails on ice for 10 minutes. Nuclear fraction was further lysed with vortex all the time. The nuclear extracts were the supernatants collected after centrifugation at 14,000 rpm for 5 minutes at 4 °C. The cytoplasmic and nuclear extracts were further processed for immunoblot analyses.

Immunoblot Analyses

Cells were lysed in the cell lysis buffer with 1mM PMSF on ice for 30 minutes. The total protein concentration of the cell lysates was determined by using BCA protein assay kit. The cell lysates were then mixed with SDS loading buffer and boiled for 10 minutes. Cell lysates were loaded on SDS-polyacrylamide gels containing 8, 10, 12 or 15% (w/v) acrylamide. Proteins were separated by electrophoresis, transferred on to PVDF membranes. The membranes were blocked with 5% (w/v) non-fat milk in TBST for 1 hour at room temperature, bound with primary antibodies overnight at 4 °C and incubated with HRP-conjugated secondary antibodies for 2 hours at room temperature. Proteins were detected by ECL Prime Western Blotting Detection Reagents. The exposed X-ray films were processed using developer and fixer, scanned into image files.

The relative intensity of a band to internal control was measured using ImageJ software. The catalog numbers and dilutions of primary antibodies are listed in the Table 4.

Table 4. Catalog Numbers and Dilutions of Primary Antibodies-II.

Antibody	Catalog Number	Dilution
P27	Santa Cruz, #776	1:1000
p-P27	Santa Cruz, #130603	1:1000
Bcl-2	Santa Cruz, #47778	1:1000
p-Bcl-2	Santa Cruz, #377576	1:1000
Beclin 1	Santa Cruz, #11427	1:1000
PI3KCIII	Cell Signaling, #4263	1:1000
ATG4B	Cell Signaling, #5299	1:1000
ATG5-12	Santa Cruz, #33210	1:1000
P62	Santa Cruz, #25730	1:1000
Poly-Ub	Santa Cruz, #8017	1:500
14-3-3	Cell Signaling, #7413	1:1000
Lamin B	Santa Cruz, #20682	1:2000
β-Tubulin	Santa Cruz, #9104	1:2000
p-HDAC4 (S632)	Cell Signaling, #3424	1:1000
p-HDAC4 (S246)	Cell Signaling, #3443	1:1000

Immunoprecipitation

To analyze levels of acetylated MAP1S by immunoprecipitation, cell lysates were prepared by using RIPA buffer with 1 mM PMSF, protease inhibitor cocktails, 5 mM NAM and 10 μM TSA; and centrifuged at 14,000 rpm for 15 minutes at 4 °C to

isolate the supernatants. Lysates of same amount of total proteins were mixed with 30 µl anti-acetyl-lysine agarose conjugate overnight at 4 °C for precipitation of total acetylated lysine proteins.

To study the interaction between HDAC4 and MAP1S or 14-3-3 by immunoprecipitation, cell lysates were prepared by using NP-40 buffer with 1mM PMSF and protease inhibitor cocktails. The supernatants were collected after centrifugation at 14,000 rpm for 15 minutes at 4 °C. Same amount of lysates with 1.5 mg of total protein were subjected to immunoprecipitation with 2 µg antibodies against MAP1S, HDAC4, HA, or the respective IgG control, and incubated with 30 µl Protein G-Sepharose beads. After overnight rotation at 4 °C, beads that binds with antibodies and the bound proteins were precipitated and washed extensively with the NP-40 buffer four times. The final precipitates were resuspended in 100 µl lysis buffer containing SDS loading buffer and boiled for 10 minutes for further immunoblot analyses.

Protein Half-life Measurement

MEF cells were seeded in 35 mm culture dishes and treated with 100 µM spermidine. After 4 hours of spermidine treatment, the protein synthesis inhibitor 10 µg/ml CHX was added into the culture media. Cell lysates were harvested at the indicated time points for further immunoblot analyses.

Site-directed Mutagenesis

HA-MAP1S K520R mutation was introduced into the full length HA-MAP1S using QuikChange II kit (Agilent Technologies, #200523), according to the manufacturer's recommended instruction. HA-MAP1S K520R was PCR amplified from HA-MAP1S template with primers (5'-CTCCCGGGGGGTCCTGGCTTCTTTCTC-3', 5'-GAGGAAAGAAGCCAGGACCCCCCGGGAG-3'). The restriction enzyme DpnI was then added into the mixture after PCR reaction for digesting the template of full length HA-MAP1S. After transformation, the positive colonies were picked and verified by DNA sequencing.

Dihydroethidium (DHE) Staining

A part of frozen samples was cryosectioned and used for measurement of oxidative stress. As previously described (4), the cryosections were stained with 2 mM dihydroethidium hydrochloride (Invitrogen, #D-1168) for 30 minutes at 37 °C. DHE permeates into cells and reacts with reactive oxygen species (ROS). The products of DHE and cytosolic superoxide intercalate into genomic DNA upon oxidation, and label nuclear with red fluorescent signals monitored by fluorescence microscopy analyses. The intensities of red fluorescent signals were quantified by ImageJ software.

Histology

Paraffin sections were re-hydrated for hematoxylin (Fisher Scientific, #SH26) and eosin (Sigma, #HT110116) (H&E) staining. The area of sinusoidal space was

quantified using ImageJ software. For immunohistochemistry staining, slides were boiled in citrate buffer (10 mM sodium citrate, 0.05% Tween-20), pH 8.0 for 20 minutes for antigen retrieval after re-hydration. Slides were further processed and stained with γ-H2AX (Cell Signaling, #9718, dilution 1:480) using HRP/ 3, 3'-Diaminobenzidine (DAB) detection IHC kit (Abcam, #64261) according to manufacturer's recommended instruction. The nuclei were counter stained with hematoxylin. Positive staining of γ-H2AX was measured by ImageJ software.

Statistical Analyses

Statistical significance was determined by Student's t-test, with significance set to *, $p \leq 0.05$; **, $P \leq 0.01$; and ***, $P \leq 0.001$. Error bars indicate standard deviation. The overall survival and median survival were analyzed by the Kaplan-Meier method. Cox proportional hazard analysis was used to explore the effect of variables on overall survival.

Results

Spermidine Enhances MAP1S Protein Level and Accelerates Autophagic Flux

To study the impact of spermidine on autophagic flux, MEF or HeLa cells were first treated with spermidine for different amount of time or different concentrations of spermidine. Increased levels of MAP1S as well as autophagy marker LC3-II in a time and dose-dependent manner were observed when cells were treated with spermidine (Figure 18A, B). Levels of LC3-II in the presence of lysosome inhibitor BAF were elevated upon exposure to 100 μM spermidine for 4 hours (Figure 18C, D), suggesting that spermidine accelerated autophagic flux. Meanwhile, HeLa cells stably expressing RFP-LC3 were utilized to determine the impact of spermidine on autophagic flux. Accumulation of RFP-LC3 punctate foci induced by spermidine treatment, in the absence or presence of BAF, further confirmed that spermidine induced autophagy activation (Figure 18E, F). All the results indicate that spermidine increases levels of MAP1S protein and accelerates autophagic flux.

Spermidine-induced Activation of Autophagic Flux Depends on MAP1S

To understand the role of MAP1S in spermidine-induced autophagy, levels of LC3 were examined in wild-type or MAP1S$^{-/-}$ mice treated with spermidine. Levels of MAP1S and LC3-II were increased after spermidine treatment in livers, as well as other organs of mice including brain and heart, in wild-type mice with presence of MAP1S protein but not MAP1S$^{-/-}$ mice (Figure 19A, B). This suggested that MAP1S might be responsible for the impact of spermidine on autophagy. In addition, MEF cells derived

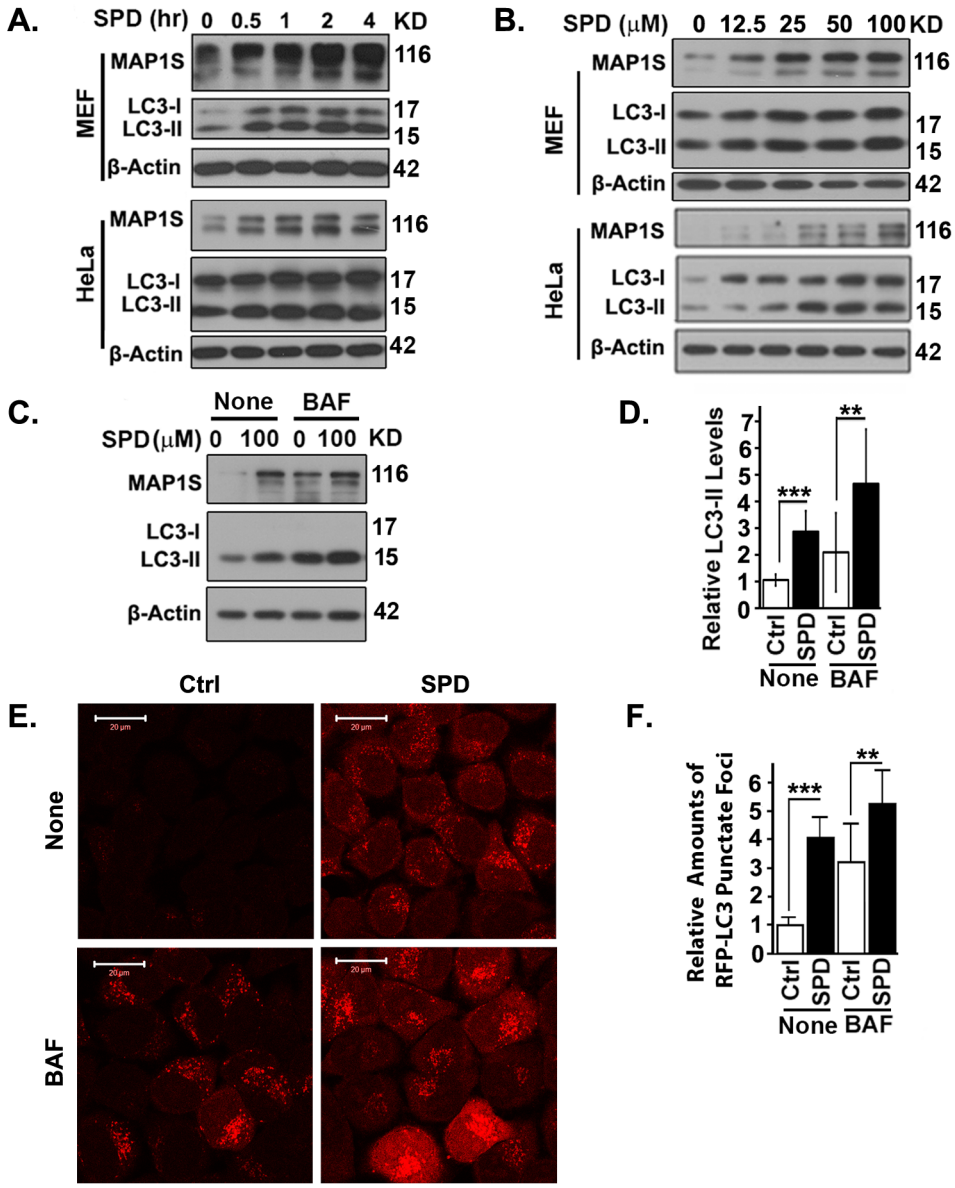

Figure 18. Spermidine Accelerates Autophagic Flux. (**A**, **B**) Spermidine enhances levels of MAP1S and LC3 in a time and dose-dependent manner. Representative immunoblot results show levels of MAP1S and LC3 in MEF or HeLa cells treated with 100 μM spermidine (SPD) for different amount of time (**A**) or different concentrations of spermidine for 4 hours (**B**). (**C**, **D**) Spermidine enhances levels of MAP1S and LC3-II. Representative immunoblot results (**C**) and quantification (**D**) show the impact of spermidine on levels of MAP1S and LC3 in HeLa cells in the absence (None) or presence of BAF. (**E**, **F**) Spermidine induces accumulation of RFP-LC3 punctate foci. Representative fluorescent images (**E**) and quantification (**F**) of the number of RFP-LC3 punctate foci in HeLa cells stably expressing RFP-LC3 untreated (Ctrl) or treated with spermidine (SPD) in the absence (None) or presence of BAF.

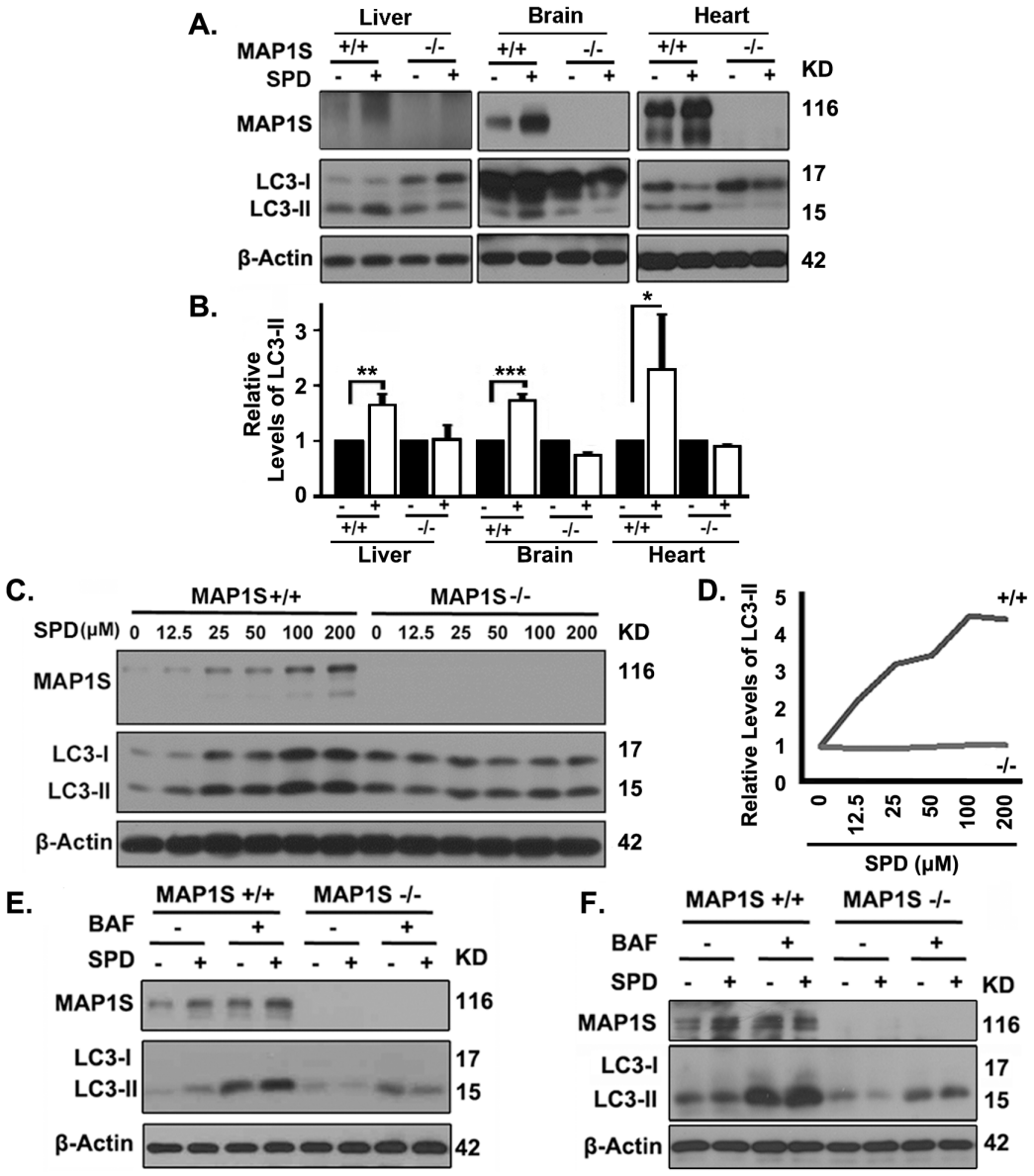

Figure 19. Spermidine-induced Autophagy Depends on MAP1S. (**A**, **B**) Spermidine enhances levels of LC3-II in wild-type mice but not MAP1S$^{-/-}$ mice. Representative immunoblot analyses (**A**) and quantification (**B**) show the impact of spermidine on levels of LC3-II in organs collected from wild-type or MAP1S$^{-/-}$ mice. (**C**, **D**) Spermidine enhances levels of LC3 in wild-type but not MAP1S$^{-/-}$ MEFs. Representative immunoblot results (**C**) and quantification (**D**) show levels of LC3 in MEF cells derived from wild-type or MAP1S$^{-/-}$ mice treated with different concentrations of spermidine for 4 hours. (**E**, **F**) Spermidine-induced enhancement in levels of LC3 depends on MAP1S. Representative immunoblot results show the impact of spermidine on levels of LC3-II in MEF cells (**E**) or primary mouse hepatocytes (**F**) isolated from wild-type or MAP1S$^{-/-}$ mice in the absence or presence of BAF.

from wild-type or MAP1S$^{-/-}$ mice were utilized to confirm the role of MAP1S in spermidine-induced autophagy. Similarly to the results in mice, spermidine-induced enhancement in levels of LC3-II was also observed in wild-type MEF cells but not MAP1S$^{-/-}$ MEF cells (Figure 19C, D). Furthermore, spermidine-induced activation of autophagic flux as indicated by levels of LC3-II in the presence of BAF was observed in wild-type but not MAP1S$^{-/-}$ MEF cells (Figure 19E) or primary mouse hepatocytes (Figure 19F). Therefore, the activation of autophagic flux by spermidine requires the presence of MAP1S.

Spermidine Enhances Acetylation and Stability of MAP1S through HDAC4

To study the mechanism by which spermidine regulates levels of MAP1S protein, levels of acetylated MAP1S acetylation were first examined by immunoprecipitation. Consistent with a previous report (127), spermidine significantly increased levels of acetylated MAP1S (Figure 20A, B). As discussed in chapter II, acetylation is important in regulating the stability of MAP1S protein. Thus, the half-life of MAP1S protein was measured after MEF cells were untreated or treated with spermidine. Enhancement of MAP1S protein stability was observed after spermidine treatment (Figure 20C, D), which confirmed that spermidine enhanced the acetylation and stability of MAP1S protein.

HDAC4 has been identified to regulate the acetylation and protein stability of MAP1S in chapter II. To determine whether spermidine regulates the acetylation and stability of MAP1S through HDAC4, the interaction between HDAC4 and MAP1S in

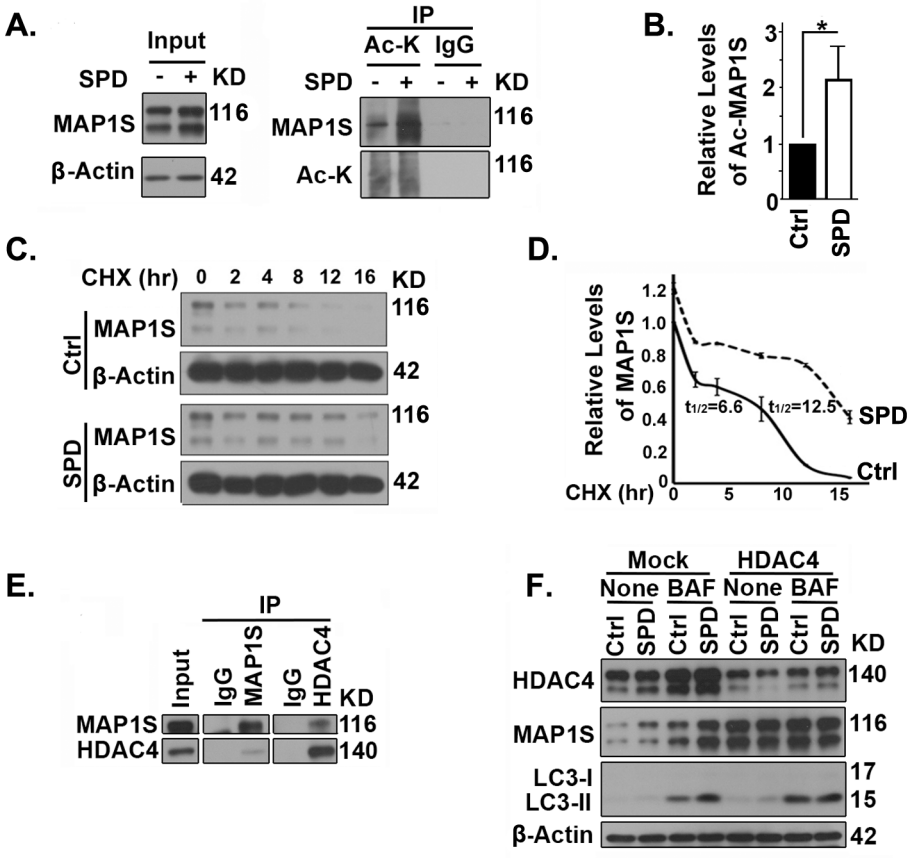

Figure 20. Spermidine Enhances the Acetylation and Stability of MAP1S Protein through HDAC4. (**A**, **B**) Spermidine increases levels of acetylated MAP1S. Representative immunoblot results (**A**) and quantification (**B**) shows the impact of spermidine on acetylated MAP1S in MEF cells. Acetylated MAP1S was precipitated with anti-acetyl-lysine agarose conjugate and immunoblotted with antibodies against MAP1S. (**C**, **D**) Spermidine enhances the stability of MAP1S protein. MEF cells were treated with spermidine, and protein synthesis was terminated with 10 μg/ml cycloheximide (CHX). Cell lysates were collected at indicated time points. Representative immunoblot results (**C**) and quantification (**D**) are shown. The values of t1/2 were the time required for half of MAP1S proteins were degraded. (**E**) HDAC4 interacts with MAP1S. Lysates of HepG2 cells were immunoprecipitated with antibodies against MAP1S or HDAC4, or the respective IgG control. (**F**) Spermidine-induced enhancement in levels of MAP1S and LC3 requires the presence of HDAC4. Representative immunoblot results show the impact of spermidine on levels of MAP1S and LC3 in HeLa cells treated with random (Mock) or HDAC4-specific siRNA in the absence (Ctrl) or presence of BAF.

HepG2 cells was re-confirmed by immunoprecipitation (Figure 20E). Suppression of HDAC4 with specific siRNA led to increased levels of MAP1S protein; while spermidine failed to further induce autophagy activation in HDAC4-suppressed cells (Figure 20F). These results suggest that spermidine enhances the acetylation and stability of MAP1S protein to activate autophagic flux through HDAC4.

Lysine 520 Residue of MAP1S Is Critical for MAP1S to Promote Autophagosomal Degradation in Spermidine-induced Autophagy

Lysine 520 residue (K520) of human MAP1S has been identified as the acetylation lysine site upon exposure to spermidine in the mass spectrometry analyses (127). To explore the role of lysine 520 of MAP1S in spermidine-induced autophagy, a point mutation of lysine 520 to arginine was introduced to establish K520R mutant MAP1S by site-directed mutagenesis. The K520R mutant MAP1S protein exhibited higher levels of expression but lower degrees of interaction with HDAC4 than the wild-type MAP1S protein, although it distributed in the cytoplasm similarly to the wild-type MAP1S (Figure 21A, B).

To study the impact of lysine 520 of MAP1S on autophagy, cells were overexpressed with wild-type or K520R mutant MAP1S in the absence or presence of BAF. Overexpression of the K520R mutant resulted in increased levels of LC3-II and accumulation of RFP-LC3 punctate foci (Figure 21C-F). Autophagy is a dynamic process; increased levels of LC3-II may be a result of activated autophagosomal biogenesis or inhibited autophagosomal degradation. Levels of accumulated LC3-II

remained intact in cells overexpressed with K520R mutant in the presence of lysosome inhibitor BAF (Figure 21C, D), which suggested that K520R mutation inhibited autophagosomal degradation rather than autophagosomal biogenesis.

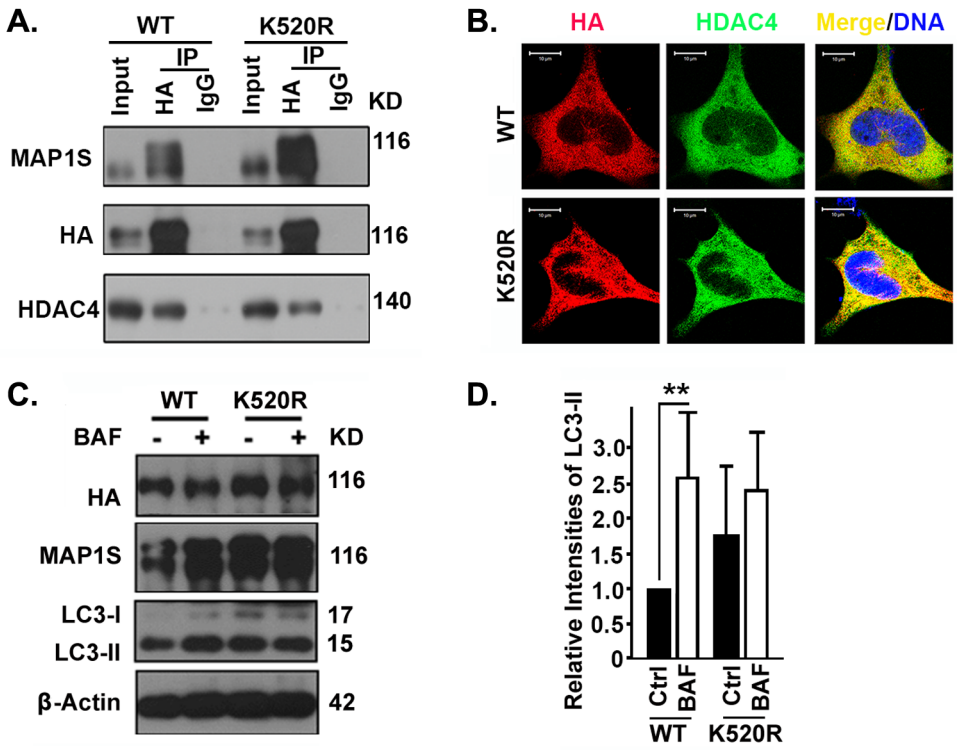

Figure 21. Mutation of MAP1S Lysine 520 Residue Inhibits Autophagy. (**A**) K520R mutant MAP1S has lower affinity with HDAC4 compared to wild-type MAP1S. Lysates of 293T cells transiently expressing HA-fused wild-type or K520R mutant MAP1S were precipitated with HA antibodies or IgG control. (**B**) HDAC4 co-localizes with wild-type or K520R mutant MAP1S in HeLa cells. (**C**-**F**) MAP1S K520R mutation suppresses autophagy degradation. Representative immunoblot results of levels of LC3-II in HeLa cells (**C**) and fluorescent images of RFP-LC3 punctate foci in HeLa cells stably expressing RFP-LC3 (**E**) and the respective quantification (**D**, **F**) are shown.

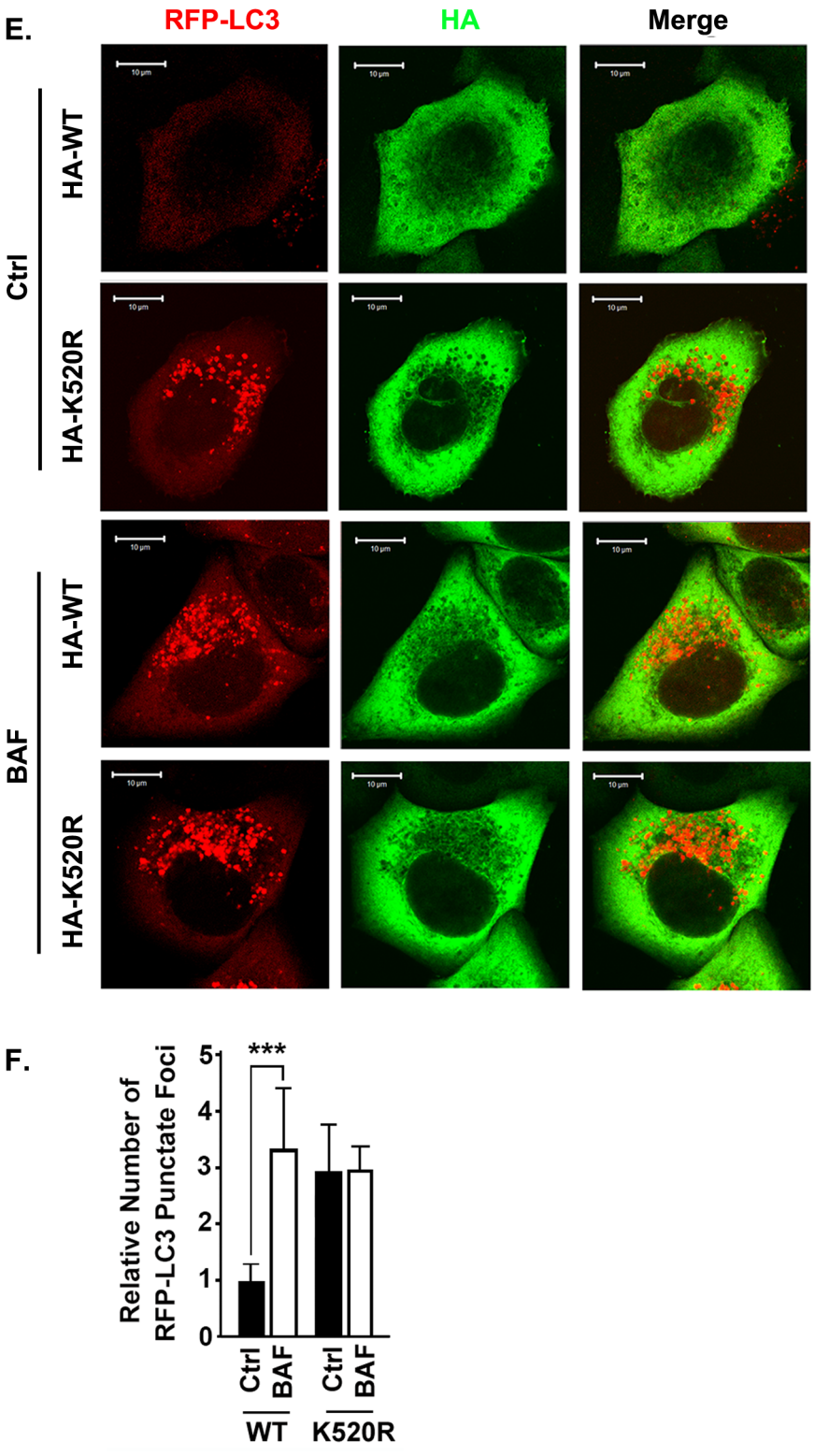

Figure 21. Continued.

Notably, the amount of punctate foci of RFP-LC3 associated with LAMP2-labeled lysosomes in cells expressing K520R mutant was elevated compared to cells expressing wild-type MAP1S (Figure 22A-C). This confirmed that the mutation of lysine 520 in MAP1S reduced the efficiency of autophagosome-lysosome fusion, one of the functions of MAP1S in autophagy (41).

To further test whether the impact of spermidine on autophagy depends on lysine 520 of MAP1S, wild-type or K520R mutant MAP1S was re-expressed in MAP1S$^{-/-}$ MEF cells. Spermidine failed to increase levels of LC3-II in MAP1S$^{-/-}$ MEF cells re-expressed with vector control in the presence of BAF, which indicated that spermidine-induced autophagy was impaired when MAP1S was depleted. Spermidine-induced autophagy was only restored in cells re-expressed with wild-type MAP1S but not K520R mutant MAP1S (Figure 22D, E), suggesting that lysine 520 residue of MAP1S is important for MAP1S to promote autophagosomal degradation in spermidine-induced autophagy.

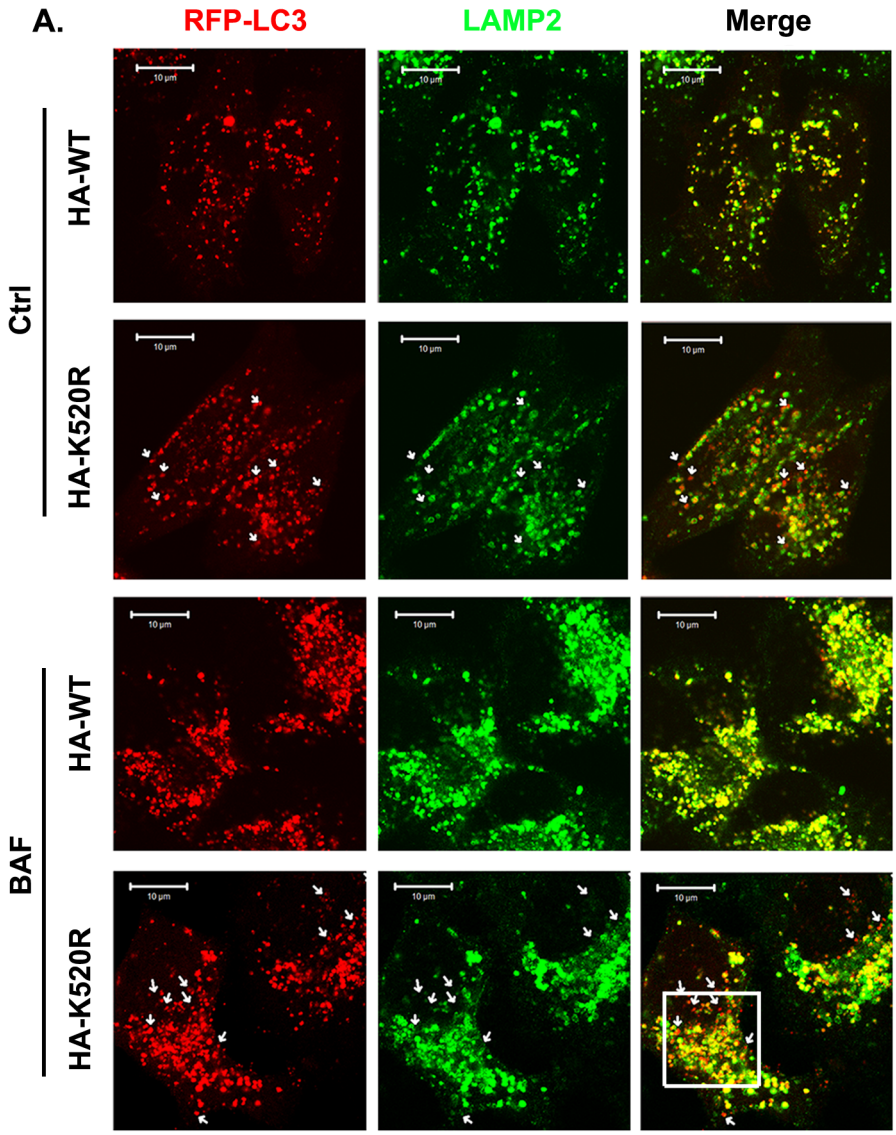

Figure 22. Lysine 520 Residue of MAP1S Is Critical in Spermidine-induced Autophagy. (**A**-**C**) Overexpression of K520R mutant inhibits autophagosome-lysosome fusion. HeLa cells stably expressing RFP-LC3 were transfected with wild-type or K520R mutant MAP1S. Lysosomes were labeled by staining with anti-LAMP2 antibodies. Representative fluorescent images (**A**, **B**) show lysosome-associated (yellow in merge) and lysosome-free RFP-LC3 punctate foci (red spots, some are indicated by white arrows). An enlarged view of lysosome-free RFP-LC3 punctate foci from (**A**) is shown (**B**). Quantification (**C**) shows the percentages of lysosome-free to total RFP-LC3 punctate foci. (**D**, **E**) Wild-type but not K520R mutant MAP1S restores spermidine-induced autophagy in MAP1S$^{-/-}$ MEF cells. Representative immunoblot results (**D**) and quantification (**E**) show the impact of spermidine on levels of LC3 in MAP1S$^{-/-}$ MEF cells re-expressed with HA, or HA-fused wild-type or K520R mutant MAP1S.

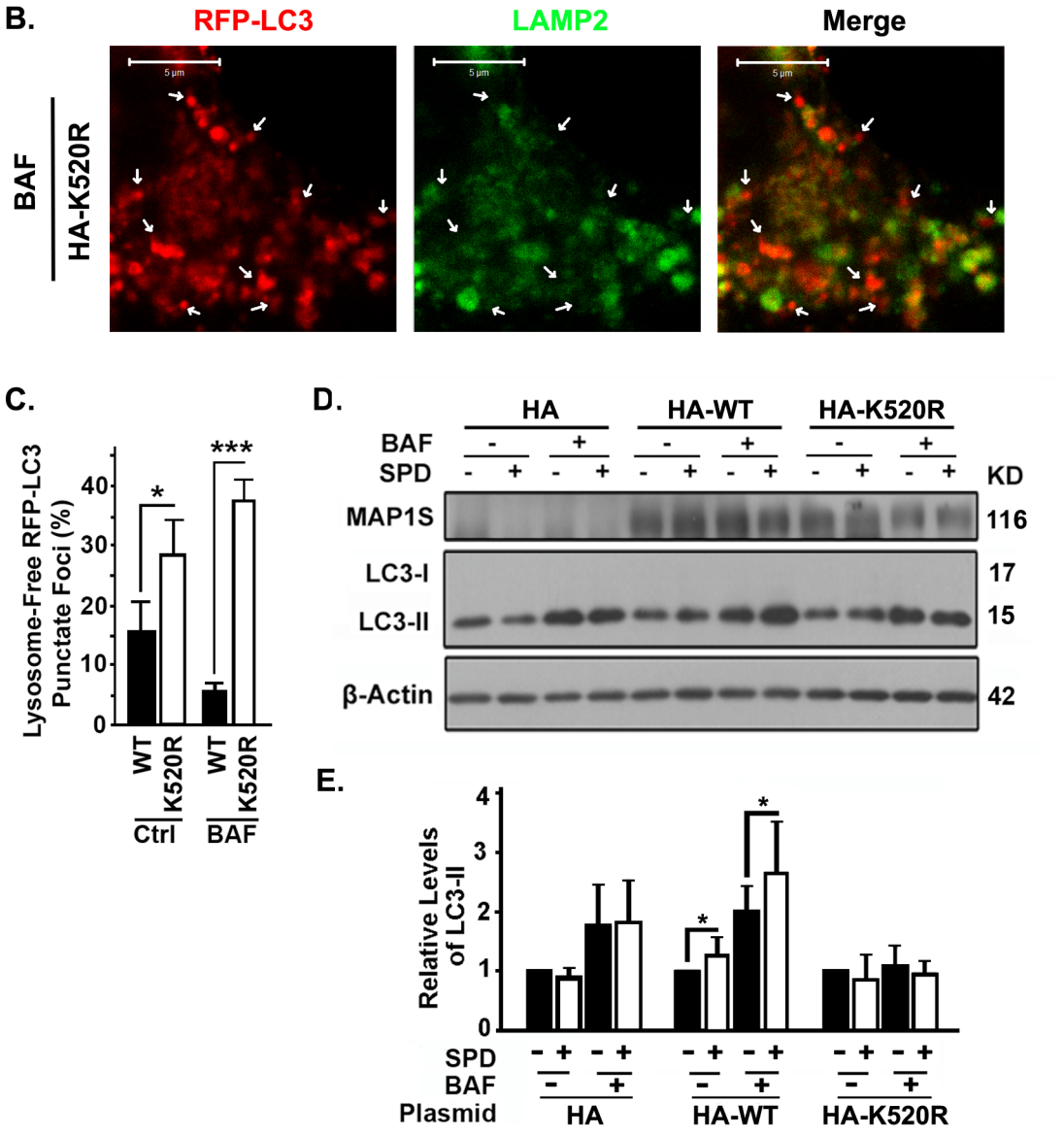

Figure 22. Continued.

Spermidine Dephosphorylates and Suppresses Cytosolic HDAC4

To test whether spermidine enhances the acetylation of MAP1S by negatively regulating HDAC4, MEF or HeLa cells were treated with different concentrations of spermidine for 4 hours. Unexpectedly, spermidine increases levels of HDAC4 protein in both cell lines (Figure 23A, B), as well as in different organs of mice (Figure 23C).

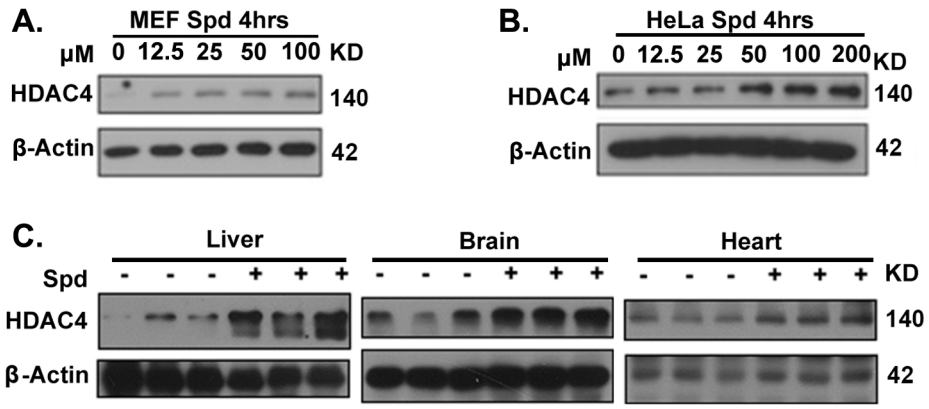

Figure 23. Spermidine Enhances Levels of HDAC4 Protein. (**A**-**C**) Spermidine increases levels of HDAC4. Represent immunoblot results show levels of HDAC4 in MEF (**A**) or HeLa (**B**) cells treated with different concentrations of spermidine for 4 hours, or in organs form 3 pairs of wild-type mice treated with spermidine (**C**).

Furthermore, HeLa or MEF cells transiently overexpressed with GFP-HDAC4 were utilized to monitor the subcellular distribution of HDAC4 after spermidine treatment. Although HDAC4 was overexpressed, spermidine enhanced the nuclear translocation of HDAC4 in different types of cells (Figure 24A-D); and the actual levels of cytosolic HDAC4 were reduced after spermidine treatment (Figure 24E, F). Therefore, spermidine causes depletion of cytosolic HDAC4.

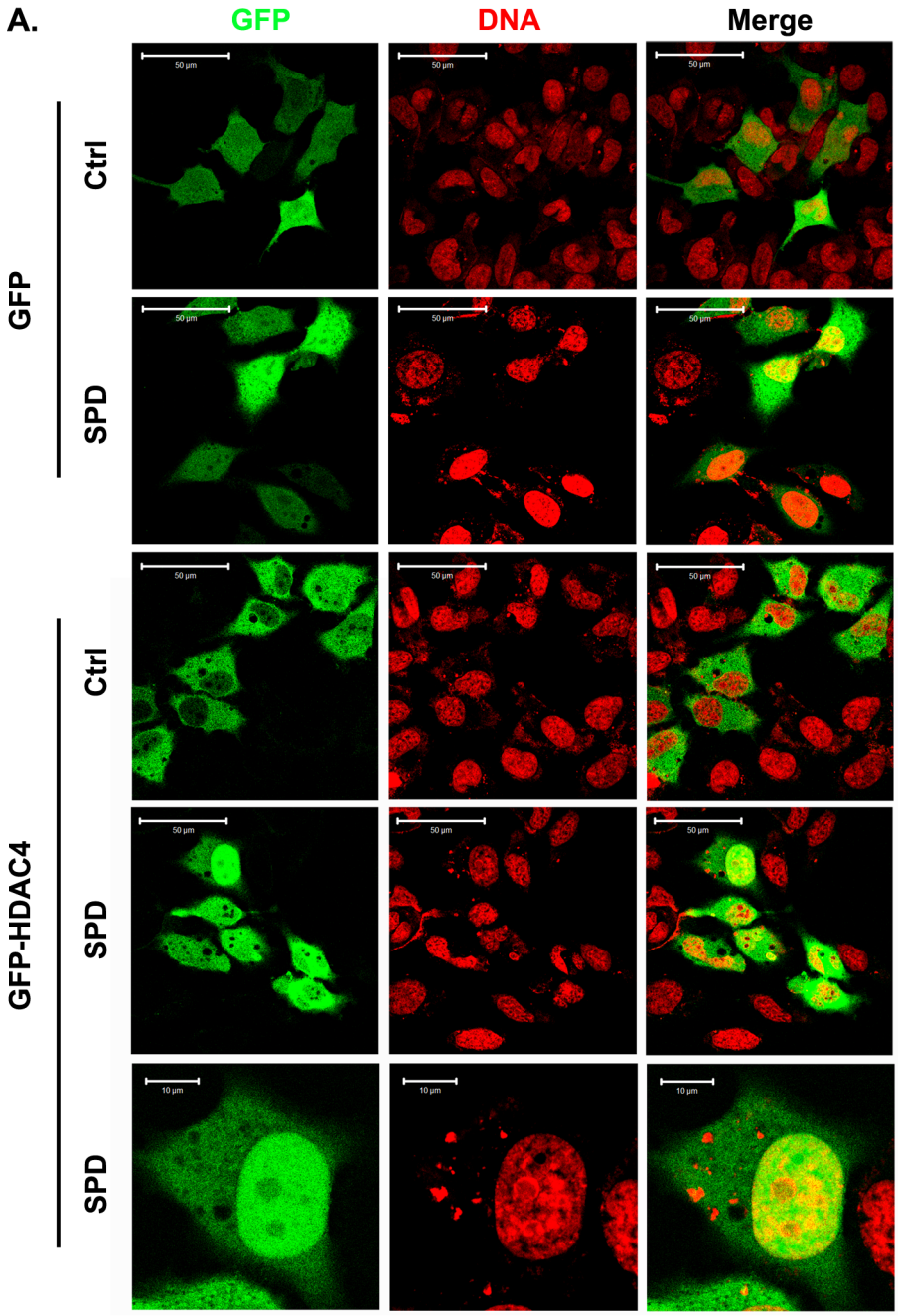

Figure 24. Spermidine Suppresses Cytosolic HDAC4. (**A-D**) Spermidine induces the nuclear translocation of HDAC4. Represent fluorescence microscopic images (**A**, **B**) and quantification (**C**, **D**) of the impact of spermidine on the distribution of GFP-HDAC4 in HeLa (**A**, **C**) or wild-type MEF (**B**, **D**) cells are shown. (**E**, **F**) Spermidine suppresses cytosolic HDAC4. Representative immunoblot results (**E**) and quantification (**F**) show the impact of spermidine on the distribution of HDAC4 in subcellular fractions of HeLa cells.

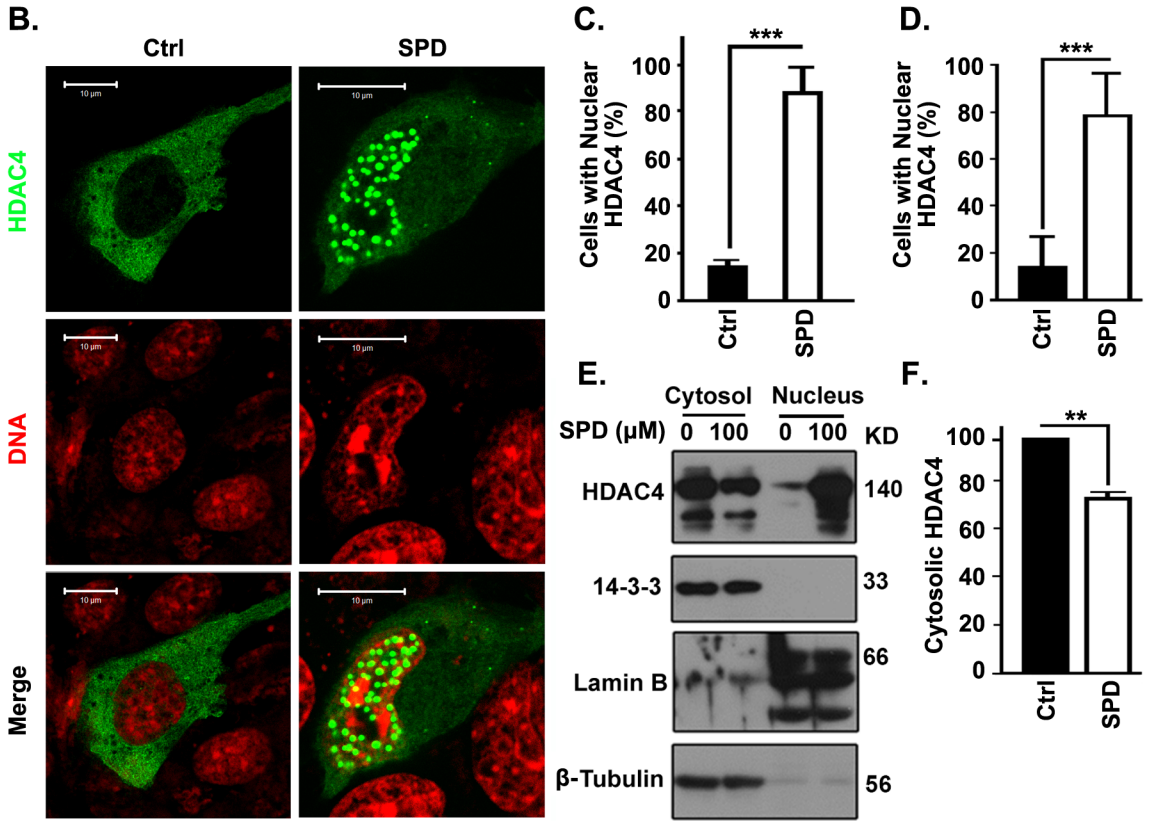

Figure 24. Continued.

As reported previously (128), phosphorylated HDAC4 binds with 14-3-3 and is retained in the cytoplasm; dephosphorylation of HDAC4 on serine 246 and serine 632 is important for HDAC4 nuclear import. Thus, levels of phosphorylated HDAC4 were first examined to understand the nuclear translocation of HDAC4 after spermidine treatment. Decreased levels of phospho-HDAC4 (S246/S632), as well as HDAC4 binding partner 14-3-3, were observed in cells treated with spermidine (Figure 25A, B). In addition, immunoprecipitation results showed that spermidine reduced the association of HDAC4 with 14-3-3 (Figure 25C, D), which confirmed that HDAC4 was released by 14-3-3 and imported to nucleus.

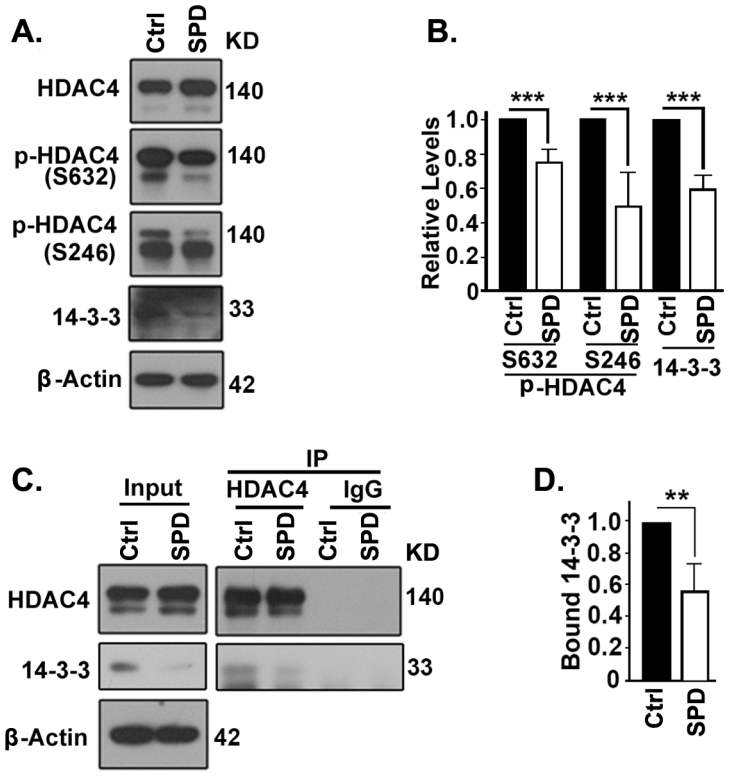

Figure 25. Spermidine Dephosphorylates HDAC4 and Induces the Dissociation of HDAC4 from 14-3-3. (**A**, **B**) Spermidine dephosphorylates HDAC4. Representative immunoblot results (**A**) and quantification (**B**) of the impact of spermidine on levels of total HDAC4, phosphorylated HDAC4, and 14-3-3. (**C**, **D**) Spermidine induces the dissociation of HDAC4 from 14-3-3. Lysates of HeLa cells untreated or treated with spermidine were precipitated with HDAC4 antibodies or IgG control. Representative immunoblot results (**C**) and quantification (**D**) are shown.

Spermidine Reduces the Interaction between HDAC4 and MAP1S

To study the impact of spermidine on HDAC4-MAP1S complex, endogenous MAP1S was first precipitated by MAP1S-specific antibodies. Reduced level of bound HDAC4 was observed after spermidine treatment (Figure 26A, B), which suggested spermidine led to the dissociation of MAP1S from HDAC4. The results were further confirmed in the 293T cells overexpressed with HDAC4 and MAP1S. Less amount of

bounded MAP1S or HDAC4 was pulled down after spermidine treatment with specific antibodies against either HDAC4 or MAP1S for immunoprecipitation (Figure 26C, D). The co-localization of HDAC4 with MAP1S in the cytoplasm was significantly reduced as detected under fluorescence microscope (Figure 26E, F). Thus, spermidine decreases the association of HDAC4 with MAP1S, although total amount of HDAC4 is increased.

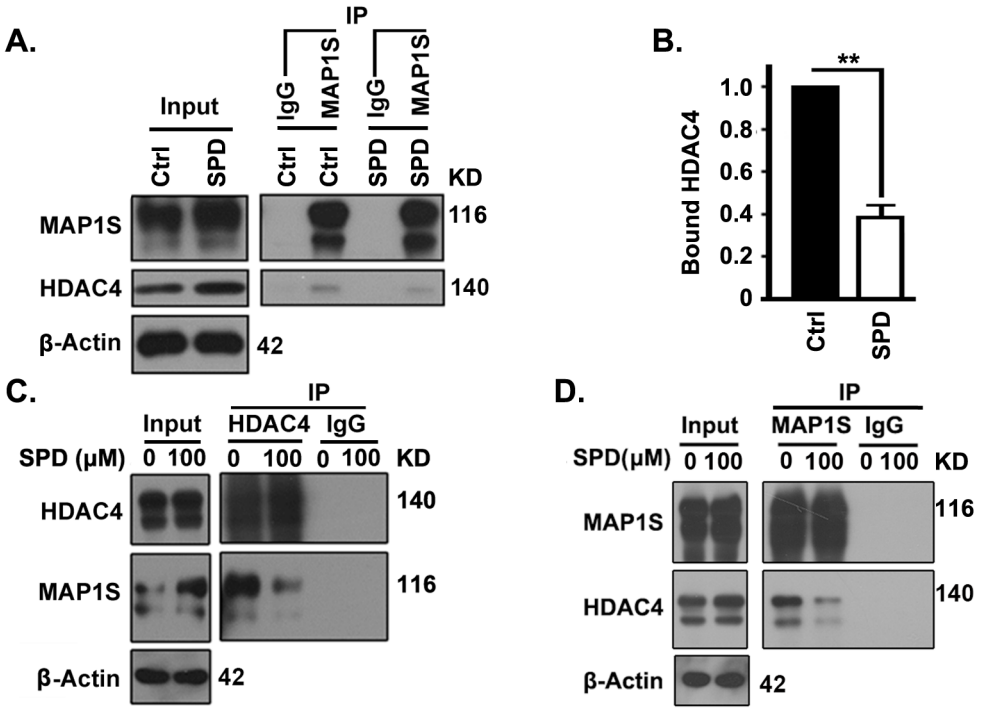

Figure 26. Spermidine Interrupts the Association of HDAC4 with MAP1S. (**A**, **B**) Spermidine induces the dissociation of endogenous HDAC4 from MAP1S. Lysates of HeLa cells untreated or treated with spermidine were precipitated with MAP1S-specific antibodies or IgG control. Representative immunoblot results (**A**) and quantification (**B**) are shown. (**C**, **D**) Spermidine reduces the interaction between exogenous HDAC4 and MAP1S. Lysates of 293T cells transiently overexpressing HDAC4 and MAP1S, treated without or with spermidine, were precipitated with HDAC4- (**C**), MAP1S- (**D**) specific antibodies or the respective IgG control. (**E**, **F**) Spermidine induces HDAC4 nuclear translocation and its dissociation from MAP1S. Representative fluorescent images (**E**) and quantification (**F**) show the co-localization between HDAC4 and MAP1S in the HeLa cells co-overexpressing HDAC4 and MAP1S untreated or treated with spermidine.

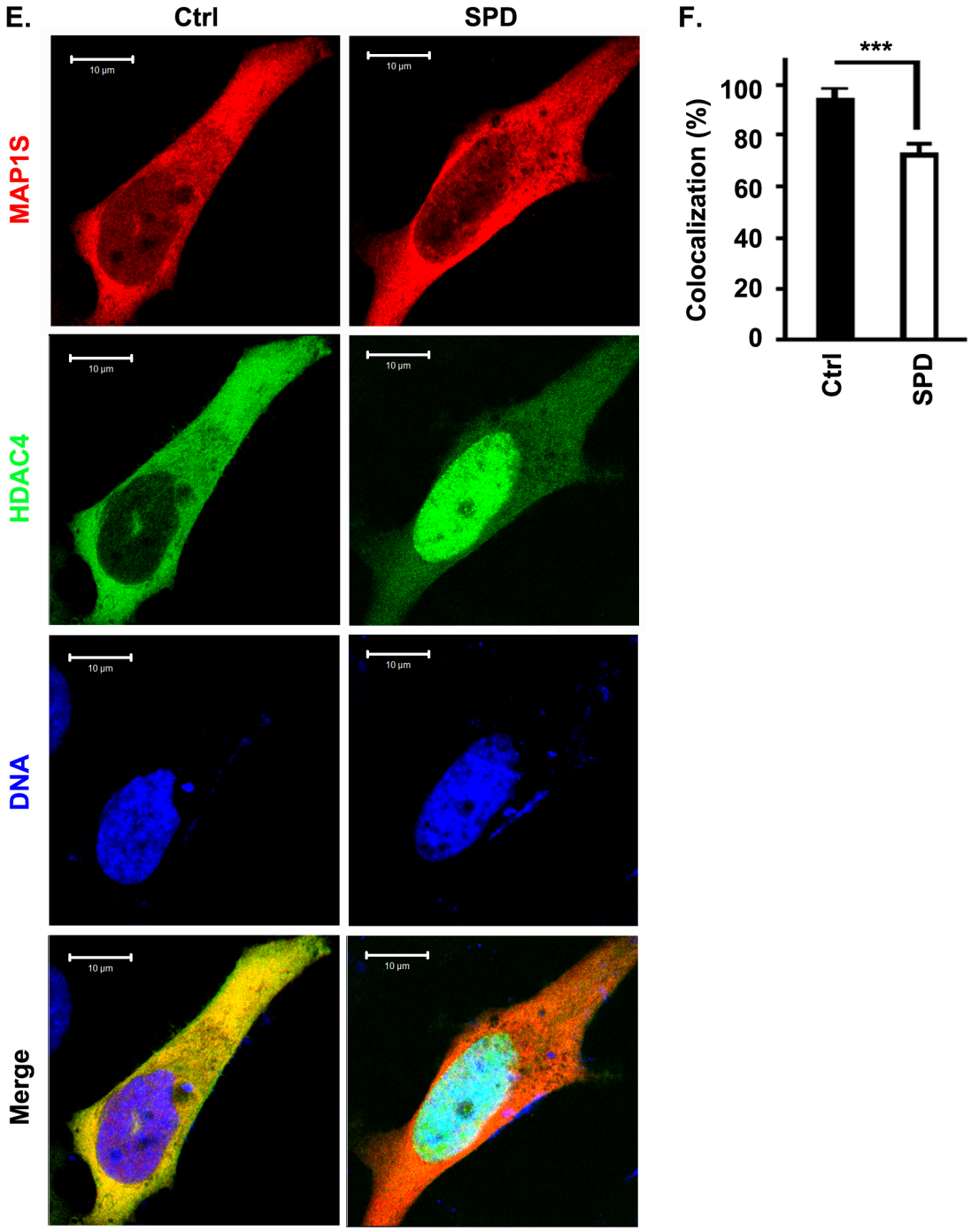

Figure 26. Continued.

Spermidine-induced Expansion of Mouse Lifespans Depends on MAP1S

Spermidine has been shown to increase the lifespans of yeast, nematodes and flies in an autophagy-dependent fashion (51). MAP1S activates autophagy to suppress oxidative stress and sustain the lifespans of mice (4). To study the impact of spermidine

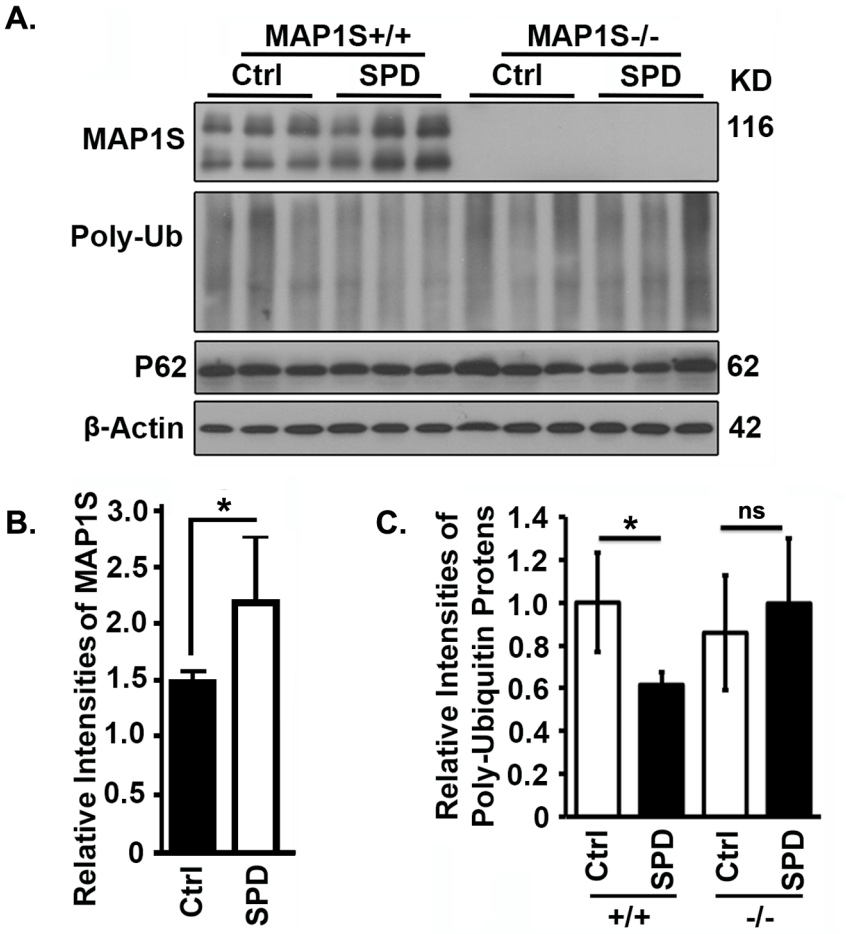

Figure 27. Feeding Mice with Spermidine for One Month Enhances Levels of MAP1S Protein and Autophagy Activity. (**A**-**C**) Feeding mice with spermidine for one month enhances levels of MAP1S protein. Wild-type or MAP1S$^{-/-}$ mice were fed with drinking water or drinking water containing 3 mM spermidine for 1 month. Representative immunoblot results (**A**) and quantification of the relative levels of MAP1S (**B**) or poly-ubiquitin proteins (**C**) of liver lysates are shown.

in vivo, wild-type or MAP1S$^{-/-}$ mice were fed with drinking water or drinking water containing 3 mM spermidine. As expected, feeding mice with spermidine for 1 month enhanced levels of MAP1S and autophagy activity as detected by reduced levels of poly-ubiquitin proteins (Figure 27A-C).

Wild-type mice that were continuously fed with drinking water containing spermidine for 18 months also sustained higher levels of MAP1S compared to wild-type mice fed with drinking water (Figure 28A). Furthermore, mice fed with drinking water containing spermidine exhibited significantly lower levels of oxidative stress in liver tissues than those fed with drinking water (Figure 28B, C).

As previously reported, deletion of MAP1S caused sinusoidal dilation in liver and shortened the median lifespans of mice from 28.0 months (wild-type mice) to 22.4 months (MAP1S$^{-/-}$ mice) (4). Histological examination revealed that spermidine treatment alleviated sinusoidal dilation in wild-type mice but not MAP1S$^{-/-}$ mice (Figure 29A, B). A 25% increase of median survival time from 26.9 months to 33.3 months was observed in wild-type mice fed with drinking water containing spermidine compared to wild-type mice fed with drinking water (Figure 29C, D), corresponding to the increase of human lifespans from 74.7 years to 92.5 years. Elevated oxidative stress and sinusoidal dilation, and reduced median lifespans from 26.9 months to 21.9 months caused by MAP1S deletion were not significantly improved by exposure to spermidine (Figure 28B, C and 29A-D). Thus, spermidine-induced expansion of lifespans depends on MAP1S.

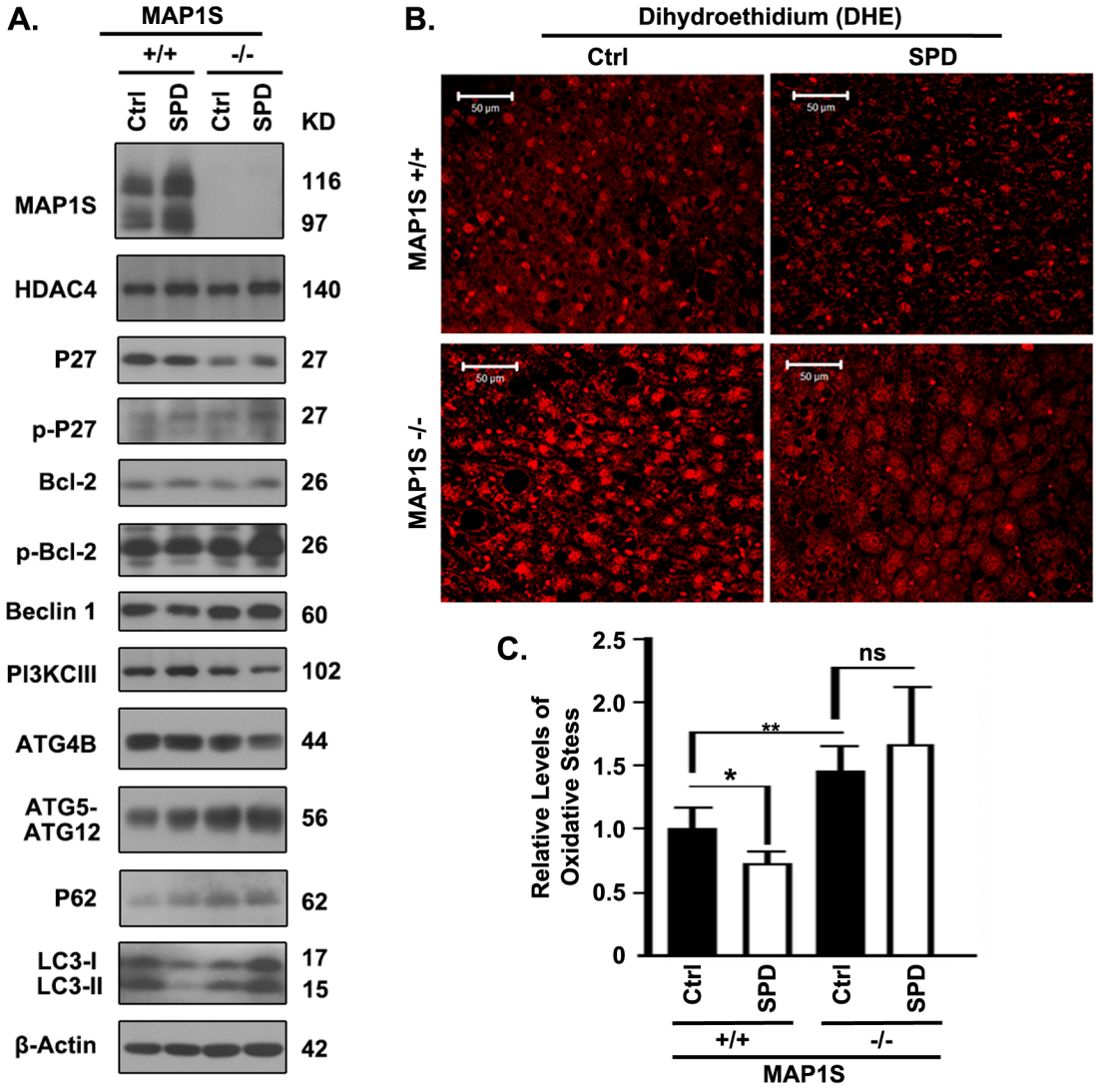

Figure 28. Feeding Mice with Spermidine for Eighteen Months Enhances MAP1S-mediated Autophagy to Suppress Oxidative Stress. (**A**) Feeding mice with spermidine for eighteen months enhances levels of MAP1S protein. Representative immunoblot results show levels of MAP1S and HDAC4 of liver lysates of wild-type or MAP1S$^{-/-}$ mice untreated or treated with spermidine for 18 months. Lysates with the same amount of total proteins were subjected to immunoblot with antibodies against MAP1S, HDAC4, P27, phosphorylated P27 (p-P27), Bcl-2, phosphorylated Bcl-2 (p-Bcl-2), Beclin 1, PI3KCIII, ATG4B, ATG5-ATG12, P62, LC3, or β-Actin. (**B**, **C**) Spermidine suppresses oxidative stress in wild-type mice but not MAP1S$^{-/-}$ mice. Representative DHE staining results (**B**) and quantification (**C**) show levels of oxidative stress among the livers from wild-type or MAP1S$^{-/-}$ mice untreated or treated with spermidine for 18 months.

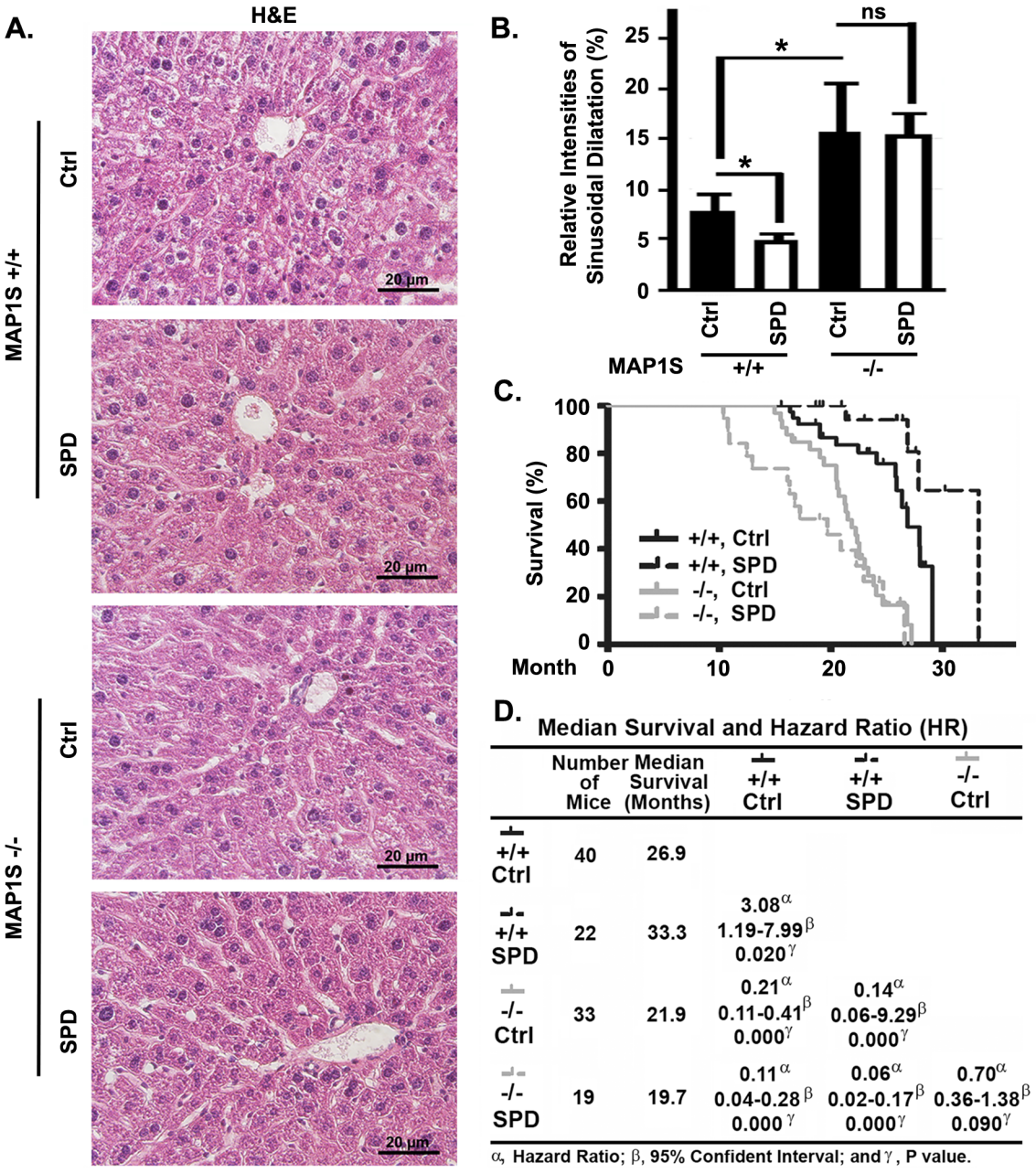

Figure 29. Spermidine-induced Lifespan Extension Is MAP1S-dependent. (**A**, **B**) Spermidine reduces sinusoidal dilatation in wild-type mice but not MAP1S$^{-/-}$ mice. Representative H&E staining results (**A**) and qualification (**B**) show the intensities of sinusoidal dilatation among the liver tissues from wild-type or MAP1S$^{-/-}$ mice untreated or treated with spermidine for 18 months. (**C**, **D**) Spermidine extends lifespans of wild-type mice but not MAP1S$^{-/-}$ mice. The Kaplan-Meier survival curves (**C**) show the survival time of wild-type or MAP1S$^{-/-}$ mice untreated or treated with spermidine. A table (**D**) summarizes median survival and hazard ratio based on the plots in (**C**).

Spermidine Suppresses Hepatocellular Carcinogenesis through MAP1S

Previous results showed that MAP1S$^{-/-}$ mice exposed to diethylnitrosamine (DEN) developed more and larger foci of hepatocellular carcinomas (HCC) than wild-type mice (33). To study the application of spermidine in suppression of tumorigenesis, DEN-induced HCC mouse model was utilized. Wild-type or MAP1S$^{-/-}$ mice were injected with a single dose of DEN on 15-day after birth and examined for tumor development at 7-month-old. It was confirmed that MAP1S suppressed the development of HCC (Figure 30A). Wild-type mice fed with drinking water containing spermidine after DEN injection exhibited reduced liver weights, liver to body weight ratios, and less surface tumors although the body weights were not altered (Figure 30B-E). The typical trabecular hepatocarcinomas as displayed by hematoxylin and eosin (H&E) staining were dramatically reduced (Figure 30F).

Spermidine treatment significantly elevated levels of MAP1S protein (Figure 31A), and suppressed genomic instability as showed by γ-H2AX, the DNA double-strand breaks marker, in the immunohistochemistry staining. The number of cells positively stained with γ-H2AX was significantly decreased in tumor area of wild-type mice fed with drinking water containing spermidine (Figure 31B, C). Depletion of MAP1S promoted the development of HCC in MAP1S$^{-/-}$ mice while further spermidine treatment exhibited no significant reduction in DNA damages and HCC (Figure 30, 31). These results indicate that suppressive role of spermidine in the development of HCC acts through MAP1S.

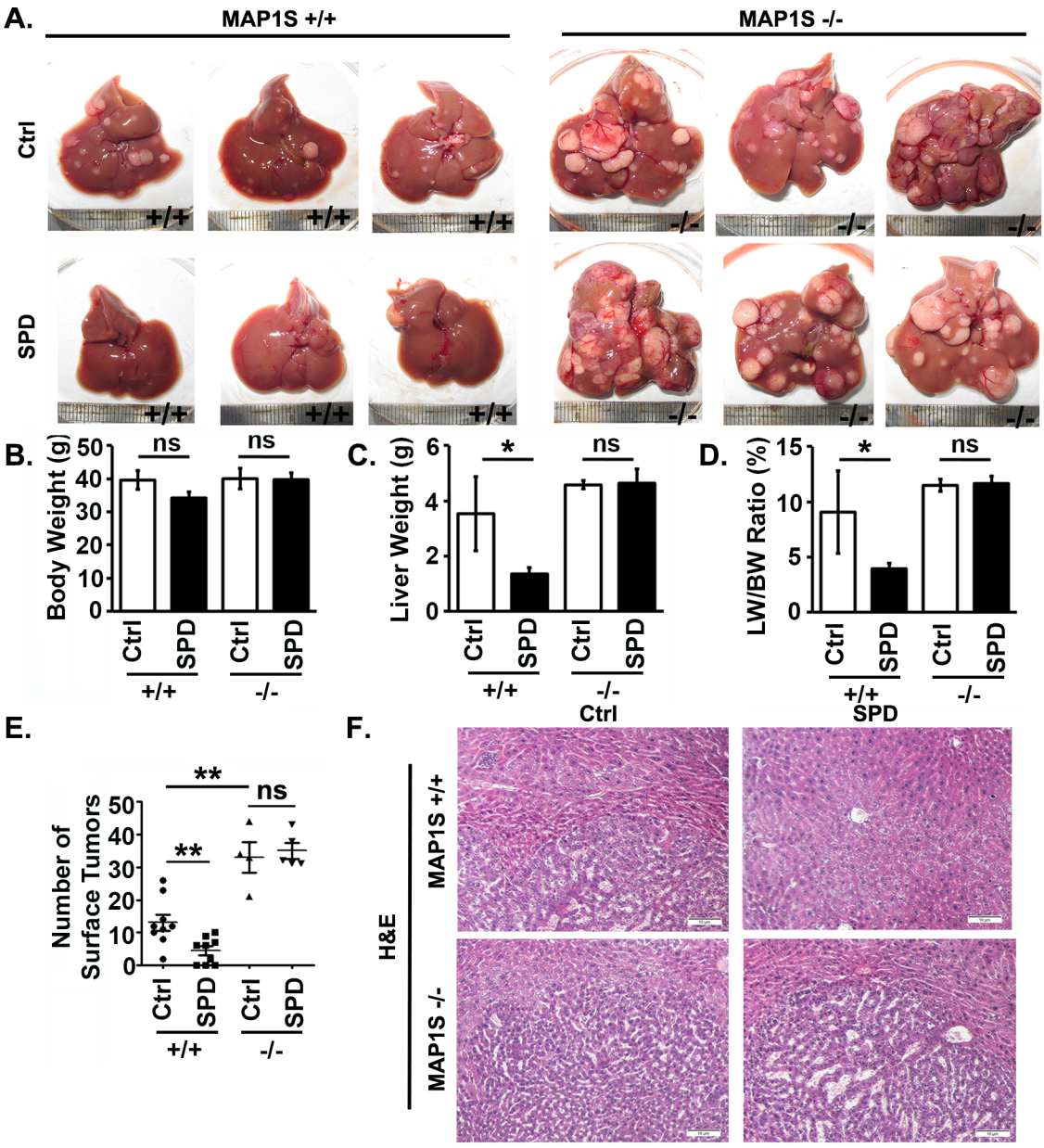

Figure 30. Spermidine Suppresses Diethylnitrosamine-induced Hepatocellular Carcinomas in the Presence of MAP1S. (**A**) Spermidine suppresses the development of DEN-induced hepatocarcinomas in wild-type mice but not MAP1S$^{-/-}$ mice. Representative images show liver tissues from DEN-treated wild-type or MAP1S$^{-/-}$ mice fed with drinking water (Ctrl) or spermidine-containing water (SPD). (**B**-**E**) Plots show the body weights (**B**), the liver weights (**C**), the ratios of liver weight to body weight (**D**) and the number of surface tumors of mice as described in (**A**). (**F**) Spermidine suppresses DEN-induced hepatocarcinomas in wild-type mice but not MAP1S$^{-/-}$ mice. Representative H&E staining results of liver sections of DEN-treated 7-month-old mice as described in (**A**) are shown. Bars in (**F**) were 10 μm.

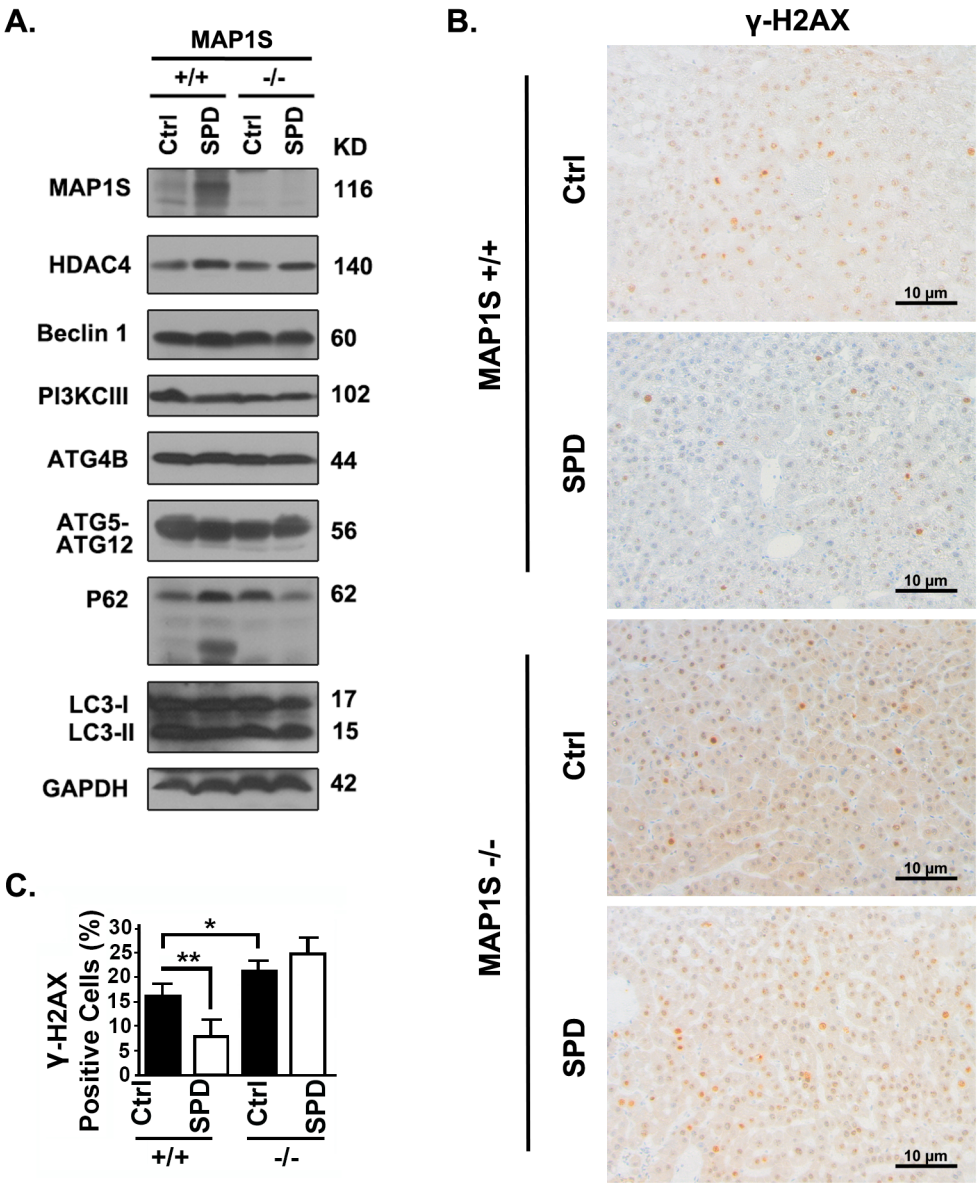

Figure 31. Spermidine Enhances Levels of MAP1S to Suppress Genomic Instability during Hepatocarcinogenesis. (**A**) Spermidine enhances levels of MAP1S in liver tissues from DEN-treated mice. Representative immunoblot results show levels of MAP1S and HDAC4 of liver lysates. Lysates with the same amount of total proteins were subjected to immunoblot analyses with antibodies against MAP1S, HDAC4, Beclin 1, PI3KCIII, ATG4B, ATG5-ATG12, P62, LC3, or GAPDH. (**B**, **C**) Spermidine decreases levels of γ-H2AX in hepatocarcinomas developed in wild-type mice but not MAP1S$^{-/-}$ mice. Representative immunohistochemistry staining results (**B**) and quantification (**C**) show γ-H2AX in tumor area in liver sections of DEN-treated mice.

Discussion

Spermidine is recently identified as an autophagy inducer to prolong lifespans in model systems (51). By inhibiting the enzyme activity of histone acetyltransferases (HAT) and reducing the acetylation of histone H3, spermidine induces global gene silencing without affecting the transcription of *atg* genes (53). Acetylproteomic and phosphoproteomic analyses also indicate that spermidine regulates the post-translational modification of various proteins in the cytoplasm or nucleus respectively through (de)acetylation and (de)phosphorylation processes (127,129). Herein, we demonstrate that spermidine promotes the nuclear translocation of HDAC4 via dephosphorylation on serine 246 and serine 632 of HDAC4, leading to decreased levels of cytosolic HDAC4 and reduction in the association of HDAC4 with MAP1S. Spermidine specifically inhibits the deacetylation of the cytosolic autophagy activator MAP1S to enhance autophagic flux. Though the mechanism by which spermidine regulates HDAC4 dephosphorylation remains unclear so far, protein phosphatase-2A (PP2A) is considered to be a potential regulator of spermidine-induced HDAC4 dephosphorylation. PP2A is an identified phosphatase that dephosphorylates HDAC4 and regulates HDAC4 nuclear import as previously reported (67). Spermidine may induce the dephosphorylation of HDAC4 through activation of PP2A (130). Other evidence suggests that suppression of LKB1-AMPK dramatically reduces levels of phosphorylated HDAC4 (131). Spermidine shows no impact on the phosphorylation of mTOR substrate, so that autophagy initiation through the LKB1-AMPK-mTOR pathway is not affected by spermidine (127), which implies spermidine may only alter the HDAC4-specific activity of LKB1.

Spermidine enhances the acetylation of MAP1S on lysine 520 as indicated in the mass spectrometry analyses (127). Our study shows that lysine 520 residue of MAP1S is critical in spermidine-induced autophagy by promoting autophagosome-lysosome fusion process. Though lysine 520 is not localized in the HDAC4-binding domain of MAP1S, mutation of lysine 520 reduces the interaction between MAP1S and HDAC4. Hence, lysine 520 seems to be important in maintaining protein structure in that future study may be focused on the function of acetylation on the lysine 520 of MAP1S.

In addition to extending lifespans in yeast, nematodes and flies, spermidine has been reported to reactivate autophagy to ameliorate myopathic defects of collagen-deficient mice (132). MAP1S-mediated autophagy is positively related to longevity. MAP1S activates autophagy to suppress oxidative stress and sustain the lifespans of mice. MAP1S deficient mice have defects in autophagy and exhibit dramatically shortened lifespans (4). Here, we, for the first time, show that spermidine treatment enhances MAP1S-mediated autophagy, leading to significantly extended lifespans of wild-type mice. The results indicate that mice fed with drinking water containing spermidine have prolonged lifespans than those of the mice fed with drinking water. The median survival has increased from 26.9 months to 33.3 months after spermidine treatment. Such an extension of lifespans in mice equals an increase of lifespans from 74.7 years to 92.5 years in humans. Short mouse lifespans are correlated with low levels of autophagy activity, high levels of oxidative stress, and high degrees of sinusoidal dilatation, as previously reported (4). Our results discover that long-term of spermidine treatment enhances levels of MAP1S protein together with other autophagy-relevant

proteins including class III PI3K, ATG4B, ATG5-12, suggesting that spermidine regulates multiple autophagy-relevant proteins that coordinately enhance autophagy activity. Autophagy defects lead to enhancement of oxidative stress (15). Mice fed with drinking water containing spermidine have high levels of autophagy activity and exhibit low levels of oxidative stress in the liver tissues than those of the mice fed with drinking water. Sinusoidal dilatation is a type of vascular liver lesions that is characterized by widening of hepatic capillaries (4,133). It impairs contractile properties of hepatic capillaries and associates with inflammatory hepatocellular adenoma which is formerly known as telangiectatic focal nodular hyperplasia (134,135). Mice fed with drinking water containing spermidine display low levels of sinusoidal dilatation in the liver tissues than those of the mice fed with drinking water, suggesting that spermidine maintains liver function to prolong lifespans.

Besides, our study shows that spermidine suppresses hepatocarcinomas in a DEN-induced mouse model. After exposure to carcinogen, mice fed with drinking water containing spermidine have lower incidence of HCC and develop less malignant tumor than those of the mice fed with drinking water. MAP1S-mediated autophagy removes aggresomes that induce oxidative stress and trigger genomic instability. MAP1S deficient mice have autophagy defects and develop more malignant tumor in DEN-induced mouse model, which suggests the importance of MAP1S in tumor suppression (33). Long-term feeding of spermidine in DEN-treated mice significantly enhances levels of MAP1S protein other than class III PI3K, ATG4B, and ATG5-12, which is different from the results in the longevity study. This points out the unique role of

MAP1S-mediated autophagy in tumor suppression. Currently, most HCC patients are diagnosed at late-stage. Thus, it is important to explore the effect of spermidine on advanced HCC as well as HCC prevention in the further study. Since spermidine is a natural product plentiful in various kinds of food, consuming spermidine via regular diet or supplements may provide a novel paradigm to prevent or treat HCC in a safe and cost-effective way.

Notably, all the impacts of spermidine on lifespan extension and HCC suppression depend on the presence of MAP1S, and are abolished in the MAP1S deficient mice. Although other biological function of spermidine may exist, the major role of spermidine in longevity and tumor suppression is mediated by MAP1S-mediated autophagy. Therefore, activation of MAP1S-mediated autophagy provides a novel strategy to enhance longevity and suppress tumorigenesis.

CHAPTER V

CONCLUSIONS

Autophagy is a cellular catabolic machinery to clean up dysfunctional organelles, misfolded proteins and aggresomes through lysosome-mediated degradation. Autophagy also serves as a major mechanism that maintains homeostasis under cellular stress, including nutrient fluctuation, growth factor deprivation, hypoxia, etc. By removing damaged and harmful organelles that produce reactive oxygen species (ROS) and cytotoxic aggregated proteins, autophagy reduces cellular damage and further protects genomic stability. Aging and aging-associated pathologies occur as a result of the accumulation of cellular damage. Induction of autophagy is a novel strategy to prolong lifespans and suppress aging-associated diseases, such as neurodegenerative diseases and cancers.

Understanding the molecular mechanism of autophagy is essential for discovery of new targets to manipulate autophagy activity. As a novel microtubule-associated autophagy activator, MAP1S has attracted our attention to explore its molecular detail in regulating autophagy. MAP1S can directly enhance autophagy by interacting with autophagosome-associated LC3 to promote autophagosome formation and transportation along microtubule; and may also indirectly enhance autophagy initiation by sustaining levels of Bcl-2 and P27. In this study, we have identified HDAC4 as the upstream regulator of MAP1S and determined the mechanism that MAP1S is regulated through acetylation and deacetylation process. Acetylation of MAP1S maintains its protein

stability. Particularly, acetylation on the lysine 520 residue of MAP1S is critical in autophagosome-lysosome fusion process. MAP1S co-localizes with HDAC4 in the cytoplasm, and interacts with HDAC4 through an HDAC4-binding domain (HBD) which is the overlapping region between the heavy chain (HC) and short chain (SC) of MAP1S. HDAC4 negatively regulates MAP1S via deacetylation, leading to the destabilization of MAP1S protein. Overexpression of HDAC4 decreases levels of MAP1S protein and suppresses MAP1S-mediated autophagy. Inhibition of HDAC4 enhances levels of MAP1S protein and promotes MAP1S-mediated autophagy.

Huntington's disease is caused by the accumulation of toxic mutant Huntingtin (mHTT) aggregates that leads to neurodegeneration. Autophagy controls the degradation of mHTT aggregates and is one of the potential treatments for the disease. HDAC4 associates with cytoplasmic mHTT aggregates and is suggested to be a target to ameliorate neurodegeneration. In this study, we have elucidated the mechanism by which HDAC4 regulates mHTT aggregation and discovered a novel approach to alleviate mHTT aggregation. HDAC4 destabilizes MAP1S through direct interaction and deacetylation, and further suppresses MAP1S-mediated autophagic clearance of mHTT aggregates. Overexpression of HBD blocks the interaction between HDAC4 and MAP1S, promotes the stabilization of MAP1S protein and activates MAP1S-mediated autophagic turnover of mHTT. In addition to HDAC4 reduction, interruption of the specific interaction between HDAC4 and MAP1S is a new therapeutic strategy to degrade cytoplasmic mHTT aggregates and treat Huntington's disease.

Spermidine is a polyamine that extends lifespans through autophagy induction in multiple organisms. As a natural product highly contained in wheat germ, citrus fruits and soybeans, spermidine enhances autophagy activity and may be a potential treatment for lifespan extension or tumor suppression. In this study, we have deciphered the essential role of MAP1S in spermidine-induced autophagy and explored the suppressive impact of spermidine on hepatocellular carcinogenesis. Spermidine induces autophagy through a MAP1S-dependent mechanism. By dephosphorylating HDAC4 on serine 246 and serine 632, spermidine leads to the release of HDAC4 from 14-3-3 and HDAC4 nuclear localization. Decreased cytosolic level of HDAC4 attenuates the interaction between HDAC4 and MAP1S. As MAP1S is dissociated from HDAC4, the acetylation of MAP1S is maintained for the stabilization of MAP1S protein. Enhancement in levels of MAP1S accelerates autophagosomal formation and autolysosomal degradation. In addition, spermidine induces acetylation on lysine 520 residue of MAP1S protein to promote autophagosome-lysosome fusion. Long-term treatment of spermidine enhances levels of MAP1S protein and autophagy activity to reduce cellular oxidative stress in mice. In wild-type mice, spermidine prolongs lifespans with an increment of 6 months in median survival time, and suppresses diethylnitrosamine-induced hepatocellular carcinomas. Depletion of MAP1S impairs spermidine-induced autophagy, which further results in the impact of spermidine on lifespan extension and tumor suppression abolished in the $MAP1S^{-/-}$ mice. This study reveals that application of spermidine to activate MAP1S-mediated autophagy is a promising strategy to suppress aging and hepatocarcinogenesis in human.

Overall, our study unravels the mechanism that MAP1S is negatively regulated by HDAC4 via deacetylation, and demonstrates the significant impact of activating MAP1S-mediated autophagy by HDAC4 inhibition on alleviating Huntington's diseases and suppressing hepatocellular carcinogenesis (Figure 32).

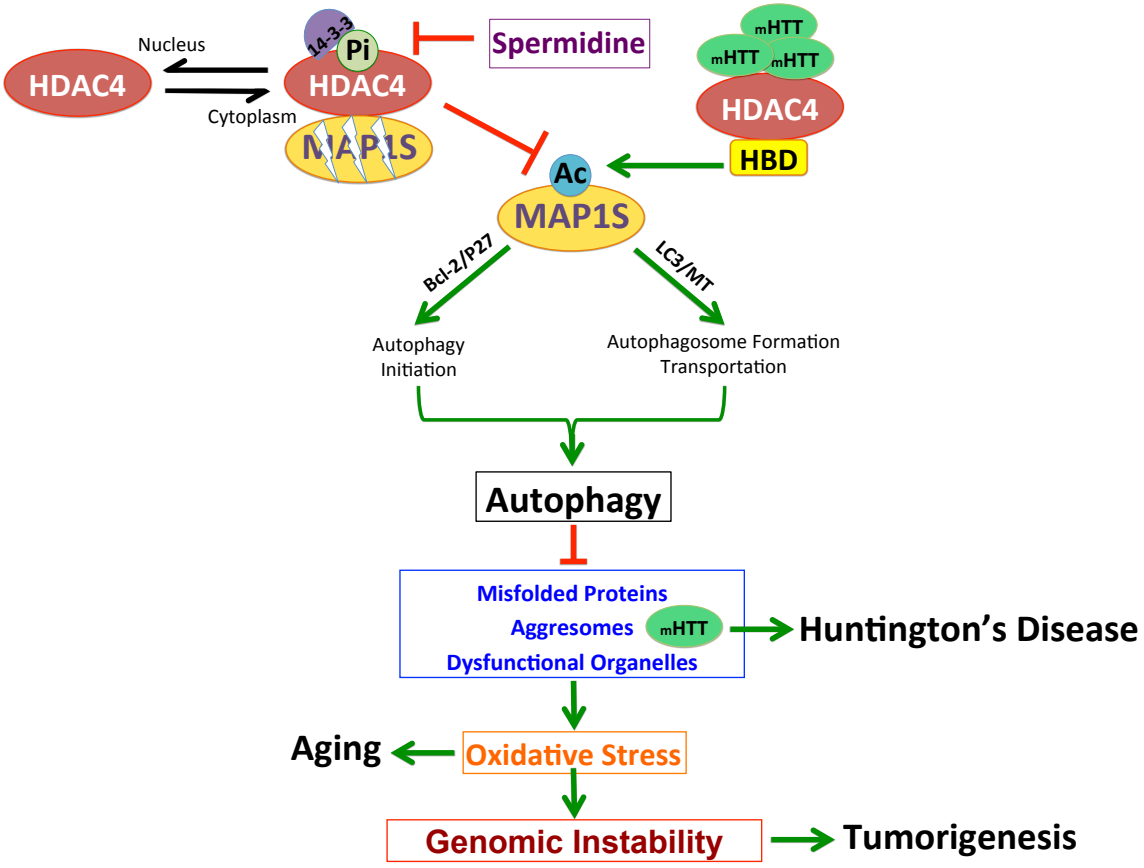

Figure 32. Proposed Model of Activation of MAP1S-mediated Autophagy by Inhibiting HDAC4 in Suppressing Aging and Aging-associated Diseases.

REFERENCES

1. Lopez, A. D., Mathers, C. D., Ezzati, M., Jamison, D. T., and Murray, C. J. (2006) Global and regional burden of disease and risk factors, 2001: systematic analysis of population health data. *Lancet (London, England)* **367**, 1747-1757
2. Collaborators., G. M. a. C. o. D. (2015) Global, regional, and national age-sex specific all-cause and cause-specific mortality for 240 causes of death, 1990-2013: a systematic analysis for the Global Burden of Disease Study 2013. *Lancet (London, England)* **385**, 117-171
3. Lopez-Otin, C., Blasco, M. A., Partridge, L., Serrano, M., and Kroemer, G. (2013) The hallmarks of aging. *Cell* **153**, 1194-1217
4. Li, W., Zou, J., Yue, F., Song, K., Chen, Q., McKeehan, W. L., Wang, F., Xu, G., Huang, H., Yi, J., and Liu, L. (2016) Defects in MAP1S-mediated autophagy cause reduction in mouse lifespans especially when fibronectin is overexpressed. *Aging Cell* **15**, 370-379
5. Duve, C. D., and Wattiaux, R. (1966) Functions of lysosomes. *Annual Review of Physiology* **28**, 435-492
6. Xie, R., Nguyen, S., McKeehan, W. L., and Liu, L. (2010) Acetylated microtubules are required for fusion of autophagosomes with lysosomes. *BMC Cell Biology* **11**, 89
7. Mizushima, N. (2007) Autophagy: process and function. *Genes & Development* **21**, 2861-2873

8. Jung, C. H., Ro, S. H., Cao, J., Otto, N. M., and Kim, D. H. (2010) mTOR regulation of autophagy. *FEBS Letter* **584**, 1287-1295

9. Kihara, A., Noda, T., Ishihara, N., and Ohsumi, Y. (2001) Two distinct Vps34 phosphatidylinositol 3-kinase complexes function in autophagy and carboxypeptidase Y sorting in Saccharomyces cerevisiae. *The Journal of Cell Biology* **152**, 519-530

10. Geng, J., and Klionsky, D. J. (2008) The Atg8 and Atg12 ubiquitin-like conjugation systems in macroautophagy. 'Protein modifications: beyond the usual suspects' review series. *EMBO Reports* **9**, 859-864

11. He, C., and Klionsky, D. J. (2009) Regulation mechanisms and signaling pathways of autophagy. *Annual Review of Genetics* **43**, 67-93

12. Mizushima, N., Kuma, A., Kobayashi, Y., Yamamoto, A., Matsubae, M., Takao, T., Natsume, T., Ohsumi, Y., and Yoshimori, T. (2003) Mouse Apg16L, a novel WD-repeat protein, targets to the autophagic isolation membrane with the Apg12-Apg5 conjugate. *Journal of Cell Science* **116**, 1679-1688

13. Kabeya, Y., Mizushima, N., Ueno, T., Yamamoto, A., Kirisako, T., Noda, T., Kominami, E., Ohsumi, Y., and Yoshimori, T. (2000) LC3, a mammalian homologue of yeast Apg8p, is localized in autophagosome membranes after processing. *The EMBO Journal* **19**, 5720-5728

14. Klionsky, D. J., Abdalla, F. C., Abeliovich, H., Abraham, R. T., Acevedo-Arozena, A., Adeli, K., Agholme, L., Agnello, M., Agostinis, P., Aguirre-Ghiso, J. A., Ahn, H. J., Ait-Mohamed, O., Ait-Si-Ali, S., Akematsu, T., Akira, S., Al-

Younes, H. M., Al-Zeer, M. A., Albert, M. L., Albin, R. L., Alegre-Abarrategui, J., Aleo, M. F., Alirezaei, M., Almasan, A., Almonte-Becerril, M., Amano, A., Amaravadi, R., Amarnath, S., Amer, A. O., Andrieu-Abadie, N., Anantharam, V., Ann, D. K., Anoopkumar-Dukie, S., Aoki, H., Apostolova, N., Arancia, G., Aris, J. P., Asanuma, K., Asare, N. Y., Ashida, H., Askanas, V., Askew, D. S., Auberger, P., Baba, M., Backues, S. K., Baehrecke, E. H., Bahr, B. A., Bai, X. Y., Bailly, Y., Baiocchi, R., Baldini, G., Balduini, W., Ballabio, A., Bamber, B. A., Bampton, E. T., Banhegyi, G., Bartholomew, C. R., Bassham, D. C., Bast, R. C., Jr., Batoko, H., Bay, B. H., Beau, I., Bechet, D. M., Begley, T. J., Behl, C., Behrends, C., Bekri, S., Bellaire, B., Bendall, L. J., Benetti, L., Berliocchi, L., Bernardi, H., Bernassola, F., Besteiro, S., Bhatia-Kissova, I., Bi, X., Biard-Piechaczyk, M., Blum, J. S., Boise, L. H., Bonaldo, P., Boone, D. L., Bornhauser, B. C., Bortoluci, K. R., Bossis, I., Bost, F., Bourquin, J. P., Boya, P., Boyer-Guittaut, M., Bozhkov, P. V., Brady, N. R., Brancolini, C., Brech, A., Brenman, J. E., Brennand, A., Bresnick, E. H., Brest, P., Bridges, D., Bristol, M. L., Brookes, P. S., Brown, E. J., Brumell, J. H., Brunetti-Pierri, N., Brunk, U. T., Bulman, D. E., Bultman, S. J., Bultynck, G., Burbulla, L. F., Bursch, W., Butchar, J. P., Buzgariu, W., Bydlowski, S. P., Cadwell, K., Cahova, M., Cai, D., Cai, J., Cai, Q., Calabretta, B., Calvo-Garrido, J., Camougrand, N., Campanella, M., Campos-Salinas, J., Candi, E., Cao, L., Caplan, A. B., Carding, S. R., Cardoso, S. M., Carew, J. S., Carlin, C. R., Carmignac, V., Carneiro, L. A., Carra, S., Caruso, R. A., Casari, G., Casas, C., Castino, R., Cebollero, E., Cecconi, F., Celli, J.,

Chaachouay, H., Chae, H. J., Chai, C. Y., Chan, D. C., Chan, E. Y., Chang, R. C., Che, C. M., Chen, C. C., Chen, G. C., Chen, G. Q., Chen, M., Chen, Q., Chen, S. S., Chen, W., Chen, X., Chen, X., Chen, X., Chen, Y. G., Chen, Y., Chen, Y., Chen, Y. J., Chen, Z., Cheng, A., Cheng, C. H., Cheng, Y., Cheong, H., Cheong, J. H., Cherry, S., Chess-Williams, R., Cheung, Z. H., Chevet, E., Chiang, H. L., Chiarelli, R., Chiba, T., Chin, L. S., Chiou, S. H., Chisari, F. V., Cho, C. H., Cho, D. H., Choi, A. M., Choi, D., Choi, K. S., Choi, M. E., Chouaib, S., Choubey, D., Choubey, V., Chu, C. T., Chuang, T. H., Chueh, S. H., Chun, T., Chwae, Y. J., Chye, M. L., Ciarcia, R., Ciriolo, M. R., Clague, M. J., Clark, R. S., Clarke, P. G., Clarke, R., Codogno, P., Coller, H. A., Colombo, M. I., Comincini, S., Condello, M., Condorelli, F., Cookson, M. R., Coombs, G. H., Coppens, I., Corbalan, R., Cossart, P., Costelli, P., Costes, S., Coto-Montes, A., Couve, E., Coxon, F. P., Cregg, J. M., Crespo, J. L., Cronje, M. J., Cuervo, A. M., Cullen, J. J., Czaja, M. J., D'Amelio, M., Darfeuille-Michaud, A., Davids, L. M., Davies, F. E., De Felici, M., de Groot, J. F., de Haan, C. A., De Martino, L., De Milito, A., De Tata, V., Debnath, J., Degterev, A., Dehay, B., Delbridge, L. M., Demarchi, F., Deng, Y. Z., Dengjel, J., Dent, P., Denton, D., Deretic, V., Desai, S. D., Devenish, R. J., Di Gioacchino, M., Di Paolo, G., Di Pietro, C., Diaz-Araya, G., Diaz-Laviada, I., Diaz-Meco, M. T., Diaz-Nido, J., Dikic, I., Dinesh-Kumar, S. P., Ding, W. X., Distelhorst, C. W., Diwan, A., Djavaheri-Mergny, M., Dokudovskaya, S., Dong, Z., Dorsey, F. C., Dosenko, V., Dowling, J. J., Doxsey, S., Dreux, M., Drew, M. E., Duan, Q., Duchosal, M. A., Duff, K., Dugail, I., Durbeej, M., Duszenko, M.,

Edelstein, C. L., Edinger, A. L., Egea, G., Eichinger, L., Eissa, N. T., Ekmekcioglu, S., El-Deiry, W. S., Elazar, Z., Elgendy, M., Ellerby, L. M., Eng, K. E., Engelbrecht, A. M., Engelender, S., Erenpreisa, J., Escalante, R., Esclatine, A., Eskelinen, E. L., Espert, L., Espina, V., Fan, H., Fan, J., Fan, Q. W., Fan, Z., Fang, S., Fang, Y., Fanto, M., Fanzani, A., Farkas, T., Farre, J. C., Faure, M., Fechheimer, M., Feng, C. G., Feng, J., Feng, Q., Feng, Y., Fesus, L., Feuer, R., Figueiredo-Pereira, M. E., Fimia, G. M., Fingar, D. C., Finkbeiner, S., Finkel, T., Finley, K. D., Fiorito, F., Fisher, E. A., Fisher, P. B., Flajolet, M., Florez-McClure, M. L., Florio, S., Fon, E. A., Fornai, F., Fortunato, F., Fotedar, R., Fowler, D. H., Fox, H. S., Franco, R., Frankel, L. B., Fransen, M., Fuentes, J. M., Fueyo, J., Fujii, J., Fujisaki, K., Fujita, E., Fukuda, M., Furukawa, R. H., Gaestel, M., Gailly, P., Gajewska, M., Galliot, B., Galy, V., Ganesh, S., Ganetzky, B., Ganley, I. G., Gao, F. B., Gao, G. F., Gao, J., Garcia, L., Garcia-Manero, G., Garcia-Marcos, M., Garmyn, M., Gartel, A. L., Gatti, E., Gautel, M., Gawriluk, T. R., Gegg, M. E., Geng, J., Germain, M., Gestwicki, J. E., Gewirtz, D. A., Ghavami, S., Ghosh, P., Giammarioli, A. M., Giatromanolaki, A. N., Gibson, S. B., Gilkerson, R. W., Ginger, M. L., Ginsberg, H. N., Golab, J., Goligorsky, M. S., Golstein, P., Gomez-Manzano, C., Goncu, E., Gongora, C., Gonzalez, C. D., Gonzalez, R., Gonzalez-Estevez, C., Gonzalez-Polo, R. A., Gonzalez-Rey, E., Gorbunov, N. V., Gorski, S., Goruppi, S., Gottlieb, R. A., Gozuacik, D., Granato, G. E., Grant, G. D., Green, K. N., Gregorc, A., Gros, F., Grose, C., Grunt, T. W., Gual, P., Guan, J. L., Guan, K. L., Guichard, S. M., Gukovskaya, A. S.,

Gukovsky, I., Gunst, J., Gustafsson, A. B., Halayko, A. J., Hale, A. N., Halonen, S. K., Hamasaki, M., Han, F., Han, T., Hancock, M. K., Hansen, M., Harada, H., Harada, M., Hardt, S. E., Harper, J. W., Harris, A. L., Harris, J., Harris, S. D., Hashimoto, M., Haspel, J. A., Hayashi, S., Hazelhurst, L. A., He, C., He, Y. W., Hebert, M. J., Heidenreich, K. A., Helfrich, M. H., Helgason, G. V., Henske, E. P., Herman, B., Herman, P. K., Hetz, C., Hilfiker, S., Hill, J. A., Hocking, L. J., Hofman, P., Hofmann, T. G., Hohfeld, J., Holyoake, T. L., Hong, M. H., Hood, D. A., Hotamisligil, G. S., Houwerzijl, E. J., Hoyer-Hansen, M., Hu, B., Hu, C. A., Hu, H. M., Hua, Y., Huang, C., Huang, J., Huang, S., Huang, W. P., Huber, T. B., Huh, W. K., Hung, T. H., Hupp, T. R., Hur, G. M., Hurley, J. B., Hussain, S. N., Hussey, P. J., Hwang, J. J., Hwang, S., Ichihara, A., Ilkhanizadeh, S., Inoki, K., Into, T., Iovane, V., Iovanna, J. L., Ip, N. Y., Isaka, Y., Ishida, H., Isidoro, C., Isobe, K., Iwasaki, A., Izquierdo, M., Izumi, Y., Jaakkola, P. M., Jaattela, M., Jackson, G. R., Jackson, W. T., Janji, B., Jendrach, M., Jeon, J. H., Jeung, E. B., Jiang, H., Jiang, H., Jiang, J. X., Jiang, M., Jiang, Q., Jiang, X., Jiang, X., Jimenez, A., Jin, M., Jin, S., Joe, C. O., Johansen, T., Johnson, D. E., Johnson, G. V., Jones, N. L., Joseph, B., Joseph, S. K., Joubert, A. M., Juhasz, G., Juillerat-Jeanneret, L., Jung, C. H., Jung, Y. K., Kaarniranta, K., Kaasik, A., Kabuta, T., Kadowaki, M., Kagedal, K., Kamada, Y., Kaminskyy, V. O., Kampinga, H. H., Kanamori, H., Kang, C., Kang, K. B., Kang, K. I., Kang, R., Kang, Y. A., Kanki, T., Kanneganti, T. D., Kanno, H., Kanthasamy, A. G., Kanthasamy, A., Karantza, V., Kaushal, G. P., Kaushik, S., Kawazoe, Y., Ke, P. Y., Kehrl, J. H., Kelekar, A.,

Kerkhoff, C., Kessel, D. H., Khalil, H., Kiel, J. A., Kiger, A. A., Kihara, A., Kim, D. R., Kim, D. H., Kim, D. H., Kim, E. K., Kim, H. R., Kim, J. S., Kim, J. H., Kim, J. C., Kim, J. K., Kim, P. K., Kim, S. W., Kim, Y. S., Kim, Y., Kimchi, A., Kimmelman, A. C., King, J. S., Kinsella, T. J., Kirkin, V., Kirshenbaum, L. A., Kitamoto, K., Kitazato, K., Klein, L., Klimecki, W. T., Klucken, J., Knecht, E., Ko, B. C., Koch, J. C., Koga, H., Koh, J. Y., Koh, Y. H., Koike, M., Komatsu, M., Kominami, E., Kong, H. J., Kong, W. J., Korolchuk, V. I., Kotake, Y., Koukourakis, M. I., Kouri Flores, J. B., Kovacs, A. L., Kraft, C., Krainc, D., Kramer, H., Kretz-Remy, C., Krichevsky, A. M., Kroemer, G., Kruger, R., Krut, O., Ktistakis, N. T., Kuan, C. Y., Kucharczyk, R., Kumar, A., Kumar, R., Kumar, S., Kundu, M., Kung, H. J., Kurz, T., Kwon, H. J., La Spada, A. R., Lafont, F., Lamark, T., Landry, J., Lane, J. D., Lapaquette, P., Laporte, J. F., Laszlo, L., Lavandero, S., Lavoie, J. N., Layfield, R., Lazo, P. A., Le, W., Le Cam, L., Ledbetter, D. J., Lee, A. J., Lee, B. W., Lee, G. M., Lee, J., Lee, J. H., Lee, M., Lee, M. S., Lee, S. H., Leeuwenburgh, C., Legembre, P., Legouis, R., Lehmann, M., Lei, H. Y., Lei, Q. Y., Leib, D. A., Leiro, J., Lemasters, J. J., Lemoine, A., Lesniak, M. S., Lev, D., Levenson, V. V., Levine, B., Levy, E., Li, F., Li, J. L., Li, L., Li, S., Li, W., Li, X. J., Li, Y. B., Li, Y. P., Liang, C., Liang, Q., Liao, Y. F., Liberski, P. P., Lieberman, A., Lim, H. J., Lim, K. L., Lim, K., Lin, C. F., Lin, F. C., Lin, J., Lin, J. D., Lin, K., Lin, W. W., Lin, W. C., Lin, Y. L., Linden, R., Lingor, P., Lippincott-Schwartz, J., Lisanti, M. P., Liton, P. B., Liu, B., Liu, C. F., Liu, K., Liu, L., Liu, Q. A., Liu, W., Liu, Y. C., Liu, Y., Lockshin, R. A., Lok, C.

N., Lonial, S., Loos, B., Lopez-Berestein, G., Lopez-Otin, C., Lossi, L., Lotze, M. T., Low, P., Lu, B., Lu, B., Lu, B., Lu, Z., Luciano, F., Lukacs, N. W., Lund, A. H., Lynch-Day, M. A., Ma, Y., Macian, F., MacKeigan, J. P., Macleod, K. F., Madeo, F., Maiuri, L., Maiuri, M. C., Malagoli, D., Malicdan, M. C., Malorni, W., Man, N., Mandelkow, E. M., Manon, S., Manov, I., Mao, K., Mao, X., Mao, Z., Marambaud, P., Marazziti, D., Marcel, Y. L., Marchbank, K., Marchetti, P., Marciniak, S. J., Marcondes, M., Mardi, M., Marfe, G., Marino, G., Markaki, M., Marten, M. R., Martin, S. J., Martinand-Mari, C., Martinet, W., Martinez-Vicente, M., Masini, M., Matarrese, P., Matsuo, S., Matteoni, R., Mayer, A., Mazure, N. M., McConkey, D. J., McConnell, M. J., McDermott, C., McDonald, C., McInerney, G. M., McKenna, S. L., McLaughlin, B., McLean, P. J., McMaster, C. R., McQuibban, G. A., Meijer, A. J., Meisler, M. H., Melendez, A., Melia, T. J., Melino, G., Mena, M. A., Menendez, J. A., Menna-Barreto, R. F., Menon, M. B., Menzies, F. M., Mercer, C. A., Merighi, A., Merry, D. E., Meschini, S., Meyer, C. G., Meyer, T. F., Miao, C. Y., Miao, J. Y., Michels, P. A., Michiels, C., Mijaljica, D., Milojkovic, A., Minucci, S., Miracco, C., Miranti, C. K., Mitroulis, I., Miyazawa, K., Mizushima, N., Mograbi, B., Mohseni, S., Molero, X., Mollereau, B., Mollinedo, F., Momoi, T., Monastyrska, I., Monick, M. M., Monteiro, M. J., Moore, M. N., Mora, R., Moreau, K., Moreira, P. I., Moriyasu, Y., Moscat, J., Mostowy, S., Mottram, J. C., Motyl, T., Moussa, C. E., Muller, S., Muller, S., Munger, K., Munz, C., Murphy, L. O., Murphy, M. E., Musaro, A., Mysorekar, I., Nagata, E., Nagata, K., Nahimana, A., Nair, U., Nakagawa, T.,

Nakahira, K., Nakano, H., Nakatogawa, H., Nanjundan, M., Naqvi, N. I., Narendra, D. P., Narita, M., Navarro, M., Nawrocki, S. T., Nazarko, T. Y., Nemchenko, A., Netea, M. G., Neufeld, T. P., Ney, P. A., Nezis, I. P., Nguyen, H. P., Nie, D., Nishino, I., Nislow, C., Nixon, R. A., Noda, T., Noegel, A. A., Nogalska, A., Noguchi, S., Notterpek, L., Novak, I., Nozaki, T., Nukina, N., Nurnberger, T., Nyfeler, B., Obara, K., Oberley, T. D., Oddo, S., Ogawa, M., Ohashi, T., Okamoto, K., Oleinick, N. L., Oliver, F. J., Olsen, L. J., Olsson, S., Opota, O., Osborne, T. F., Ostrander, G. K., Otsu, K., Ou, J. H., Ouimet, M., Overholtzer, M., Ozpolat, B., Paganetti, P., Pagnini, U., Pallet, N., Palmer, G. E., Palumbo, C., Pan, T., Panaretakis, T., Pandey, U. B., Papackova, Z., Papassideri, I., Paris, I., Park, J., Park, O. K., Parys, J. B., Parzych, K. R., Patschan, S., Patterson, C., Pattingre, S., Pawelek, J. M., Peng, J., Perlmutter, D. H., Perrotta, I., Perry, G., Pervaiz, S., Peter, M., Peters, G. J., Petersen, M., Petrovski, G., Phang, J. M., Piacentini, M., Pierre, P., Pierrefite-Carle, V., Pierron, G., Pinkas-Kramarski, R., Piras, A., Piri, N., Platanias, L. C., Poggeler, S., Poirot, M., Poletti, A., Pous, C., Pozuelo-Rubio, M., Praetorius-Ibba, M., Prasad, A., Prescott, M., Priault, M., Produit-Zengaffinen, N., Progulske-Fox, A., Proikas-Cezanne, T., Przedborski, S., Przyklenk, K., Puertollano, R., Puyal, J., Qian, S. B., Qin, L., Qin, Z. H., Quaggin, S. E., Raben, N., Rabinowich, H., Rabkin, S. W., Rahman, I., Rami, A., Ramm, G., Randall, G., Randow, F., Rao, V. A., Rathmell, J. C., Ravikumar, B., Ray, S. K., Reed, B. H., Reed, J. C., Reggiori, F., Regnier-Vigouroux, A., Reichert, A. S., Reiners, J. J., Jr., Reiter, R. J., Ren, J., Revuelta,

J. L., Rhodes, C. J., Ritis, K., Rizzo, E., Robbins, J., Roberge, M., Roca, H., Roccheri, M. C., Rocchi, S., Rodemann, H. P., Rodriguez de Cordoba, S., Rohrer, B., Roninson, I. B., Rosen, K., Rost-Roszkowska, M. M., Rouis, M., Rouschop, K. M., Rovetta, F., Rubin, B. P., Rubinsztein, D. C., Ruckdeschel, K., Rucker, E. B., 3rd, Rudich, A., Rudolf, E., Ruiz-Opazo, N., Russo, R., Rusten, T. E., Ryan, K. M., Ryter, S. W., Sabatini, D. M., Sadoshima, J., Saha, T., Saitoh, T., Sakagami, H., Sakai, Y., Salekdeh, G. H., Salomoni, P., Salvaterra, P. M., Salvesen, G., Salvioli, R., Sanchez, A. M., Sanchez-Alcazar, J. A., Sanchez-Prieto, R., Sandri, M., Sankar, U., Sansanwal, P., Santambrogio, L., Saran, S., Sarkar, S., Sarwal, M., Sasakawa, C., Sasnauskiene, A., Sass, M., Sato, K., Sato, M., Schapira, A. H., Scharl, M., Schatzl, H. M., Scheper, W., Schiaffino, S., Schneider, C., Schneider, M. E., Schneider-Stock, R., Schoenlein, P. V., Schorderet, D. F., Schuller, C., Schwartz, G. K., Scorrano, L., Sealy, L., Seglen, P. O., Segura-Aguilar, J., Seiliez, I., Seleverstov, O., Sell, C., Seo, J. B., Separovic, D., Setaluri, V., Setoguchi, T., Settembre, C., Shacka, J. J., Shanmugam, M., Shapiro, I. M., Shaulian, E., Shaw, R. J., Shelhamer, J. H., Shen, H. M., Shen, W. C., Sheng, Z. H., Shi, Y., Shibuya, K., Shidoji, Y., Shieh, J. J., Shih, C. M., Shimada, Y., Shimizu, S., Shintani, T., Shirihai, O. S., Shore, G. C., Sibirny, A. A., Sidhu, S. B., Sikorska, B., Silva-Zacarin, E. C., Simmons, A., Simon, A. K., Simon, H. U., Simone, C., Simonsen, A., Sinclair, D. A., Singh, R., Sinha, D., Sinicrope, F. A., Sirko, A., Siu, P. M., Sivridis, E., Skop, V., Skulachev, V. P., Slack, R. S., Smaili, S. S., Smith, D. R., Soengas, M. S.,

Soldati, T., Song, X., Sood, A. K., Soong, T. W., Sotgia, F., Spector, S. A., Spies, C. D., Springer, W., Srinivasula, S. M., Stefanis, L., Steffan, J. S., Stendel, R., Stenmark, H., Stephanou, A., Stern, S. T., Sternberg, C., Stork, B., Stralfors, P., Subauste, C. S., Sui, X., Sulzer, D., Sun, J., Sun, S. Y., Sun, Z. J., Sung, J. J., Suzuki, K., Suzuki, T., Swanson, M. S., Swanton, C., Sweeney, S. T., Sy, L. K., Szabadkai, G., Tabas, I., Taegtmeyer, H., Tafani, M., Takacs-Vellai, K., Takano, Y., Takegawa, K., Takemura, G., Takeshita, F., Talbot, N. J., Tan, K. S., Tanaka, K., Tanaka, K., Tang, D., Tang, D., Tanida, I., Tannous, B. A., Tavernarakis, N., Taylor, G. S., Taylor, G. A., Taylor, J. P., Terada, L. S., Terman, A., Tettamanti, G., Thevissen, K., Thompson, C. B., Thorburn, A., Thumm, M., Tian, F., Tian, Y., Tocchini-Valentini, G., Tolkovsky, A. M., Tomino, Y., Tonges, L., Tooze, S. A., Tournier, C., Tower, J., Towns, R., Trajkovic, V., Travassos, L. H., Tsai, T. F., Tschan, M. P., Tsubata, T., Tsung, A., Turk, B., Turner, L. S., Tyagi, S. C., Uchiyama, Y., Ueno, T., Umekawa, M., Umemiya-Shirafuji, R., Unni, V. K., Vaccaro, M. I., Valente, E. M., Van den Berghe, G., van der Klei, I. J., van Doorn, W., van Dyk, L. F., van Egmond, M., van Grunsven, L. A., Vandenabeele, P., Vandenberghe, W. P., Vanhorebeek, I., Vaquero, E. C., Velasco, G., Vellai, T., Vicencio, J. M., Vierstra, R. D., Vila, M., Vindis, C., Viola, G., Viscomi, M. T., Voitsekhovskaja, O. V., von Haefen, C., Votruba, M., Wada, K., Wade-Martins, R., Walker, C. L., Walsh, C. M., Walter, J., Wan, X. B., Wang, A., Wang, C., Wang, D., Wang, F., Wang, F., Wang, G., Wang, H., Wang, H. G., Wang, H. D., Wang, J., Wang, K., Wang, M., Wang, R. C., Wang, X., Wang, X.,

Wang, Y. J., Wang, Y., Wang, Z., Wang, Z. C., Wang, Z., Wansink, D. G., Ward, D. M., Watada, H., Waters, S. L., Webster, P., Wei, L., Weihl, C. C., Weiss, W. A., Welford, S. M., Wen, L. P., Whitehouse, C. A., Whitton, J. L., Whitworth, A. J., Wileman, T., Wiley, J. W., Wilkinson, S., Willbold, D., Williams, R. L., Williamson, P. R., Wouters, B. G., Wu, C., Wu, D. C., Wu, W. K., Wyttenbach, A., Xavier, R. J., Xi, Z., Xia, P., Xiao, G., Xie, Z., Xie, Z., Xu, D. Z., Xu, J., Xu, L., Xu, X., Yamamoto, A., Yamamoto, A., Yamashina, S., Yamashita, M., Yan, X., Yanagida, M., Yang, D. S., Yang, E., Yang, J. M., Yang, S. Y., Yang, W., Yang, W. Y., Yang, Z., Yao, M. C., Yao, T. P., Yeganeh, B., Yen, W. L., Yin, J. J., Yin, X. M., Yoo, O. J., Yoon, G., Yoon, S. Y., Yorimitsu, T., Yoshikawa, Y., Yoshimori, T., Yoshimoto, K., You, H. J., Youle, R. J., Younes, A., Yu, L., Yu, L., Yu, S. W., Yu, W. H., Yuan, Z. M., Yue, Z., Yun, C. H., Yuzaki, M., Zabirnyk, O., Silva-Zacarin, E., Zacks, D., Zacksenhaus, E., Zaffaroni, N., Zakeri, Z., Zeh, H. J., 3rd, Zeitlin, S. O., Zhang, H., Zhang, H. L., Zhang, J., Zhang, J. P., Zhang, L., Zhang, L., Zhang, M. Y., Zhang, X. D., Zhao, M., Zhao, Y. F., Zhao, Y., Zhao, Z. J., Zheng, X., Zhivotovsky, B., Zhong, Q., Zhou, C. Z., Zhu, C., Zhu, W. G., Zhu, X. F., Zhu, X., Zhu, Y., Zoladek, T., Zong, W. X., Zorzano, A., Zschocke, J., and Zuckerbraun, B. (2012) Guidelines for the use and interpretation of assays for monitoring autophagy. *Autophagy* **8**, 445-544

15. Liu, L., McKeehan, W. L., Wang, F., and Xie, R. (2012) MAP1S enhances autophagy to suppress tumorigenesis. *Autophagy* **8**, 278-280

16. Yen, W. L., and Klionsky, D. J. (2008) How to live long and prosper: autophagy, mitochondria, and aging. *Physiology* **23**, 248-262

17. Madeo, F., Zimmermann, A., Maiuri, M. C., and Kroemer, G. (2015) Essential role for autophagy in life span extension. *The Journal of Clinical Investigation* **125**, 85-93

18. Martinez-Vicente, M., and Cuervo, A. M. (2007) Autophagy and neurodegeneration: when the cleaning crew goes on strike. *Lancet Neurology* **6**, 352-361

19. Pouladi, M. A., Morton, A. J., and Hayden, M. R. (2013) Choosing an animal model for the study of Huntington's disease. *Nature Reviews Neuroscience* **14**, 708-721

20. Yue, F., Li, W., Zou, J., Chen, Q., Xu, G., Huang, H., Xu, Z., Zhang, S., Gallinari, P., Wang, F., McKeehan, W. L., and Liu, L. (2015) Blocking the association of HDAC4 with MAP1S accelerates autophagy clearance of mutant Huntingtin. *Aging* **7**, 839-853

21. Pringsheim, T., Wiltshire, K., Day, L., Dykeman, J., Steeves, T., and Jette, N. (2012) The incidence and prevalence of Huntington's disease: a systematic review and meta-analysis. *Movement Disorders Journal* **27**, 1083-1091

22. Rawlins, M. D., Wexler, N. S., Wexler, A. R., Tabrizi, S. J., Douglas, I., Evans, S. J., and Smeeth, L. (2016) The Prevalence of Huntington's Disease. *Neuroepidemiology* **46**, 144-153

23. Martin, D. D., Ladha, S., Ehrnhoefer, D. E., and Hayden, M. R. (2015) Autophagy in Huntington disease and huntingtin in autophagy. *Trends in Neurosciences* **38**, 26-35

24. Bjorkoy, G., Lamark, T., Brech, A., Outzen, H., Perander, M., Overvatn, A., Stenmark, H., and Johansen, T. (2005) p62/SQSTM1 forms protein aggregates degraded by autophagy and has a protective effect on huntingtin-induced cell death. *The Journal of Cell Biology* **171**, 603-614

25. Torre, L. A., Bray, F., Siegel, R. L., Ferlay, J., Lortet-Tieulent, J., and Jemal, A. (2015) Global cancer statistics, 2012. *CA: a Cancer Journal for Clinicians* **65**, 87-108

26. Siegel, R. L., Miller, K. D., and Jemal, A. (2016) Cancer statistics, 2016. *CA: a Cancer Journal for Clinicians* **66**, 7-30

27. Boring, C. C., Squires, T. S., and Tong, T. (1991) Cancer statistics, 1991. *CA: a Cancer Journal for Clinicians* **41**, 19-36

28. Mittal, S., and El-Serag, H. B. (2013) Epidemiology of hepatocellular carcinoma: consider the population. *Journal of Clinical Gastroenterology* **47 Suppl**, S2-6

29. Zhang, D. Y., and Friedman, S. L. (2012) Fibrosis-dependent mechanisms of hepatocarcinogenesis. *Hepatology (Baltimore, Md.)* **56**, 769-775

30. Singh, S., Singh, P. P., Roberts, L. R., and Sanchez, W. (2014) Chemopreventive strategies in hepatocellular carcinoma. *Nature Reviews Gastroenterology & Hepatology* **11**, 45-54

31. McGlynn, K. A., and London, W. T. (2011) The global epidemiology of hepatocellular carcinoma: present and future. *Clinical Liver Disease* **15**, 223-243, vii-x

32. Takamura, A., Komatsu, M., Hara, T., Sakamoto, A., Kishi, C., Waguri, S., Eishi, Y., Hino, O., Tanaka, K., and Mizushima, N. (2011) Autophagy-deficient mice develop multiple liver tumors. *Genes & Development* **25**, 795-800

33. Xie, R., Wang, F., McKeehan, W. L., and Liu, L. (2011) Autophagy enhanced by microtubule- and mitochondrion-associated MAP1S suppresses genome instability and hepatocarcinogenesis. *Cancer Research* **71**, 7537-7546

34. Jiang, X., Li, X., Huang, H., Jiang, F., Lin, Z., He, H., Chen, Y., Yue, F., Zou, J., He, Y., You, P., Wang, W., Yang, W., Zhao, H., Lai, Y., Wang, F., Zhong, W., and Liu, L. (2014) Elevated levels of mitochondrion-associated autophagy inhibitor LRPPRC are associated with poor prognosis in patients with prostate cancer. *Cancer* **120**, 1228-1236

35. Jiang, X., Zhong, W., Huang, H., He, H., Jiang, F., Chen, Y., Yue, F., Zou, J., Li, X., He, Y., You, P., Yang, W., Lai, Y., Wang, F., and Liu, L. (2015) Autophagy defects suggested by low levels of autophagy activator MAP1S and high levels of autophagy inhibitor LRPPRC predict poor prognosis of prostate cancer patients. *Molecular Carcinogenesis* **54**, 1194-1204

36. Xu, G., Jiang, Y., Xiao, Y., Liu, X. D., Yue, F., Li, W., Li, X., He, Y., Jiang, X., Huang, H., Chen, Q., Jonasch, E., and Liu, L. (2016) Fast clearance of lipid

droplets through MAP1S-activated autophagy suppresses clear cell renal cell carcinomas and promotes patient survival. *Oncotarget* **7**, 6255-6265

37. Liu, L., and McKeehan, W. L. (2002) Sequence analysis of LRPPRC and its SEC1 domain interaction partners suggests roles in cytoskeletal organization, vesicular trafficking, nucleocytosolic shuttling, and chromosome activity. *Genomics* **79**, 124-136

38. Liu, L., Vo, A., Liu, G., and McKeehan, W. L. (2005) Distinct structural domains within C19ORF5 support association with stabilized microtubules and mitochondrial aggregation and genome destruction. *Cancer Research* **65**, 4191-4201

39. Orbán-Németh, Z., Simader, H., Badurek, S., Trančiková, A., and Propst, F. (2005) Microtubule-associated protein 1S, a short and ubiquitously expressed member of the microtubule-associated protein 1 family. *The Journal of Biological Chemistry* **280**, 2257-2265

40. Liu, L., Xie, R., Yang, C., and McKeehan, W. L. (2009) Dual function microtubule- and mitochondria-associated proteins mediate mitotic cell death. *Cell Oncology* **31**, 393-405

41. Xie, R., Nguyen, S., McKeehan, K., Wang, F., McKeehan, W. L., and Liu, L. (2011) Microtubule-associated protein 1S (MAP1S) bridges autophagic components with microtubules and mitochondria to affect autophagosomal biogenesis and degradation. *The Journal of Biological Chemistry* **286**, 10367-10377

42. Liang, J., Shao, S. H., Xu, Z.-X., Hennessy, B., Ding, Z., Larrea, M., Kondo, S., Dumont, D. J., Gutterman, J. U., Walker, C. L., Slingerland, J. M., and Mills, G. B. (2007) The energy sensing LKB1-AMPK pathway regulates p27(kip1) phosphorylation mediating the decision to enter autophagy or apoptosis. *Nature Cell Biology* **9**, 218-224

43. Glozak, M. A., and Seto, E. (2007) Histone deacetylases and cancer. *Oncogene* **26**, 5420-5432

44. Dokmanovic, M., Clarke, C., and Marks, P. A. (2007) Histone deacetylase inhibitors: overview and perspectives. *Molecular Cancer Research* **5**, 981-989

45. Struhl, K. (1998) Histone acetylation and transcriptional regulatory mechanisms. *Genes & Development* **12**, 599-606

46. Sadoul, K., Wang, J., Diagouraga, B., and Khochbin, S. (2011) The tale of protein lysine acetylation in the cytoplasm. *Journal of Biomedicine and Biotechnology* **2011**, 970382

47. Eisenberg, T., Schroeder, S., Andryushkova, A., Pendl, T., Kuttner, V., Bhukel, A., Marino, G., Pietrocola, F., Harger, A., Zimmermann, A., Moustafa, T., Sprenger, A., Jany, E., Buttner, S., Carmona-Gutierrez, D., Ruckenstuhl, C., Ring, J., Reichelt, W., Schimmel, K., Leeb, T., Moser, C., Schatz, S., Kamolz, L. P., Magnes, C., Sinner, F., Sedej, S., Frohlich, K. U., Juhasz, G., Pieber, T. R., Dengjel, J., Sigrist, S. J., Kroemer, G., and Madeo, F. (2014) Nucleocytosolic depletion of the energy metabolite acetyl-coenzyme a stimulates autophagy and prolongs lifespan. *Cell Metabolism* **19**, 431-444

48. Howitz, K. T., Bitterman, K. J., Cohen, H. Y., Lamming, D. W., Lavu, S., Wood, J. G., Zipkin, R. E., Chung, P., Kisielewski, A., Zhang, L. L., Scherer, B., and Sinclair, D. A. (2003) Small molecule activators of sirtuins extend Saccharomyces cerevisiae lifespan. *Nature* **425**, 191-196

49. Shao, Y., Gao, Z., Marks, P. A., and Jiang, X. (2004) Apoptotic and autophagic cell death induced by histone deacetylase inhibitors. *Proceedings of the National Academy of Sciences of the United States of America* **101**, 18030-18035

50. Gammoh, N., Lam, D., Puente, C., Ganley, I., Marks, P. A., and Jiang, X. (2012) Role of autophagy in histone deacetylase inhibitor-induced apoptotic and nonapoptotic cell death. *Proceedings of the National Academy of Sciences of the United States of America* **109**, 6561-6565

51. Eisenberg, T., Knauer, H., Schauer, A., Büttner, S., Ruckenstuhl, C., Carmona-Gutierrez, D., Ring, J., Schroeder, S., Magnes, C., Antonacci, L., Fussi, H., Deszcz, L., Hartl, R., Schraml, E., Criollo, A., Megalou, E., Weiskopf, D., Laun, P., Heeren, G., Breitenbach, M., Grubeck-Loebenstein, B., Herker, E., Fahrenkrog, B., Fröhlich, K.-U., Sinner, F., Tavernarakis, N., Minois, N., Kroemer, G., and Madeo, F. (2009) Induction of autophagy by spermidine promotes longevity. *Nature Cell Biology* **11**, 1305-1314

52. Ali, M. A., Poortvliet, E., Strömberg, R., and Yngve, A. (2011) Polyamines in foods: development of a food database. *Food & Nutrtion Research* **55**, 55-72

53. Madeo, F., Eisenberg, T., Büttner, S., Ruckenstuhl, C., and Kroemer, G. (2010) Spermidine: a novel autophagy inducer and longevity elixir. *Autophagy* **6**, 160-162

54. Liu, L., Vo, A., and McKeehan, W. L. (2005) Specificity of the methylation-suppressed A isoform of candidate tumor suppressor RASSF1 for microtubule hyperstabilization is determined by cell death inducer C19ORF5. *Cancer Research* **65**, 1830-1838

55. Vairo, G., Soos, T. J., Upton, T. M., Zalvide, J., DeCaprio, J. A., Ewen, M. E., Koff, A., and Adams, J. M. (2000) Bcl-2 retards cell cycle entry through p27(Kip1), pRB relative p130, and altered E2F regulation. *Molecular and Cellular Biology* **20**, 4745-4753

56. Zhang, G., Park, M. A., Mitchell, C., Walker, T., Hamed, H., Studer, E., Graf, M., Rahmani, M., Gupta, S., Hylemon, P. B., Fisher, P. B., Grant, S., and Dent, P. (2008) Multiple cyclin kinase inhibitors promote bile acid-induced apoptosis and autophagy in primary hepatocytes via p53-CD95-dependent signaling. *The Journal of Biological Chemistry* **283**, 24343-24358

57. Liu, L., Trimarchi, J. R., Smith, P. J. S., and Keefe, D. L. (2002) Mitochondrial dysfunction leads to telomere attrition and genomic instability. *Aging Cell* **1**, 40-46

58. Zou, J., Yue, F., Jiang, X., Li, W., Yi, J., and Liu, L. (2013) Mitochondrion-associated protein LRPPRC suppresses the initiation of basal levels of autophagy via enhancing Bcl-2 stability. *Biochemical Journal* **454**, 447-457

59. Miska, E. A., Karlsson, C., Langley, E., Nielsen, S. J., Pines, J., and Kouzarides, T. (1999) HDAC4 deacetylase associates with and represses the MEF2 transcription factor. *The EMBO Journal* **18**, 5099-5107

60. Vega, R. B., Matsuda, K., Oh, J., Barbosa, A. C., Yang, X., Meadows, E., McAnally, J., Pomajzl, C., Shelton, J. M., Richardson, J. A., Karsenty, G., and Olson, E. N. (2004) Histone deacetylase 4 controls chondrocyte hypertrophy during skeletogenesis. *Cell* **119**, 555-566

61. Geng, H., Harvey, C. T., Pittsenbarger, J., Liu, Q., Beer, T. M., Xue, C., and Qian, D. Z. (2011) HDAC4 protein regulates HIF1alpha protein lysine acetylation and cancer cell response to hypoxia. *The Journal of Biological Chemistry* **286**, 38095-38102

62. Choi, M. C., Cohen, T. J., Barrientos, T., Wang, B., Li, M., Simmons, B. J., Yang, J. S., Cox, G. A., Zhao, Y., and Yao, T. P. (2012) A direct HDAC4-MAP kinase crosstalk activates muscle atrophy program. *Molecular Cell* **47**, 122-132

63. Stronach, E. A., Alfraidi, A., Rama, N., Datler, C., Studd, J. B., Agarwal, R., Guney, T. G., Gourley, C., Hennessy, B. T., Mills, G. B., Mai, A., Brown, R., Dina, R., and Gabra, H. (2011) HDAC4-regulated STAT1 activation mediates platinum resistance in ovarian cancer. *Cancer Research* **71**, 4412-4422

64. Wang, Z., Qin, G., and Zhao, T. C. (2014) Histone Deacetylase 4 (HDAC4): Mechanism of Regulations and Biological Functions. *Epigenomics* **6**, 139-150

65. Wang, A. H., Grégoire, S., Zika, E., Xiao, L., Li, C. S., Li, H., Wright, K. L., Ting, J. P., and Yang, X.-J. (2005) Identification of the ankyrin repeat proteins

ANKRA and RFXANK as novel partners of class IIa histone deacetylases. *The Journal of Biological Chemistry* **280**, 29117-29127

66. Lahm, A., Paolini, C., Pallaoro, M., Nardi, M. C., Jones, P., Neddermann, P., Sambucini, S., Bottomley, M. J., Surdo, P. L., Carfi´, A., Koch, U., Francesco, R. D., hler, C. S., and Gallinari, P. (2007) Unraveling the hidden catalytic activity of vertebrate class IIa histone deacetylases. *Proceedings of the National Academy of Sciences of the United States of America* **104**, 17335-17340

67. Paroni, G., Cernotta, N., Dello Russo, C., Gallinari, P., Pallaoro, M., Foti, C., Talamo, F., Orsatti, L., Steinkühler, C., and Brancolini, C. (2008) PP2A regulates HDAC4 nuclear import. *Molecular Biology of the Cell* **19**, 655-667

68. Ahn, M. Y., Ahn, S. G., and Yoon, J. H. (2011) Apicidin, a histone deaceylase inhibitor, induces both apoptosis and autophagy in human oral squamous carcinoma cells. *Oral Oncology* **47**, 1032-1038

69. Arrowsmith, C. H., Bountra, C., Fish, P. V., Lee, K., and Schapira, M. (2012) Epigenetic protein families: a new frontier for drug discovery. *Nature Reviews Drug Discovery* **11**, 384-400

70. Glozak, M. A., Sengupta, N., Zhang, X., and Seto, E. (2005) Acetylation and deacetylation of non-histone proteins. *Gene* **363**, 15-23

71. Gu, W., and Roeder, R. G. (1997) Activation of p53 sequence-specific DNA binding by acetylation of the p53 C-terminal domain. *Cell* **90**, 595-606

72. Espinosa, J. M., and Emerson, B. M. (2001) Transcriptional regulation by p53 through intrinsic DNA/chromatin binding and site-directed cofactor recruitment. *Molecular Cell* **8**, 57-69

73. Ito, A., Kawaguchi, Y., Lai, C. H., Kovacs, J. J., Higashimoto, Y., Appella, E., and Yao, T. P. (2002) MDM2-HDAC1-mediated deacetylation of p53 is required for its degradation. *The EMBO Journal* **21**, 6236-6245

74. Hubbert, C., Guardiola, A., Shao, R., Kawaguchi, Y., Ito, A., Nixon, A., Yoshida, M., Wang, X. F., and Yao, T. P. (2002) HDAC6 is a microtubule-associated deacetylase. *Nature* **417**, 455-458

75. Zhang, Y., Li, N., Caron, C., Matthias, G., Hess, D., Khochbin, S., and Matthias, P. (2003) HDAC6 interacts with and deacetylates tubulin and microtubules in vivo. *The EMBO Journal* **22**, 1168-1179

76. Iwata, A., Riley, B. E., Johnston, J. A., and Kopito, R. R. (2005) HDAC6 and microtubules are required for autophagic degradation of aggregated huntingtin. *The Journal of Biological Chemistry* **280**, 40282-40292

77. Lee, J. Y., Koga, H., Kawaguchi, Y., Tang, W., Wong, E., Gao, Y. S., Pandey, U. B., Kaushik, S., Tresse, E., Lu, J., Taylor, J. P., Cuervo, A. M., and Yao, T. P. (2010) HDAC6 controls autophagosome maturation essential for ubiquitin-selective quality-control autophagy. *The EMBO Journal* **29**, 969-980

78. Pandey, U. B., Nie, Z., Batlevi, Y., McCray, B. A., Ritson, G. P., Nedelsky, N. B., Schwartz, S. L., DiProspero, N. A., Knight, M. A., Schuldiner, O., Padmanabhan, R., Hild, M., Berry, D. L., Garza, D., Hubbert, C. C., Yao, T. P.,

Baehrecke, E. H., and Taylor, J. P. (2007) HDAC6 rescues neurodegeneration and provides an essential link between autophagy and the UPS. *Nature* **447**, 859-863

79. Chen, Q., Yue, F., Li, W., Zou, J., Xu, T., Huang, C., Zhang, Y., Song, K., Huang, G., Xu, G., Huang, H., Li, J., and Liu, L. (2015) Potassium Bisperoxo(1,10-phenanthroline)oxovanadate (bpV(phen)) Induces Apoptosis and Pyroptosis and Disrupts the P62-HDAC6 Protein Interaction to Suppress the Acetylated Microtubule-dependent Degradation of Autophagosomes. *The Journal of Biological Chemistry* **290**, 26051-26058

80. Greco, T. M., Yu, F., Guise, A. J., and Cristea, I. M. (2011) Nuclear import of histone deacetylase 5 by requisite nuclear localization signal phosphorylation. *Molecular & Cellular Proteomics* **10**, M110.004317

81. Backs, J., Backs, T., Bezprozvannaya, S., McKinsey, T. A., and Olson, E. N. (2008) Histone deacetylase 5 acquires calcium/calmodulin-dependent kinase II responsiveness by oligomerization with histone deacetylase 4. *Molecular and Cellular Biology* **28**, 3437-3445

82. Ginnan, R., Sun, L. Y., Schwarz, J. J., and Singer, H. A. (2012) MEF2 is regulated by CaMKIIdelta2 and a HDAC4-HDAC5 heterodimer in vascular smooth muscle cells. *Biochemical Journal* **444**, 105-114

83. Fischle, W., Dequiedt, F., Hendzel, M. J., Guenther, M. G., Lazar, M. A., Voelter, W., and Verdin, E. (2002) Enzymatic activity associated with class II HDACs is

dependent on a multiprotein complex containing HDAC3 and SMRT/N-CoR. *Molecular Cell* **9**, 45-57

84. Klionsky, D. J., Abdelmohsen, K., Abe, A., Abedin, M. J., Abeliovich, H., Acevedo Arozena, A., Adachi, H., Adams, C. M., Adams, P. D., Adeli, K., Adhihetty, P. J., Adler, S. G., Agam, G., Agarwal, R., Aghi, M. K., Agnello, M., Agostinis, P., Aguilar, P. V., Aguirre-Ghiso, J., Airoldi, E. M., Ait-Si-Ali, S., Akematsu, T., Akporiaye, E. T., Al-Rubeai, M., Albaiceta, G. M., Albanese, C., Albani, D., Albert, M. L., Aldudo, J., Algul, H., Alirezaei, M., Alloza, I., Almasan, A., Almonte-Beceril, M., Alnemri, E. S., Alonso, C., Altan-Bonnet, N., Altieri, D. C., Alvarez, S., Alvarez-Erviti, L., Alves, S., Amadoro, G., Amano, A., Amantini, C., Ambrosio, S., Amelio, I., Amer, A. O., Amessou, M., Amon, A., An, Z., Anania, F. A., Andersen, S. U., Andley, U. P., Andreadi, C. K., Andrieu-Abadie, N., Anel, A., Ann, D. K., Anoopkumar-Dukie, S., Antonioli, M., Aoki, H., Apostolova, N., Aquila, S., Aquilano, K., Araki, K., Arama, E., Aranda, A., Araya, J., Arcaro, A., Arias, E., Arimoto, H., Ariosa, A. R., Armstrong, J. L., Arnould, T., Arsov, I., Asanuma, K., Askanas, V., Asselin, E., Atarashi, R., Atherton, S. S., Atkin, J. D., Attardi, L. D., Auberger, P., Auburger, G., Aurelian, L., Autelli, R., Avagliano, L., Avantaggiati, M. L., Avrahami, L., Awale, S., Azad, N., Bachetti, T., Backer, J. M., Bae, D. H., Bae, J. S., Bae, O. N., Bae, S. H., Baehrecke, E. H., Baek, S. H., Baghdiguian, S., Bagniewska-Zadworna, A., Bai, H., Bai, J., Bai, X. Y., Bailly, Y., Balaji, K. N., Balduini, W., Ballabio, A., Balzan, R., Banerjee, R., Banhegyi, G., Bao, H., Barbeau, B., Barrachina, M. D.,

Barreiro, E., Bartel, B., Bartolome, A., Bassham, D. C., Bassi, M. T., Bast, R. C., Jr., Basu, A., Batista, M. T., Batoko, H., Battino, M., Bauckman, K., Baumgarner, B. L., Bayer, K. U., Beale, R., Beaulieu, J. F., Beck, G. R., Jr., Becker, C., Beckham, J. D., Bedard, P. A., Bednarski, P. J., Begley, T. J., Behl, C., Behrends, C., Behrens, G. M., Behrns, K. E., Bejarano, E., Belaid, A., Belleudi, F., Benard, G., Berchem, G., Bergamaschi, D., Bergami, M., Berkhout, B., Berliocchi, L., Bernard, A., Bernard, M., Bernassola, F., Bertolotti, A., Bess, A. S., Besteiro, S., Bettuzzi, S., Bhalla, S., Bhattacharyya, S., Bhutia, S. K., Biagosch, C., Bianchi, M. W., Biard-Piechaczyk, M., Billes, V., Bincoletto, C., Bingol, B., Bird, S. W., Bitoun, M., Bjedov, I., Blackstone, C., Blanc, L., Blanco, G. A., Blomhoff, H. K., Boada-Romero, E., Bockler, S., Boes, M., Boesze-Battaglia, K., Boise, L. H., Bolino, A., Boman, A., Bonaldo, P., Bordi, M., Bosch, J., Botana, L. M., Botti, J., Bou, G., Bouche, M., Bouchecareilh, M., Boucher, M. J., Boulton, M. E., Bouret, S. G., Boya, P., Boyer-Guittaut, M., Bozhkov, P. V., Brady, N., Braga, V. M., Brancolini, C., Braus, G. H., Bravo-San Pedro, J. M., Brennan, L. A., Bresnick, E. H., Brest, P., Bridges, D., Bringer, M. A., Brini, M., Brito, G. C., Brodin, B., Brookes, P. S., Brown, E. J., Brown, K., Broxmeyer, H. E., Bruhat, A., Brum, P. C., Brumell, J. H., Brunetti-Pierri, N., Bryson-Richardson, R. J., Buch, S., Buchan, A. M., Budak, H., Bulavin, D. V., Bultman, S. J., Bultynck, G., Bumbasirevic, V., Burelle, Y., Burke, R. E., Burmeister, M., Butikofer, P., Caberlotto, L., Cadwell, K., Cahova, M., Cai, D., Cai, J., Cai, Q., Calatayud, S., Camougrand, N., Campanella, M., Campbell, G. R., Campbell, M., Campello, S.,

Candau, R., Caniggia, I., Cantoni, L., Cao, L., Caplan, A. B., Caraglia, M., Cardinali, C., Cardoso, S. M., Carew, J. S., Carleton, L. A., Carlin, C. R., Carloni, S., Carlsson, S. R., Carmona-Gutierrez, D., Carneiro, L. A., Carnevali, O., Carra, S., Carrier, A., Carroll, B., Casas, C., Casas, J., Cassinelli, G., Castets, P., Castro-Obregon, S., Cavallini, G., Ceccherini, I., Cecconi, F., Cederbaum, A. I., Cena, V., Cenci, S., Cerella, C., Cervia, D., Cetrullo, S., Chaachouay, H., Chae, H. J., Chagin, A. S., Chai, C. Y., Chakrabarti, G., Chamilos, G., Chan, E. Y., Chan, M. T., Chandra, D., Chandra, P., Chang, C. P., Chang, R. C., Chang, T. Y., Chatham, J. C., Chatterjee, S., Chauhan, S., Che, Y., Cheetham, M. E., Cheluvappa, R., Chen, C. J., Chen, G., Chen, G. C., Chen, G., Chen, H., Chen, J. W., Chen, J. K., Chen, M., Chen, M., Chen, P., Chen, Q., Chen, Q., Chen, S. D., Chen, S., Chen, S. S., Chen, W., Chen, W. J., Chen, W. Q., Chen, W., Chen, X., Chen, Y. H., Chen, Y. G., Chen, Y., Chen, Y., Chen, Y., Chen, Y. J., Chen, Y. Q., Chen, Y., Chen, Z., Chen, Z., Cheng, A., Cheng, C. H., Cheng, H., Cheong, H., Cherry, S., Chesney, J., Cheung, C. H., Chevet, E., Chi, H. C., Chi, S. G., Chiacchiera, F., Chiang, H. L., Chiarelli, R., Chiariello, M., Chieppa, M., Chin, L. S., Chiong, M., Chiu, G. N., Cho, D. H., Cho, S. G., Cho, W. C., Cho, Y. Y., Cho, Y. S., Choi, A. M., Choi, E. J., Choi, E. K., Choi, J., Choi, M. E., Choi, S. I., Chou, T. F., Chouaib, S., Choubey, D., Choubey, V., Chow, K. C., Chowdhury, K., Chu, C. T., Chuang, T. H., Chun, T., Chung, H., Chung, T., Chung, Y. L., Chwae, Y. J., Cianfanelli, V., Ciarcia, R., Ciechomska, I. A., Ciriolo, M. R., Cirone, M., Claerhout, S., Clague, M. J., Claria, J., Clarke, P. G., Clarke, R., Clementi, E.,

Cleyrat, C., Cnop, M., Coccia, E. M., Cocco, T., Codogno, P., Coers, J., Cohen, E. E., Colecchia, D., Coletto, L., Coll, N. S., Colucci-Guyon, E., Comincini, S., Condello, M., Cook, K. L., Coombs, G. H., Cooper, C. D., Cooper, J. M., Coppens, I., Corasaniti, M. T., Corazzari, M., Corbalan, R., Corcelle-Termeau, E., Cordero, M. D., Corral-Ramos, C., Corti, O., Cossarizza, A., Costelli, P., Costes, S., Cotman, S. L., Coto-Montes, A., Cottet, S., Couve, E., Covey, L. R., Cowart, L. A., Cox, J. S., Coxon, F. P., Coyne, C. B., Cragg, M. S., Craven, R. J., Crepaldi, T., Crespo, J. L., Criollo, A., Crippa, V., Cruz, M. T., Cuervo, A. M., Cuezva, J. M., Cui, T., Cutillas, P. R., Czaja, M. J., Czyzyk-Krzeska, M. F., Dagda, R. K., Dahmen, U., Dai, C., Dai, W., Dai, Y., Dalby, K. N., Dalla Valle, L., Dalmasso, G., D'Amelio, M., Damme, M., Darfeuille-Michaud, A., Dargemont, C., Darley-Usmar, V. M., Dasarathy, S., Dasgupta, B., Dash, S., Dass, C. R., Davey, H. M., Davids, L. M., Davila, D., Davis, R. J., Dawson, T. M., Dawson, V. L., Daza, P., de Belleroche, J., de Figueiredo, P., de Figueiredo, R. C., de la Fuente, J., De Martino, L., De Matteis, A., De Meyer, G. R., De Milito, A., De Santi, M., de Souza, W., De Tata, V., De Zio, D., Debnath, J., Dechant, R., Decuypere, J. P., Deegan, S., Dehay, B., Del Bello, B., Del Re, D. P., Delage-Mourroux, R., Delbridge, L. M., Deldicque, L., Delorme-Axford, E., Deng, Y., Dengjel, J., Denizot, M., Dent, P., Der, C. J., Deretic, V., Derrien, B., Deutsch, E., Devarenne, T. P., Devenish, R. J., Di Bartolomeo, S., Di Daniele, N., Di Domenico, F., Di Nardo, A., Di Paola, S., Di Pietro, A., Di Renzo, L., DiAntonio, A., Diaz-Araya, G., Diaz-Laviada, I., Diaz-Meco, M. T., Diaz-Nido,

J., Dickey, C. A., Dickson, R. C., Diederich, M., Digard, P., Dikic, I., Dinesh-Kumar, S. P., Ding, C., Ding, W. X., Ding, Z., Dini, L., Distler, J. H., Diwan, A., Djavaheri-Mergny, M., Dmytruk, K., Dobson, R. C., Doetsch, V., Dokladny, K., Dokudovskaya, S., Donadelli, M., Dong, X. C., Dong, X., Dong, Z., Donohue, T. M., Jr., Doran, K. S., D'Orazi, G., Dorn, G. W., 2nd, Dosenko, V., Dridi, S., Drucker, L., Du, J., Du, L. L., Du, L., du Toit, A., Dua, P., Duan, L., Duann, P., Dubey, V. K., Duchen, M. R., Duchosal, M. A., Duez, H., Dugail, I., Dumit, V. I., Duncan, M. C., Dunlop, E. A., Dunn, W. A., Jr., Dupont, N., Dupuis, L., Duran, R. V., Durcan, T. M., Duvezin-Caubet, S., Duvvuri, U., Eapen, V., Ebrahimi-Fakhari, D., Echard, A., Eckhart, L., Edelstein, C. L., Edinger, A. L., Eichinger, L., Eisenberg, T., Eisenberg-Lerner, A., Eissa, N. T., El-Deiry, W. S., El-Khoury, V., Elazar, Z., Eldar-Finkelman, H., Elliott, C. J., Emanuele, E., Emmenegger, U., Engedal, N., Engelbrecht, A. M., Engelender, S., Enserink, J. M., Erdmann, R., Erenpreisa, J., Eri, R., Eriksen, J. L., Erman, A., Escalante, R., Eskelinen, E. L., Espert, L., Esteban-Martinez, L., Evans, T. J., Fabri, M., Fabrias, G., Fabrizi, C., Facchiano, A., Faergeman, N. J., Faggioni, A., Fairlie, W. D., Fan, C., Fan, D., Fan, J., Fang, S., Fanto, M., Fanzani, A., Farkas, T., Faure, M., Favier, F. B., Fearnhead, H., Federici, M., Fei, E., Felizardo, T. C., Feng, H., Feng, Y., Feng, Y., Ferguson, T. A., Fernandez, A. F., Fernandez-Barrena, M. G., Fernandez-Checa, J. C., Fernandez-Lopez, A., Fernandez-Zapico, M. E., Feron, O., Ferraro, E., Ferreira-Halder, C. V., Fesus, L., Feuer, R., Fiesel, F. C., Filippi-Chiela, E. C., Filomeni, G., Fimia, G. M., Fingert, J. H., Finkbeiner, S., Finkel, T., Fiorito, F.,

Fisher, P. B., Flajolet, M., Flamigni, F., Florey, O., Florio, S., Floto, R. A., Folini, M., Follo, C., Fon, E. A., Fornai, F., Fortunato, F., Fraldi, A., Franco, R., Francois, A., Francois, A., Frankel, L. B., Fraser, I. D., Frey, N., Freyssenet, D. G., Frezza, C., Friedman, S. L., Frigo, D. E., Fu, D., Fuentes, J. M., Fueyo, J., Fujitani, Y., Fujiwara, Y., Fujiya, M., Fukuda, M., Fulda, S., Fusco, C., Gabryel, B., Gaestel, M., Gailly, P., Gajewska, M., Galadari, S., Galili, G., Galindo, I., Galindo, M. F., Galliciotti, G., Galluzzi, L., Galluzzi, L., Galy, V., Gammoh, N., Gandy, S., Ganesan, A. K., Ganesan, S., Ganley, I. G., Gannage, M., Gao, F. B., Gao, F., Gao, J. X., Garcia Nannig, L., Garcia Vescovi, E., Garcia-Macia, M., Garcia-Ruiz, C., Garg, A. D., Garg, P. K., Gargini, R., Gassen, N. C., Gatica, D., Gatti, E., Gavard, J., Gavathiotis, E., Ge, L., Ge, P., Ge, S., Gean, P. W., Gelmetti, V., Genazzani, A. A., Geng, J., Genschik, P., Gerner, L., Gestwicki, J. E., Gewirtz, D. A., Ghavami, S., Ghigo, E., Ghosh, D., Giammarioli, A. M., Giampieri, F., Giampietri, C., Giatromanolaki, A., Gibbings, D. J., Gibellini, L., Gibson, S. B., Ginet, V., Giordano, A., Giorgini, F., Giovannetti, E., Girardin, S. E., Gispert, S., Giuliano, S., Gladson, C. L., Glavic, A., Gleave, M., Godefroy, N., Gogal, R. M., Jr., Gokulan, K., Goldman, G. H., Goletti, D., Goligorsky, M. S., Gomes, A. V., Gomes, L. C., Gomez, H., Gomez-Manzano, C., Gomez-Sanchez, R., Goncalves, D. A., Goncu, E., Gong, Q., Gongora, C., Gonzalez, C. B., Gonzalez-Alegre, P., Gonzalez-Cabo, P., Gonzalez-Polo, R. A., Goping, I. S., Gorbea, C., Gorbunov, N. V., Goring, D. R., Gorman, A. M., Gorski, S. M., Goruppi, S., Goto-Yamada, S., Gotor, C., Gottlieb, R. A., Gozes, I., Gozuacik, D.,

Graba, Y., Graef, M., Granato, G. E., Grant, G. D., Grant, S., Gravina, G. L., Green, D. R., Greenhough, A., Greenwood, M. T., Grimaldi, B., Gros, F., Grose, C., Groulx, J. F., Gruber, F., Grumati, P., Grune, T., Guan, J. L., Guan, K. L., Guerra, B., Guillen, C., Gulshan, K., Gunst, J., Guo, C., Guo, L., Guo, M., Guo, W., Guo, X. G., Gust, A. A., Gustafsson, A. B., Gutierrez, E., Gutierrez, M. G., Gwak, H. S., Haas, A., Haber, J. E., Hadano, S., Hagedorn, M., Hahn, D. R., Halayko, A. J., Hamacher-Brady, A., Hamada, K., Hamai, A., Hamann, A., Hamasaki, M., Hamer, I., Hamid, Q., Hammond, E. M., Han, F., Han, W., Handa, J. T., Hanover, J. A., Hansen, M., Harada, M., Harhaji-Trajkovic, L., Harper, J. W., Harrath, A. H., Harris, A. L., Harris, J., Hasler, U., Hasselblatt, P., Hasui, K., Hawley, R. G., Hawley, T. S., He, C., He, C. Y., He, F., He, G., He, R. R., He, X. H., He, Y. W., He, Y. Y., Heath, J. K., Hebert, M. J., Heinzen, R. A., Helgason, G. V., Hensel, M., Henske, E. P., Her, C., Herman, P. K., Hernandez, A., Hernandez, C., Hernandez-Tiedra, S., Hetz, C., Hiesinger, P. R., Higaki, K., Hilfiker, S., Hill, B. G., Hill, J. A., Hill, W. D., Hino, K., Hofius, D., Hofman, P., Hoglinger, G. U., Hohfeld, J., Holz, M. K., Hong, Y., Hood, D. A., Hoozemans, J. J., Hoppe, T., Hsu, C., Hsu, C. Y., Hsu, L. C., Hu, D., Hu, G., Hu, H. M., Hu, H., Hu, M. C., Hu, Y. C., Hu, Z. W., Hua, F., Hua, Y., Huang, C., Huang, H. L., Huang, K. H., Huang, K. Y., Huang, S., Huang, S., Huang, W. P., Huang, Y. R., Huang, Y., Huang, Y., Huber, T. B., Huebbe, P., Huh, W. K., Hulmi, J. J., Hur, G. M., Hurley, J. H., Husak, Z., Hussain, S. N., Hussain, S., Hwang, J. J., Hwang, S., Hwang, T. I., Ichihara, A., Imai, Y., Imbriano, C., Inomata, M., Into, T.,

Iovane, V., Iovanna, J. L., Iozzo, R. V., Ip, N. Y., Irazoqui, J. E., Iribarren, P., Isaka, Y., Isakovic, A. J., Ischiropoulos, H., Isenberg, J. S., Ishaq, M., Ishida, H., Ishii, I., Ishmael, J. E., Isidoro, C., Isobe, K. I., Isono, E., Issazadeh-Navikas, S., Itahana, K., Itakura, E., Ivanov, A. I., Iyer, A. K., Izquierdo, J. M., Izumi, Y., Izzo, V., Jaattela, M., Jaber, N., Jackson, D. J., Jackson, W. T., Jacob, T. G., Jacques, T. S., Jagannath, C., Jain, A., Jana, N. R., Jang, B. K., Jani, A., Janji, B., Jannig, P. R., Jansson, P. J., Jean, S., Jendrach, M., Jeon, J. H., Jessen, N., Jeung, E. B., Jia, K., Jia, L., Jiang, H., Jiang, H., Jiang, L., Jiang, T., Jiang, X., Jiang, X., Jiang, X., Jiang, Y., Jiang, Y., Jimenez, A., Jin, C., Jin, H., Jin, L., Jin, M., Jin, S., Jinwal, U. K., Jo, E. K., Johansen, T., Johnson, D. E., Johnson, G. V., Johnson, J. D., Jonasch, E., Jones, C., Joosten, L. A., Jordan, J., Joseph, A. M., Joseph, B., Joubert, A. M., Ju, D., Ju, J., Juan, H. F., Juenemann, K., Juhasz, G., Jung, H. S., Jung, J. U., Jung, Y. K., Jungbluth, H., Justice, M. J., Jutten, B., Kaakoush, N. O., Kaarniranta, K., Kaasik, A., Kabuta, T., Kaeffer, B., Kagedal, K., Kahana, A., Kajimura, S., Kakhlon, O., Kalia, M., Kalvakolanu, D. V., Kamada, Y., Kambas, K., Kaminskyy, V. O., Kampinga, H. H., Kandouz, M., Kang, C., Kang, R., Kang, T. C., Kanki, T., Kanneganti, T. D., Kanno, H., Kanthasamy, A. G., Kantorow, M., Kaparakis-Liaskos, M., Kapuy, O., Karantza, V., Karim, M. R., Karmakar, P., Kaser, A., Kaushik, S., Kawula, T., Kaynar, A. M., Ke, P. Y., Ke, Z. J., Kehrl, J. H., Keller, K. E., Kemper, J. K., Kenworthy, A. K., Kepp, O., Kern, A., Kesari, S., Kessel, D., Ketteler, R., Kettelhut, I. D., Khambu, B., Khan, M. M., Khandelwal, V. K., Khare, S., Kiang, J. G., Kiger, A. A., Kihara, A., Kim,

A. L., Kim, C. H., Kim, D. R., Kim, D. H., Kim, E. K., Kim, H. Y., Kim, H. R., Kim, J. S., Kim, J. H., Kim, J. C., Kim, J. H., Kim, K. W., Kim, M. D., Kim, M. M., Kim, P. K., Kim, S. W., Kim, S. Y., Kim, Y. S., Kim, Y., Kimchi, A., Kimmelman, A. C., Kimura, T., King, J. S., Kirkegaard, K., Kirkin, V., Kirshenbaum, L. A., Kishi, S., Kitajima, Y., Kitamoto, K., Kitaoka, Y., Kitazato, K., Kley, R. A., Klimecki, W. T., Klinkenberg, M., Klucken, J., Knaevelsrud, H., Knecht, E., Knuppertz, L., Ko, J. L., Kobayashi, S., Koch, J. C., Koechlin-Ramonatxo, C., Koenig, U., Koh, Y. H., Kohler, K., Kohlwein, S. D., Koike, M., Komatsu, M., Kominami, E., Kong, D., Kong, H. J., Konstantakou, E. G., Kopp, B. T., Korcsmaros, T., Korhonen, L., Korolchuk, V. I., Koshkina, N. V., Kou, Y., Koukourakis, M. I., Koumenis, C., Kovacs, A. L., Kovacs, T., Kovacs, W. J., Koya, D., Kraft, C., Krainc, D., Kramer, H., Kravic-Stevovic, T., Krek, W., Kretz-Remy, C., Krick, R., Krishnamurthy, M., Kriston-Vizi, J., Kroemer, G., Kruer, M. C., Kruger, R., Ktistakis, N. T., Kuchitsu, K., Kuhn, C., Kumar, A. P., Kumar, A., Kumar, A., Kumar, D., Kumar, D., Kumar, R., Kumar, S., Kundu, M., Kung, H. J., Kuno, A., Kuo, S. H., Kuret, J., Kurz, T., Kwok, T., Kwon, T. K., Kwon, Y. T., Kyrmizi, I., La Spada, A. R., Lafont, F., Lahm, T., Lakkaraju, A., Lam, T., Lamark, T., Lancel, S., Landowski, T. H., Lane, D. J., Lane, J. D., Lanzi, C., Lapaquette, P., Lapierre, L. R., Laporte, J., Laukkarinen, J., Laurie, G. W., Lavandero, S., Lavie, L., LaVoie, M. J., Law, B. Y., Law, H. K., Law, K. B., Layfield, R., Lazo, P. A., Le Cam, L., Le Roch, K. G., Le Stunff, H., Leardkamolkarn, V., Lecuit, M., Lee, B. H., Lee, C. H., Lee, E. F., Lee, G. M.,

Lee, H. J., Lee, H., Lee, J. K., Lee, J., Lee, J. H., Lee, J. H., Lee, M., Lee, M. S., Lee, P. J., Lee, S. W., Lee, S. J., Lee, S. J., Lee, S. Y., Lee, S. H., Lee, S. S., Lee, S. J., Lee, S., Lee, Y. R., Lee, Y. J., Lee, Y. H., Leeuwenburgh, C., Lefort, S., Legouis, R., Lei, J., Lei, Q. Y., Leib, D. A., Leibowitz, G., Lekli, I., Lemaire, S. D., Lemasters, J. J., Lemberg, M. K., Lemoine, A., Leng, S., Lenz, G., Lenzi, P., Lerman, L. O., Lettieri Barbato, D., Leu, J. I., Leung, H. Y., Levine, B., Lewis, P. A., Lezoualc'h, F., Li, C., Li, F., Li, F. J., Li, J., Li, K., Li, L., Li, M., Li, M., Li, Q., Li, R., Li, S., Li, W., Li, W., Li, X., Li, Y., Lian, J., Liang, C., Liang, Q., Liao, Y., Liberal, J., Liberski, P. P., Lie, P., Lieberman, A. P., Lim, H. J., Lim, K. L., Lim, K., Lima, R. T., Lin, C. S., Lin, C. F., Lin, F., Lin, F., Lin, F. C., Lin, K., Lin, K. H., Lin, P. H., Lin, T., Lin, W. W., Lin, Y. S., Lin, Y., Linden, R., Lindholm, D., Lindqvist, L. M., Lingor, P., Linkermann, A., Liotta, L. A., Lipinski, M. M., Lira, V. A., Lisanti, M. P., Liton, P. B., Liu, B., Liu, C., Liu, C. F., Liu, F., Liu, H. J., Liu, J., Liu, J. J., Liu, J. L., Liu, K., Liu, L., Liu, L., Liu, Q., Liu, R. Y., Liu, S., Liu, S., Liu, W., Liu, X. D., Liu, X., Liu, X. H., Liu, X., Liu, X., Liu, X., Liu, Y., Liu, Y., Liu, Z., Liu, Z., Liuzzi, J. P., Lizard, G., Ljujic, M., Lodhi, I. J., Logue, S. E., Lokeshwar, B. L., Long, Y. C., Lonial, S., Loos, B., Lopez-Otin, C., Lopez-Vicario, C., Lorente, M., Lorenzi, P. L., Lorincz, P., Los, M., Lotze, M. T., Lovat, P. E., Lu, B., Lu, B., Lu, J., Lu, Q., Lu, S. M., Lu, S., Lu, Y., Luciano, F., Luckhart, S., Lucocq, J. M., Ludovico, P., Lugea, A., Lukacs, N. W., Lum, J. J., Lund, A. H., Luo, H., Luo, J., Luo, S., Luparello, C., Lyons, T., Ma, J., Ma, Y., Ma, Y., Ma, Z., Machado, J., Machado-Santelli, G. M., Macian,

F., MacIntosh, G. C., MacKeigan, J. P., Macleod, K. F., MacMicking, J. D., MacMillan-Crow, L. A., Madeo, F., Madesh, M., Madrigal-Matute, J., Maeda, A., Maeda, T., Maegawa, G., Maellaro, E., Maes, H., Magarinos, M., Maiese, K., Maiti, T. K., Maiuri, L., Maiuri, M. C., Maki, C. G., Malli, R., Malorni, W., Maloyan, A., Mami-Chouaib, F., Man, N., Mancias, J. D., Mandelkow, E. M., Mandell, M. A., Manfredi, A. A., Manie, S. N., Manzoni, C., Mao, K., Mao, Z., Mao, Z. W., Marambaud, P., Marconi, A. M., Marelja, Z., Marfe, G., Margeta, M., Margittai, E., Mari, M., Mariani, F. V., Marin, C., Marinelli, S., Marino, G., Markovic, I., Marquez, R., Martelli, A. M., Martens, S., Martin, K. R., Martin, S. J., Martin, S., Martin-Acebes, M. A., Martin-Sanz, P., Martinand-Mari, C., Martinet, W., Martinez, J., Martinez-Lopez, N., Martinez-Outschoorn, U., Martinez-Velazquez, M., Martinez-Vicente, M., Martins, W. K., Mashima, H., Mastrianni, J. A., Matarese, G., Matarrese, P., Mateo, R., Matoba, S., Matsumoto, N., Matsushita, T., Matsuura, A., Matsuzawa, T., Mattson, M. P., Matus, S., Maugeri, N., Mauvezin, C., Mayer, A., Maysinger, D., Mazzolini, G. D., McBrayer, M. K., McCall, K., McCormick, C., McInerney, G. M., McIver, S. C., McKenna, S., McMahon, J. J., McNeish, I. A., Mechta-Grigoriou, F., Medema, J. P., Medina, D. L., Megyeri, K., Mehrpour, M., Mehta, J. L., Mei, Y., Meier, U. C., Meijer, A. J., Melendez, A., Melino, G., Melino, S., de Melo, E. J., Mena, M. A., Meneghini, M. D., Menendez, J. A., Menezes, R., Meng, L., Meng, L. H., Meng, S., Menghini, R., Menko, A. S., Menna-Barreto, R. F., Menon, M. B., Meraz-Rios, M. A., Merla, G., Merlini, L., Merlot, A. M., Meryk, A., Meschini,

S., Meyer, J. N., Mi, M. T., Miao, C. Y., Micale, L., Michaeli, S., Michiels, C., Migliaccio, A. R., Mihailidou, A. S., Mijaljica, D., Mikoshiba, K., Milan, E., Miller-Fleming, L., Mills, G. B., Mills, I. G., Minakaki, G., Minassian, B. A., Ming, X. F., Minibayeva, F., Minina, E. A., Mintern, J. D., Minucci, S., Miranda-Vizuete, A., Mitchell, C. H., Miyamoto, S., Miyazawa, K., Mizushima, N., Mnich, K., Mograbi, B., Mohseni, S., Moita, L. F., Molinari, M., Molinari, M., Moller, A. B., Mollereau, B., Mollinedo, F., Mongillo, M., Monick, M. M., Montagnaro, S., Montell, C., Moore, D. J., Moore, M. N., Mora-Rodriguez, R., Moreira, P. I., Morel, E., Morelli, M. B., Moreno, S., Morgan, M. J., Moris, A., Moriyasu, Y., Morrison, J. L., Morrison, L. A., Morselli, E., Moscat, J., Moseley, P. L., Mostowy, S., Motori, E., Mottet, D., Mottram, J. C., Moussa, C. E., Mpakou, V. E., Mukhtar, H., Mulcahy Levy, J. M., Muller, S., Munoz-Moreno, R., Munoz-Pinedo, C., Munz, C., Murphy, M. E., Murray, J. T., Murthy, A., Mysorekar, I. U., Nabi, I. R., Nabissi, M., Nader, G. A., Nagahara, Y., Nagai, Y., Nagata, K., Nagelkerke, A., Nagy, P., Naidu, S. R., Nair, S., Nakano, H., Nakatogawa, H., Nanjundan, M., Napolitano, G., Naqvi, N. I., Nardacci, R., Narendra, D. P., Narita, M., Nascimbeni, A. C., Natarajan, R., Navegantes, L. C., Nawrocki, S. T., Nazarko, T. Y., Nazarko, V. Y., Neill, T., Neri, L. M., Netea, M. G., Netea-Maier, R. T., Neves, B. M., Ney, P. A., Nezis, I. P., Nguyen, H. T., Nguyen, H. P., Nicot, A. S., Nilsen, H., Nilsson, P., Nishimura, M., Nishino, I., Niso-Santano, M., Niu, H., Nixon, R. A., Njar, V. C., Noda, T., Noegel, A. A., Nolte, E. M., Norberg, E., Norga, K. K., Noureini, S. K., Notomi, S., Notterpek,

L., Nowikovsky, K., Nukina, N., Nurnberger, T., O'Donnell, V. B., O'Donovan, T., O'Dwyer, P. J., Oehme, I., Oeste, C. L., Ogawa, M., Ogretmen, B., Ogura, Y., Oh, Y. J., Ohmuraya, M., Ohshima, T., Ojha, R., Okamoto, K., Okazaki, T., Oliver, F. J., Ollinger, K., Olsson, S., Orban, D. P., Ordonez, P., Orhon, I., Orosz, L., O'Rourke, E. J., Orozco, H., Ortega, A. L., Ortona, E., Osellame, L. D., Oshima, J., Oshima, S., Osiewacz, H. D., Otomo, T., Otsu, K., Ou, J. J., Outeiro, T. F., Ouyang, D. Y., Ouyang, H., Overholtzer, M., Ozbun, M. A., Ozdinler, P. H., Ozpolat, B., Pacelli, C., Paganetti, P., Page, G., Pages, G., Pagnini, U., Pajak, B., Pak, S. C., Pakos-Zebrucka, K., Pakpour, N., Palkova, Z., Palladino, F., Pallauf, K., Pallet, N., Palmieri, M., Paludan, S. R., Palumbo, C., Palumbo, S., Pampliega, O., Pan, H., Pan, W., Panaretakis, T., Pandey, A., Pantazopoulou, A., Papackova, Z., Papademetrio, D. L., Papassideri, I., Papini, A., Parajuli, N., Pardo, J., Parekh, V. V., Parenti, G., Park, J. I., Park, J., Park, O. K., Parker, R., Parlato, R., Parys, J. B., Parzych, K. R., Pasquet, J. M., Pasquier, B., Pasumarthi, K. B., Patschan, D., Patterson, C., Pattingre, S., Pattison, S., Pause, A., Pavenstadt, H., Pavone, F., Pedrozo, Z., Pena, F. J., Penalva, M. A., Pende, M., Peng, J., Penna, F., Penninger, J. M., Pensalfini, A., Pepe, S., Pereira, G. J., Pereira, P. C., Perez-de la Cruz, V., Perez-Perez, M. E., Perez-Rodriguez, D., Perez-Sala, D., Perier, C., Perl, A., Perlmutter, D. H., Perrotta, I., Pervaiz, S., Pesonen, M., Pessin, J. E., Peters, G. J., Petersen, M., Petrache, I., Petrof, B. J., Petrovski, G., Phang, J. M., Piacentini, M., Pierdominici, M., Pierre, P., Pierrefite-Carle, V., Pietrocola, F., Pimentel-Muinos, F. X., Pinar, M., Pineda, B.,

Pinkas-Kramarski, R., Pinti, M., Pinton, P., Piperdi, B., Piret, J. M., Platanias, L. C., Platta, H. W., Plowey, E. D., Poggeler, S., Poirot, M., Polcic, P., Poletti, A., Poon, A. H., Popelka, H., Popova, B., Poprawa, I., Poulose, S. M., Poulton, J., Powers, S. K., Powers, T., Pozuelo-Rubio, M., Prak, K., Prange, R., Prescott, M., Priault, M., Prince, S., Proia, R. L., Proikas-Cezanne, T., Prokisch, H., Promponas, V. J., Przyklenk, K., Puertollano, R., Pugazhenthi, S., Puglielli, L., Pujol, A., Puyal, J., Pyeon, D., Qi, X., Qian, W. B., Qin, Z. H., Qiu, Y., Qu, Z., Quadrilatero, J., Quinn, F., Raben, N., Rabinowich, H., Radogna, F., Ragusa, M. J., Rahmani, M., Raina, K., Ramanadham, S., Ramesh, R., Rami, A., Randall-Demllo, S., Randow, F., Rao, H., Rao, V. A., Rasmussen, B. B., Rasse, T. M., Ratovitski, E. A., Rautou, P. E., Ray, S. K., Razani, B., Reed, B. H., Reggiori, F., Rehm, M., Reichert, A. S., Rein, T., Reiner, D. J., Reits, E., Ren, J., Ren, X., Renna, M., Reusch, J. E., Revuelta, J. L., Reyes, L., Rezaie, A. R., Richards, R. I., Richardson, D. R., Richetta, C., Riehle, M. A., Rihn, B. H., Rikihisa, Y., Riley, B. E., Rimbach, G., Rippo, M. R., Ritis, K., Rizzi, F., Rizzo, E., Roach, P. J., Robbins, J., Roberge, M., Roca, G., Roccheri, M. C., Rocha, S., Rodrigues, C. M., Rodriguez, C. I., de Cordoba, S. R., Rodriguez-Muela, N., Roelofs, J., Rogov, V. V., Rohn, T. T., Rohrer, B., Romanelli, D., Romani, L., Romano, P. S., Roncero, M. I., Rosa, J. L., Rosello, A., Rosen, K. V., Rosenstiel, P., Rost-Roszkowska, M., Roth, K. A., Roue, G., Rouis, M., Rouschop, K. M., Ruan, D. T., Ruano, D., Rubinsztein, D. C., Rucker, E. B., 3rd, Rudich, A., Rudolf, E., Rudolf, R., Ruegg, M. A., Ruiz-Roldan, C., Ruparelia, A. A., Rusmini, P., Russ,

D. W., Russo, G. L., Russo, G., Russo, R., Rusten, T. E., Ryabovol, V., Ryan, K. M., Ryter, S. W., Sabatini, D. M., Sacher, M., Sachse, C., Sack, M. N., Sadoshima, J., Saftig, P., Sagi-Eisenberg, R., Sahni, S., Saikumar, P., Saito, T., Saitoh, T., Sakakura, K., Sakoh-Nakatogawa, M., Sakuraba, Y., Salazar-Roa, M., Salomoni, P., Saluja, A. K., Salvaterra, P. M., Salvioli, R., Samali, A., Sanchez, A. M., Sanchez-Alcazar, J. A., Sanchez-Prieto, R., Sandri, M., Sanjuan, M. A., Santaguida, S., Santambrogio, L., Santoni, G., Dos Santos, C. N., Saran, S., Sardiello, M., Sargent, G., Sarkar, P., Sarkar, S., Sarrias, M. R., Sarwal, M. M., Sasakawa, C., Sasaki, M., Sass, M., Sato, K., Sato, M., Satriano, J., Savaraj, N., Saveljeva, S., Schaefer, L., Schaible, U. E., Scharl, M., Schatzl, H. M., Schekman, R., Scheper, W., Schiavi, A., Schipper, H. M., Schmeisser, H., Schmidt, J., Schmitz, I., Schneider, B. E., Schneider, E. M., Schneider, J. L., Schon, E. A., Schonenberger, M. J., Schonthal, A. H., Schorderet, D. F., Schroder, B., Schuck, S., Schulze, R. J., Schwarten, M., Schwarz, T. L., Sciarretta, S., Scotto, K., Scovassi, A. I., Screaton, R. A., Screen, M., Seca, H., Sedej, S., Segatori, L., Segev, N., Seglen, P. O., Segui-Simarro, J. M., Segura-Aguilar, J., Seki, E., Seiliez, I., Sell, C., Semenkovich, C. F., Semenza, G. L., Sen, U., Serra, A. L., Serrano-Puebla, A., Sesaki, H., Setoguchi, T., Settembre, C., Shacka, J. J., Shajahan-Haq, A. N., Shapiro, I. M., Sharma, S., She, H., Shen, C. J., Shen, C. C., Shen, H. M., Shen, S., Shen, W., Sheng, R., Sheng, X., Sheng, Z. H., Shepherd, T. G., Shi, J., Shi, Q., Shi, Q., Shi, Y., Shibutani, S., Shibuya, K., Shidoji, Y., Shieh, J. J., Shih, C. M., Shimada, Y., Shimizu, S., Shin, D. W.,

Shinohara, M. L., Shintani, M., Shintani, T., Shioi, T., Shirabe, K., Shiri-Sverdlov, R., Shirihai, O., Shore, G. C., Shu, C. W., Shukla, D., Sibirny, A. A., Sica, V., Sigurdson, C. J., Sigurdsson, E. M., Sijwali, P. S., Sikorska, B., Silveira, W. A., Silvente-Poirot, S., Silverman, G. A., Simak, J., Simmet, T., Simon, A. K., Simon, H. U., Simone, C., Simons, M., Simonsen, A., Singh, R., Singh, S. V., Singh, S. K., Sinha, D., Sinha, S., Sinicrope, F. A., Sirko, A., Sirohi, K., Sishi, B. J., Sittler, A., Siu, P. M., Sivridis, E., Skwarska, A., Slack, R., Slaninova, I., Slavov, N., Smaili, S. S., Smalley, K. S., Smith, D. R., Soenen, S. J., Soleimanpour, S. A., Solhaug, A., Somasundaram, K., Son, J. H., Sonawane, A., Song, C., Song, F., Song, H. K., Song, J. X., Song, W., Soo, K. Y., Sood, A. K., Soong, T. W., Soontornniyomkij, V., Sorice, M., Sotgia, F., Soto-Pantoja, D. R., Sotthibundhu, A., Sousa, M. J., Spaink, H. P., Span, P. N., Spang, A., Sparks, J. D., Speck, P. G., Spector, S. A., Spies, C. D., Springer, W., Clair, D. S., Stacchiotti, A., Staels, B., Stang, M. T., Starczynowski, D. T., Starokadomskyy, P., Steegborn, C., Steele, J. W., Stefanis, L., Steffan, J., Stellrecht, C. M., Stenmark, H., Stepkowski, T. M., Stern, S. T., Stevens, C., Stockwell, B. R., Stoka, V., Storchova, Z., Stork, B., Stratoulias, V., Stravopodis, D. J., Strnad, P., Strohecker, A. M., Strom, A. L., Stromhaug, P., Stulik, J., Su, Y. X., Su, Z., Subauste, C. S., Subramaniam, S., Sue, C. M., Suh, S. W., Sui, X., Sukseree, S., Sulzer, D., Sun, F. L., Sun, J., Sun, J., Sun, S. Y., Sun, Y., Sun, Y., Sun, Y., Sundaramoorthy, V., Sung, J., Suzuki, H., Suzuki, K., Suzuki, N., Suzuki, T., Suzuki, Y. J., Swanson, M. S., Swanton, C., Sward, K., Swarup, G., Sweeney, S.

T., Sylvester, P. W., Szatmari, Z., Szegezdi, E., Szlosarek, P. W., Taegtmeyer, H., Tafani, M., Taillebourg, E., Tait, S. W., Takacs-Vellai, K., Takahashi, Y., Takats, S., Takemura, G., Takigawa, N., Talbot, N. J., Tamagno, E., Tamburini, J., Tan, C. P., Tan, L., Tan, M. L., Tan, M., Tan, Y. J., Tanaka, K., Tanaka, M., Tang, D., Tang, D., Tang, G., Tanida, I., Tanji, K., Tannous, B. A., Tapia, J. A., Tasset-Cuevas, I., Tatar, M., Tavassoly, I., Tavernarakis, N., Taylor, A., Taylor, G. S., Taylor, G. A., Taylor, J. P., Taylor, M. J., Tchetina, E. V., Tee, A. R., Teixeira-Clerc, F., Telang, S., Tencomnao, T., Teng, B. B., Teng, R. J., Terro, F., Tettamanti, G., Theiss, A. L., Theron, A. E., Thomas, K. J., Thome, M. P., Thomes, P. G., Thorburn, A., Thorner, J., Thum, T., Thumm, M., Thurston, T. L., Tian, L., Till, A., Ting, J. P., Titorenko, V. I., Toker, L., Toldo, S., Tooze, S. A., Topisirovic, I., Torgersen, M. L., Torosantucci, L., Torriglia, A., Torrisi, M. R., Tournier, C., Towns, R., Trajkovic, V., Travassos, L. H., Triola, G., Tripathi, D. N., Trisciuoglio, D., Troncoso, R., Trougakos, I. P., Truttmann, A. C., Tsai, K. J., Tschan, M. P., Tseng, Y. H., Tsukuba, T., Tsung, A., Tsvetkov, A. S., Tu, S., Tuan, H. Y., Tucci, M., Tumbarello, D. A., Turk, B., Turk, V., Turner, R. F., Tveita, A. A., Tyagi, S. C., Ubukata, M., Uchiyama, Y., Udelnow, A., Ueno, T., Umekawa, M., Umemiya-Shirafuji, R., Underwood, B. R., Ungermann, C., Ureshino, R. P., Ushioda, R., Uversky, V. N., Uzcategui, N. L., Vaccari, T., Vaccaro, M. I., Vachova, L., Vakifahmetoglu-Norberg, H., Valdor, R., Valente, E. M., Vallette, F., Valverde, A. M., Van den Berghe, G., Van Den Bosch, L., van den Brink, G. R., van der Goot, F. G., van der Klei, I. J., van der Laan, L. J.,

van Doorn, W. G., van Egmond, M., van Golen, K. L., Van Kaer, L., van Lookeren Campagne, M., Vandenabeele, P., Vandenberghe, W., Vanhorebeek, I., Varela-Nieto, I., Vasconcelos, M. H., Vasko, R., Vavvas, D. G., Vega-Naredo, I., Velasco, G., Velentzas, A. D., Velentzas, P. D., Vellai, T., Vellenga, E., Vendelbo, M. H., Venkatachalam, K., Ventura, N., Ventura, S., Veras, P. S., Verdier, M., Vertessy, B. G., Viale, A., Vidal, M., Vieira, H., Vierstra, R. D., Vigneswaran, N., Vij, N., Vila, M., Villar, M., Villar, V. H., Villarroya, J., Vindis, C., Viola, G., Viscomi, M. T., Vitale, G., Vogl, D. T., Voitsekhovskaja, O. V., von Haefen, C., von Schwarzenberg, K., Voth, D. E., Vouret-Craviari, V., Vuori, K., Vyas, J. M., Waeber, C., Walker, C. L., Walker, M. J., Walter, J., Wan, L., Wan, X., Wang, B., Wang, C., Wang, C. Y., Wang, C., Wang, C., Wang, C., Wang, D., Wang, F., Wang, F., Wang, G., Wang, H. J., Wang, H., Wang, H. G., Wang, H., Wang, H. D., Wang, J., Wang, J., Wang, M., Wang, M. Q., Wang, P. Y., Wang, P., Wang, R. C., Wang, S., Wang, T. F., Wang, X., Wang, X. J., Wang, X. W., Wang, X., Wang, X., Wang, Y., Wang, Y., Wang, Y., Wang, Y. J., Wang, Y., Wang, Y., Wang, Y. T., Wang, Y., Wang, Z. N., Wappner, P., Ward, C., Ward, D. M., Warnes, G., Watada, H., Watanabe, Y., Watase, K., Weaver, T. E., Weekes, C. D., Wei, J., Weide, T., Weihl, C. C., Weindl, G., Weis, S. N., Wen, L., Wen, X., Wen, Y., Westermann, B., Weyand, C. M., White, A. R., White, E., Whitton, J. L., Whitworth, A. J., Wiels, J., Wild, F., Wildenberg, M. E., Wileman, T., Wilkinson, D. S., Wilkinson, S., Willbold, D., Williams, C., Williams, K., Williamson, P. R., Winklhofer, K. F., Witkin, S. S., Wohlgemuth, S. E., Wollert,

T., Wolvetang, E. J., Wong, E., Wong, G. W., Wong, R. W., Wong, V. K., Woodcock, E. A., Wright, K. L., Wu, C., Wu, D., Wu, G. S., Wu, J., Wu, J., Wu, M., Wu, M., Wu, S., Wu, W. K., Wu, Y., Wu, Z., Xavier, C. P., Xavier, R. J., Xia, G. X., Xia, T., Xia, W., Xia, Y., Xiao, H., Xiao, J., Xiao, S., Xiao, W., Xie, C. M., Xie, Z., Xie, Z., Xilouri, M., Xiong, Y., Xu, C., Xu, C., Xu, F., Xu, H., Xu, H., Xu, J., Xu, J., Xu, J., Xu, L., Xu, X., Xu, Y., Xu, Y., Xu, Z. X., Xu, Z., Xue, Y., Yamada, T., Yamamoto, A., Yamanaka, K., Yamashina, S., Yamashiro, S., Yan, B., Yan, B., Yan, X., Yan, Z., Yanagi, Y., Yang, D. S., Yang, J. M., Yang, L., Yang, M., Yang, P. M., Yang, P., Yang, Q., Yang, W., Yang, W. Y., Yang, X., Yang, Y., Yang, Y., Yang, Z., Yang, Z., Yao, M. C., Yao, P. J., Yao, X., Yao, Z., Yao, Z., Yasui, L. S., Ye, M., Yedvobnick, B., Yeganeh, B., Yeh, E. S., Yeyati, P. L., Yi, F., Yi, L., Yin, X. M., Yip, C. K., Yoo, Y. M., Yoo, Y. H., Yoon, S. Y., Yoshida, K. I., Yoshimori, T., Young, K. H., Yu, H., Yu, J. J., Yu, J. T., Yu, J., Yu, L., Yu, W. H., Yu, X. F., Yu, Z., Yuan, J., Yuan, Z. M., Yue, B. Y., Yue, J., Yue, Z., Zacks, D. N., Zacksenhaus, E., Zaffaroni, N., Zaglia, T., Zakeri, Z., Zecchini, V., Zeng, J., Zeng, M., Zeng, Q., Zervos, A. S., Zhang, D. D., Zhang, F., Zhang, G., Zhang, G. C., Zhang, H., Zhang, H., Zhang, H., Zhang, H., Zhang, J., Zhang, J., Zhang, J., Zhang, J., Zhang, J. P., Zhang, L., Zhang, L., Zhang, L., Zhang, L., Zhang, M. Y., Zhang, X., Zhang, X. D., Zhang, Y., Zhang, Y., Zhang, Y., Zhang, Y., Zhang, Y., Zhao, M., Zhao, W. L., Zhao, X., Zhao, Y. G., Zhao, Y., Zhao, Y., Zhao, Y. X., Zhao, Z., Zhao, Z. J., Zheng, D., Zheng, X. L., Zheng, X., Zhivotovsky, B., Zhong, Q., Zhou, G. Z., Zhou, G., Zhou, H.,

Zhou, S. F., Zhou, X. J., Zhu, H., Zhu, H., Zhu, W. G., Zhu, W., Zhu, X. F., Zhu, Y., Zhuang, S. M., Zhuang, X., Ziparo, E., Zois, C. E., Zoladek, T., Zong, W. X., Zorzano, A., and Zughaier, S. M. (2016) Guidelines for the use and interpretation of assays for monitoring autophagy (3rd edition). *Autophagy* **12**, 1-222

85. Lee, I. H., and Finkel, T. (2009) Regulation of autophagy by the p300 acetyltransferase. *The Journal of Biological Chemistry* **284**, 6322-6328

86. Lee, I. H., Cao, L., Mostoslavsky, R., Lombard, D. B., Liu, J., Bruns, N. E., Tsokos, M., Alt, F. W., and Finkel, T. (2008) A role for the NAD-dependent deacetylase Sirt1 in the regulation of autophagy. *Proceedings of the National Academy of Sciences of the United States of America* **105**, 3374-3379

87. Mizushima, N., Levine, B., Cuervo, A. M., and Klionsky, D. J. (2008) Autophagy fights disease through cellular self-digestion. *Nature* **451**, 1069-1075

88. Harris, H., and Rubinsztein, D. C. (2012) Control of autophagy as a therapy for neurodegenerative disease. *Nature Reviews Neurology* **8**, 108-117

89. Tsien, J. Z., Huerta, P. T., and Tonegawa, S. (1996) The essential role of hippocampal CA1 NMDA receptor-dependent synaptic plasticity in spatial memory. *Cell* **87**, 1327-1338

90. Perez-Otano, I., Lujan, R., Tavalin, S. J., Plomann, M., Modregger, J., Liu, X. B., Jones, E. G., Heinemann, S. F., Lo, D. C., and Ehlers, M. D. (2006) Endocytosis and synaptic removal of NR3A-containing NMDA receptors by PACSIN1/syndapin1. *Nature Neuroscience* **9**, 611-621

91. Eriksson, M., Samuelsson, H., Samuelsson, E. B., Liu, L., McKeehan, W. L., Benedikz, E., and Sundström, E. (2007) The NMDAR subunit NR3A interacts with microtubule-associated protein 1S in the brain. *Biochemical and Biophysical Research Communications* **361**, 127-132

92. Zou, J., Yue, F., Li, W., Song, K., Jiang, X., Yi, J., and Liu, L. (2014) Autophagy Inhibitor LRPPRC Suppresses Mitophagy through Interaction with Mitophagy Initiator Parkin. *PLoS ONE* **9**, e94903

93. Mielcarek, M., Landles, C., Weiss, A., Bradaia, A., Seredenina, T., Inuabasi, L., Osborne, G. F., Wadel, K., Touller, C., Butler, R., Robertson, J., Franklin, S. A., Smith, D. L., Park, L., Marks, P. A., Wanker, E. E., Olson, E. N., Luthi-Carter, R., van der Putten, H., Beaumont, V., and Bates, G. P. (2013) HDAC4 reduction: a novel therapeutic strategy to target cytoplasmic huntingtin and ameliorate neurodegeneration. *PLoS Biology* **11**, e1001717

94. Zhang, S., Binari, R., Zhou, R., and Perrimon, N. (2010) A genomewide RNA interference screen for modifiers of aggregates formation by mutant Huntingtin in Drosophila. *Genetics* **184**, 1165-1179

95. Weiss, A., Klein, C., Woodman, B., Sathasivam, K., Bibel, M., Regulier, E., Bates, G. P., and Paganetti, P. (2008) Sensitive biochemical aggregate detection reveals aggregation onset before symptom development in cellular and murine models of Huntington's disease. *Journal of Neurochemistry* **104**, 846-858

96. Ravikumar, B., Duden, R., and Rubinsztein, D. C. (2002) Aggregate-prone proteins with polyglutamine and polyalanine expansions are degraded by autophagy. *Human Molecular Genetics* **11**, 1107-1117

97. Firdaus, W. J., Wyttenbach, A., Diaz-Latoud, C., Currie, R. W., and Arrigo, A. P. (2006) Analysis of oxidative events induced by expanded polyglutamine huntingtin exon 1 that are differentially restored by expression of heat shock proteins or treatment with an antioxidant. *FEBS Jounal* **273**, 3076-3093

98. Jeong, H., Then, F., Melia, T. J., Jr., Mazzulli, J. R., Cui, L., Savas, J. N., Voisine, C., Paganetti, P., Tanese, N., Hart, A. C., Yamamoto, A., and Krainc, D. (2009) Acetylation targets mutant huntingtin to autophagosomes for degradation. *Cell* **137**, 60-72

99. Cattaneo, E., Rigamonti, D., Goffredo, D., Zuccato, C., Squitieri, F., and Sipione, S. (2001) Loss of normal huntingtin function: new developments in Huntington's disease research. *Trends in Neurosciences* **24**, 182-188

100. Cattaneo, E., Zuccato, C., and Tartari, M. (2005) Normal huntingtin function: an alternative approach to Huntington's disease. *Nature Reviews Neuroscience* **6**, 919-930

101. Sathasivam, K., Neueder, A., Gipson, T. A., Landles, C., Benjamin, A. C., Bondulich, M. K., Smith, D. L., Faull, R. L., Roos, R. A., Howland, D., Detloff, P. J., Housman, D. E., and Bates, G. P. (2013) Aberrant splicing of HTT generates the pathogenic exon 1 protein in Huntington disease. *Proceedings of*

the National Academy of Sciences of the United States of America **110**, 2366-2370

102. Schapira, A. H., Olanow, C. W., Greenamyre, J. T., and Bezard, E. (2014) Slowing of neurodegeneration in Parkinson's disease and Huntington's disease: future therapeutic perspectives. *Lancet (London, England)* **384**, 545-555

103. Mielcarek, M., Seredenina, T., Stokes, M. P., Osborne, G. F., Landles, C., Inuabasi, L., Franklin, S. A., Silva, J. C., Luthi-Carter, R., Beaumont, V., and Bates, G. P. (2013) HDAC4 does not act as a protein deacetylase in the postnatal murine brain in vivo. *PLoS ONE* **8**, e80849

104. Reiner, A., Dragatsis, I., Zeitlin, S., and Goldowitz, D. (2003) Wild-type huntingtin plays a role in brain development and neuronal survival. *Molecular Neurobiology* **28**, 259-276

105. Gauthier, L. R., Charrin, B. C., Borrell-Pages, M., Dompierre, J. P., Rangone, H., Cordelieres, F. P., De Mey, J., MacDonald, M. E., Lessmann, V., Humbert, S., and Saudou, F. (2004) Huntingtin controls neurotrophic support and survival of neurons by enhancing BDNF vesicular transport along microtubules. *Cell* **118**, 127-138

106. Hoffner, G., Kahlem, P., and Djian, P. (2002) Perinuclear localization of huntingtin as a consequence of its binding to microtubules through an interaction with beta-tubulin: relevance to Huntington's disease. *Journal of Cell Science* **115**, 941-948

107. DiFiglia, M., Sapp, E., Chase, K., Schwarz, C., Meloni, A., Young, C., Martin, E., Vonsattel, J. P., Carraway, R., Reeves, S. A., and et al. (1995) Huntingtin is a cytoplasmic protein associated with vesicles in human and rat brain neurons. *Neuron* **14**, 1075-1081

108. Zuccato, C., Tartari, M., Crotti, A., Goffredo, D., Valenza, M., Conti, L., Cataudella, T., Leavitt, B. R., Hayden, M. R., Timmusk, T., Rigamonti, D., and Cattaneo, E. (2003) Huntingtin interacts with REST/NRSF to modulate the transcription of NRSE-controlled neuronal genes. *Nature Genetics* **35**, 76-83

109. Rigamonti, D., Bauer, J. H., De-Fraja, C., Conti, L., Sipione, S., Sciorati, C., Clementi, E., Hackam, A., Hayden, M. R., Li, Y., Cooper, J. K., Ross, C. A., Govoni, S., Vincenz, C., and Cattaneo, E. (2000) Wild-type huntingtin protects from apoptosis upstream of caspase-3. *The Journal of Neuroscience* **20**, 3705-3713

110. Steffan, J. S. (2010) Does Huntingtin play a role in selective macroautophagy? *Cell Cycle* **9**, 3401-3413

111. Rui, Y. N., Xu, Z., Patel, B., Chen, Z., Chen, D., Tito, A., David, G., Sun, Y., Stimming, E. F., Bellen, H., Cuervo, A. M., and Zhang, S. (2015) Huntingtin Functions as a Scaffold for Selective Macroautophagy. *Nature Cell Biology* **17**, 262-275

112. Wong, Y. C., and Holzbaur, E. L. (2014) The regulation of autophagosome dynamics by huntingtin and HAP1 is disrupted by expression of mutant

huntingtin, leading to defective cargo degradation. *The Journal of Neuroscience* **34**, 1293-1305

113. Mahalingam, D., Mita, M., Sarantopoulos, J., Wood, L., Amaravadi, R. K., Davis, L. E., Mita, A. C., Curiel, T. J., Espitia, C. M., Nawrocki, S. T., Giles, F. J., and Carew, J. S. (2014) Combined autophagy and HDAC inhibition: A phase I safety, tolerability, pharmacokinetic, and pharmacodynamic analysis of hydroxychloroquine in combination with the HDAC inhibitor vorinostat in patients with advanced solid tumors. *Autophagy* **10**, 1403-1414

114. Chuang, D. M., Leng, Y., Marinova, Z., Kim, H. J., and Chiu, C. T. (2009) Multiple roles of HDAC inhibition in neurodegenerative conditions. *Trends in Neurosciences* **32**, 591-601

115. Beconi, M., Aziz, O., Matthews, K., Moumne, L., O'Connell, C., Yates, D., Clifton, S., Pett, H., Vann, J., Crowley, L., Haughan, A. F., Smith, D. L., Woodman, B., Bates, G. P., Brookfield, F., Burli, R. W., McAllister, G., Dominguez, C., Munoz-Sanjuan, I., and Beaumont, V. (2012) Oral administration of the pimelic diphenylamide HDAC inhibitor HDACi 4b is unsuitable for chronic inhibition of HDAC activity in the CNS in vivo. *PLoS ONE* **7**, e44498

116. Moumne, L., Campbell, K., Howland, D., Ouyang, Y., and Bates, G. P. (2012) Genetic knock-down of HDAC3 does not modify disease-related phenotypes in a mouse model of Huntington's disease. *PLoS ONE* **7**, e31080

117. Bobrowska, A., Paganetti, P., Matthias, P., and Bates, G. P. (2011) Hdac6 knock-out increases tubulin acetylation but does not modify disease progression in the R6/2 mouse model of Huntington's disease. *PLoS ONE* **6**, e20696

118. Benn, C. L., Butler, R., Mariner, L., Nixon, J., Moffitt, H., Mielcarek, M., Woodman, B., and Bates, G. P. (2009) Genetic knock-down of HDAC7 does not ameliorate disease pathogenesis in the R6/2 mouse model of Huntington's disease. *PLoS ONE* **4**, e5747

119. Cao, H., Phan, H., and Yang, L. X. (2012) Improved chemotherapy for hepatocellular carcinoma. *Anticancer Research* **32**, 1379-1386

120. Heindryckx, F., Colle, I., and Vlierberghe, H. V. (2009) Experimental mouse models for hepatocellular carcinoma research. *International Journal of Experimental Pathology* **90**, 367-386

121. Chen, B., Liu, L., Castonguay, A., Maronpot, R. R., Anderson, M. W., and You, M. (1993) Dose-dependent ras mutation spectra in N-nitrosodiethylamine induced mouse liver tumors and 4-(methylnitrosamino)-1-(3-pyridyl)-1-butanone induced mouse lung tumors. *Carcinogenesis* **14**, 1603-1608

122. Yamada, K., Yamamiya, I., and Utsumi, H. (2006) In vivo detection of free radicals induced by diethylnitrosamine in rat liver tissue. *Free Radical Biology & Medicine* **40**, 2040-2046

123. Thorgeirsson, S. S., and Santoni-Rugiu, E. (1996) Transgenic mouse models in carcinogenesis: interaction of c-myc with transforming growth factor alpha and

hepatocyte growth factor in hepatocarcinogenesis. *British Journal of Clinical Pharmacology* **42**, 43-52

124. Harada, N., Oshima, H., Katoh, M., Tamai, Y., Oshima, M., and Taketo, M. M. (2004) Hepatocarcinogenesis in mice with beta-catenin and Ha-ras gene mutations. *Cancer Research* **64**, 48-54

125. Hanahan, D., and Weinberg, R. A. (2011) Hallmarks of cancer: the next generation. *Cell* **144**, 646-674

126. Miller-Fleming, L., Olin-Sandoval, V., Campbell, K., and Ralser, M. (2015) Remaining Mysteries of Molecular Biology: The Role of Polyamines in the Cell. *Journal of Molecular Biology* **427**, 3389-3406

127. Morselli, E., Mariño, G., Bennetzen, M. V., Eisenberg, T., Megalou, E., Schroeder, S., Cabrera, S., Bénit, P., Rustin, P., Criollo, A., Kepp, O., Galluzzi, L., Shen, S., Malik, S. A., Maiuri, M. C., Horio, Y., López-Otín, C., Andersen, J. S., Tavernarakis, N., Madeo, F., and Kroemer, G. (2011) Spermidine and resveratrol induce autophagy by distinct pathways converging on the acetylproteome. *The Journal of Cell Biology* **192**, 615-629

128. Wang, A. H., and Yang, X.-J. (2001) Histone deacetylase 4 possesses intrinsic nuclear import and export signals. *Molecular and Cellular Biology* **21**, 5992-6005

129. Bennetzen, M. V., Mariño, G., Pultz, D., Morselli, E., Færgeman, N. J., Kroemer, G., and Andersen, J. S. (2012) Phosphoproteomic analysis of cells treated with longevity-related autophagy inducers. *Cell Cycle* **11**, 1827-1840

130. Tung, H. Y., Pelech, S., Fisher, M. J., Pogson, C. I., and Cohen, P. (1985) The protein phosphatases involved in cellular regulation. Influence of polyamines on the activities of protein phosphatase-1 and protein phosphatase-2A. *European Journal of Biochemistry* **149**, 305-313

131. Mihaylova, M. M., Vasquez, D. S., Ravnskjaer, K., Denechaud, P. D., Yu, R. T., Alvarez, J. G., Downes, M., Evans, R. M., Montminy, M., and Shaw, R. J. (2011) Class IIa histone deacetylases are hormone-activated regulators of FOXO and mammalian glucose homeostasis. *Cell* **145**, 607-621

132. Chrisam, M., Pirozzi, M., Castagnaro, S., Blaauw, B., Polishchuck, R., Cecconi, F., Grumati, P., and Bonaldo, P. (2015) Reactivation of autophagy by spermidine ameliorates the myopathic defects of collagen VI-null mice. *Autophagy* **11**, 2142-2152

133. Saadoun, D., Cazals-Hatem, D., Denninger, M. H., Boudaoud, L., Pham, B. N., Mallet, V., Condat, B., Briere, J., and Valla, D. (2004) Association of idiopathic hepatic sinusoidal dilatation with the immunological features of the antiphospholipid syndrome. *Gut* **53**, 1516-1519

134. Laumonier, H., Bioulac-Sage, P., Laurent, C., Zucman-Rossi, J., Balabaud, C., and Trillaud, H. (2008) Hepatocellular adenomas: magnetic resonance imaging features as a function of molecular pathological classification. *Hepatology (Baltimore, Md.)* **48**, 808-818

135. Paradis, V., Benzekri, A., Dargere, D., Bieche, I., Laurendeau, I., Vilgrain, V., Belghiti, J., Vidaud, M., Degott, C., and Bedossa, P. (2004) Telangiectatic focal

nodular hyperplasia: a variant of hepatocellular adenoma. *Gastroenterology* **126**, 1323-1329